Doctor Thesis

Shibaura Institute of Technology

Study of Biped Robot Walking Behavior: an Analysis of Toe Effect by Using the Gait Generation Method

2014 September

Krissana Nerakae

Abstract

The study of biped robot has long history and continuation, in order to develop the robot walking process and movement ability like a human. The human walking process is stable and flexible then it can be adapted to various surfaces. In a previous research, the gait pattern design has been studying for improvement of walking control algorithm and a robot foot design etc. For a robot foot design, the research has been focused on a toe component of the biped robot. The biped robot with a toe had shown the good walking ability. From the results, it can conclude that the toe will improve the biped robot walking stability and reduce the load on any joints of the legs. The robot with toe can walk human-like walking. As a reason, I interested in the study of the toe effect emphasized on the bigtoe mechanism. I consider the bigtoe of the foot that is an important component, which distinguishes from the abnormal bigtoe such as bigtoe pain or hallux valgus. It will affect the human walking process. In addition, some medical research papers shown that some body weight are transmitted to the toe during conventional human walking and the bigtoe has a maximum supporting force area. In preceding researches, they have no obvious presentation of the robot with bigtoe.

This paper presents a study of biped robot walking process affected by the bigtoe. Furthermore, I will consider an appropriate bigtoe size that make a robot can walk with specified conditions. This research utilizes gait generation method for generating gait pattern of the robot joints. Additionally, the research concentrates on a situation that the robot walks on flat ground and friction is assume to be constant. From the results of our experiments, I obtained a good result from model B (a model composed of bigtoe, tiptoe and heel), which a ratio between bigtoe width and foot width equal 0.28. Moreover, the range of this ratio is in a scope of human bigtoe size. The expected outcome from this research, which results from the effect of the bigtoe, is an application in the robot's foot utilized, to analyze and compare the results. I expect that the bigtoe will has important benefit in the development of biped robot walking ability.

“I am a slow walker, but I never walk backwards”

-Abraham Lincoln-

“I can accept failure, but I can’t accept not trying”

-Michael Jordan-

Acknowledgements

This doctoral dissertation would not have been completed without considerable help and encouragement of Professor Hiroshi Hasegawa, my thesis advisor. His knowledge, advice, and guidance were very helpful and useful to this dissertation. Also, I would like to thank you for his care and hospitality in daily life while I was in Japan. I acknowledge Shibaura University of Technology (SIT) for providing me a scholarship which is the best opportunity in my life. Many thanks go to all staff who coordinated and helped me throughout the study. I would also like to thank Suranaree University of Technology (SUT) for granting me an opportunity to get this scholarship. I wish to thank Assoc. Prof. Flt. Lt. Dr. Kontorn Chamniprasart for his support on carrying out the research at SUT and his advice during my experiments. To my friends, special thanks to Mr. Chanyut Khajorntraidet and Mr. Chitapong Wechtaisong for their encouragement, support, and friendship.

I would like to thank all the lecturers who have taught me until now and to all people who deserve my acknowledgement for their support and advice which I cannot mention.

Finally, I would especially like to thank my father, Mr. Wichean Nerakae, and my mother, Mrs. Sunisa Nerakae, for their deep understanding and warm-hearted encouragement over the years of my study. Thanks Mr. Phansak Nerakae, my younger brother, for his love, care, and patience which are the most important for my successful.

Contents

List of Figures

List of Tables

Glossary

ZMP	Zero Moment Point; a concept related with dynamics and control of legged locomotion, e.g., for humanoid robots
CoM	Center of Mass: the unique point at the center of a distribution of mass in space that has the property that the weighted position vectors relative to this point sum to zero.
ODE	Open Dynamics Engine; a physics engine written in C/C++. Its two main components are a rigid body dynamics simulation engine and a collision detection engine
APGA	Adaptive Plan System with Genetic Algorithm; a optimization proposed to reduce a large amount of calculation cost and to improve stability in convergence to an optimal solution
GA	Genetic Algorithm; a search heuristic that mimics the process of natural evolution to generate useful solutions to optimization and search problems
ERP	Error Reduction Parameter; a parameter which corrects joint error for ODE
GRF	Ground Reaction Force; he reaction force supplied by the ground is specifically, which is basically the reaction to the force the body exerts on the ground
DOF	Degree of Freedom; the number of independent parameters that define the configuration to the analysis of systems of bodies
CFM	Constraint Force Mixing; specific parameter of the ODE, which changes stiffness of a joint.
RFM	Response Surface Model; to use a sequence of designed experiments to obtain an optimal response

1

Introduction

1.1 Background and Signification of Research Problem

Nowadays, the study of robot is popular and widely spread. This is because robots have the important role related to human life. The robots in the presence have variety duties and characteristics. For instance, the robots compose of simple links for grab an object, certain type of them is in the form of vehicle, and some kind of them have the feature human-like or animal. In the beginning of robot design, the robot can work only following the command form human. However, the presence robots are developed and their controllers are sophisticated then they can work automatically based on the reasons of each work. In additional, they have more efficiency while their size is reduced. This is because of the high performance controllers of the robots. The calculation time of the decision process is reduced. Additionally, they made from high quality materials.

Humanoid robot or biped robots are fashioned from the idea of human structure. This type of robot may compose of only legs part or completely important body part. The design concept of this type of robot make the robots have flexible structure and can adapt in any environments of application. The robots can complete the objective in many works because of these reasons. The biped robots are different from other robots that have the specific working condition. The important movement of the robot that is

very interesting is walking. The walking of robot similar to human walking and its velocity and stability are developed. The walking robots can operate in several frameworks, for example in rough area, walking up and down the step. Application in the field of medicine, they are used to carry out the patient from one position to another required position. When compare the walking process of biped robot and another type of robot that has several legs, the biped robots always has smaller size and lower weight. Moreover, they can apply in much utilization. The walking scheme of the biped robot is fashioned as human walking locomotion. In 2000, Honda Company has presented ASIMO [1] [31] that is biped robot look like human. This robot extremely stimulates the study of the biped robot both in the research and education. The results had shown the successfully developed robot technology of Honda Company. The robot efficiency has been improved, the outstanding capabilities are walking, running, walking up and down the step, and dancing. In addition, the robot composes of sound recorded system for responding the human order and it can remember the feature of human face correctly. All robot abilities made for human demands. Subsequently, the study of biped robot is continuously, for instance, WABIAN-2, WABIAN-2R [2] of Waseda University, HRP-2LT, HRP-3 and HRP-4C [3] of AIST, H6 and H7 [4] of Tokyo University. All of these ensure the development and successful technology of robots. The walking of robots is a basically important process in motion control. There are many problems in this motion control such as equilibrium of body, flexibility, and stability. These lead to development of robot mechanism, controller, and measurement system for solving the problems. The designing of biped robot has been received significant notion from human walking. The imitation of human walking that quite unique and complex is to improve the robot walking efficiency. For instance, they can walk in the rough and obstructive area spontaneously.

In the human walking process, a body weight is transferred from heel to forefoot and then to toe, ankle, knee, and hip respectively. The walking process is rhythmic and cycle, it is called gait cycle. The feet are important mechanism in robot walking process because it must support the force directly from whole body. Most robot always have simple foot shapes (flat or curve) because it easy to study and application. However, some researches present the foot shape composed of many parts that reference from human foot (heel and toe). The study of robot’s foot composed of many elements,

like human foot is not widely spread when compare with another group that change to use wheel or another structure such as the a foot like bird's foot. This paper address the robot's foot having the toe especially bigtoe, because I assume that toe will make the robot's foot has more flexibility similar to human's foot. Additionally, the robot walking process can be improved until similar to human's walking process.

There are many sizes of biped robot structure depended on the designer, the robot having the same size as human, for example, ASIMO, WABIAN and HRP. The robots mentioned above have completely components. Designing of these robots used high technology in many majors. Moreover, in the design process need the person that expert in mechanical part and physical structure because the calculation of force, momentum, and vector is very importance. Besides, the expert in mechanism for designing the transmission and movement system is also required. In the electrical driving system insist on the knowledge of electrical both digital and analog circuits. The analysis of robot's electrical circuit need much knowledge such as controller structure, measuring system, power system, and vision system. The responsive personnel in this work must have the skill in calculus and computer. Additionally, the logical thinking system and problem synthetic are required. Because of above mentioned, the robot research always use high investment budget including long time period. Because of the successful and interesting of biped robot research and education, the robots are developed and produced both in businesses and studies. The robots can response to many order and they are solutions of many problems. In the basic study, I can learn the robot's structure, design process, movement mechanism, and control system. Because of a simple structure that easy to learn, some research groups can design and produce small biped robot for study. The robot components are not expensive and easily available. These reasons make the small biped robots can be adjusted both structure and programming for each part of education.

From interesting issues and illustrated reasons, I interested in the study of the toe effect emphasized on the bigtoe mechanism. I consider the bigtoe of the foot that is an important component [15], which distinguishes from the abnormal bigtoe such as bigtoe pain or hallux valgus. It will affect the human walking process. In addition, some medical research papers shown that some body weight are transmitted to the toe during conventional human

walking and the bigtoe has a maximum supporting force area. In preceding researches, they have no obvious presentation of the robot with bigtoe. This paper presents a study of biped robot walking process affected by the bigtoe. Furthermore, I will consider an appropriate bigtoe size that make a robot can walk with specified conditions. This research utilizes gait generation method for generating gait pattern of the robot joints. I consider the bigtoe size [22]; to make our robot can walk straight forward and stay in walking conditions. Additionally, the research concentrates on a situation that the robot walks on flat ground and friction is assume to be constant.

In order to achieve the aim, I have the following sequence of steps;

First step: I make a robot simulation model composed of toes component at robot's foot to study robot walking behavior. I simulate the robot working by using gait generation method, to prove that our robot simulation model can walk and robot gait like a human gait. Moreover, in this step I use optimization method to improve robot walking and obtain long distance. I make a robot simulation model with tiptoe mechanism to study. This model study is a simple tiptoe part like another research presented model.

Second step: In this step, I design different toes type to study an effect of robot walking. I will consider that what type of toe robot simulation can improve robot walking and obtained long distance. For design toe of foot, I design base on human foot structure and foot support area during normal human walking. In this experiment, I have created four models for simulate robot walking. Model A has a foot with tiptoe mechanism same with model in first step. Model B has a bigtoe and tiptoe component consist at the robot foot. Model C is composed of tiptoe and toe part, and last one, Model D is a more complex model than another model, which the foot has a bigtoe, tiptoe and toe mechanism.

Third step: As a result of the second step, I obtained good result is a foot with bigtoe model. Therefore, I am interested in bigtoe component. Since I were aware of the bigtoe function

and expected to affect the robot walking, also presented researches about bigtoe of robot quite a few and still unclear. I study a robot with bigtoe walking. I consider the bigtoe width size to make obtain long distance and under the conditions.

1.2 Objectives

This research focuses a study of small biped robot walking process affected by the bigtoe component using the gait generation method. The hypothesis of this research is bigtoe can improve walking distance and make robot's walking behavior like a human walking. There are objective for reasons as follow.

- To create simulation model and study walking affected of small biped robot consisted toe component by using gait generation method.
- To analyze various characteristics of toe that effect to walking action in small biped robot.
- To design bigtoe width size that suitable with simulation model.
- To experiment and compare walking results from simulation model.

1.3 Scope of the Research

To define scope of dissertation in small biped robot as follow;

- Simulation model of small biped robot in this dissertation is KONDO KHR-2HV and KONDO KHR-3HV by create simulation model for consider DOF only since hip through foot.
- Studying is operated on flat ground that has constant friction.
- Characteristic of toe joint part is basic passive control by using standard size torsion spring for study.
- Walking action that focused on this research is walking as go straight under defined constraint and considers result in only final position.

1.4 Expected Benefits

After finish this dissertation, abilities that received as follow.

- Small biped robot using bigtoe can increase flexibility of walking.
- Small biped robot using bigtoe have walking action more same as human walking.
- Research results like designing and size of bigtoe can be basic detail for continue future research work and developing application in humanoid robot.

1.5 Organize of Thesis

This section discusses an overview of each chapter, which is detailed below.

In chapter2 is "Previous study": It discusses the history and origin of the Robot. Where does the word robot come from? Why build a robot? Evolutions of the robot are recorded from the past to the present. It aims for fundamental stage before into the research.

In chapter3 is "Theories of walking": It discusses human bone structure that used for general design of bipedal robots, such as human joints, human foot bone structure. The human joints, I applied to characterize the movement of the joints to make robot models for movement and mobility. The human foot bone structure, I studied for design toes part of robot model, because in the study I assumed when the robot model have a toe component it enables the flexible on the foot and a robot gait will be similar a human gait. There is also described about normal human walking gait. "What is the gait cycle?" "Where are the foot support areas during walking in stance phase?" This section connects to toes part, which I focus in this research. Order to shown that "How the toes are important for walking" and "Why I choose to study about toes which consists of bigtoe"

In chapter4 is "Methodology": It discusses physical and components of the model robot are used to walking simulation and experiment. In this research used two model robot are model KHR-2HV and model KHR-3HV of KONDO Company. I discuss the software used to make models in the simulation walking these are Msc.visual Nastran Desktop 4D and Open Dynamics Engine (ODE). Gait generation method is described in this section, which it is a method to obtain the angle position for defines into each joint to make the simulation robot move. Finally of this chapter, I discuss of design of experiment, including the experimental condition.

In chapter5 is "Design of robot's foot": It discusses design of robot's foot by reference size with real biped robot model. The experiment was divided into three phases.

- Experimental I: Robot's foot with toe mechanism, which is the first step of our study. . Therefore, the initial design is a simple design to study the effects of walking when simulation model had toes

component. To consider the locomotion in accordance with the assumption or not.

- Experimental II: Robot's foot with different type of toe mechanisms. After I obtained the results of preliminary experiments. I design and build simulation walking models with different type of toes mechanisms. The toes are designed based on the structural characteristics of human feet and pressure support on the human feet. Finally in this experiment, I compared simulation results.

- Experimental III: Robot's foot with bigtoe sizing mechanism. In this section continuation from the second experiment. The simulation model with bigtoe and tiptoe mechanism to be taken into consideration. In addition, also conducted to change a stiffness of hing spring at toes joint position, for study effects of walking. The bigtoe and tiptoe sizing is our study, in order to find appropriate size for simulation model and locomotion study.

In chapter6 is "Experimental results": It presents the results of the models with various toes to study the locomotion, walking trajectory and a rotation at the joints. Comparing the results obtained with human walking pattern.

In chapter7 is "Discussion and Conclusion": It discusses a systematic review of the experiments and the conclusion of the experiments.

2

Literature Review

2.1 The History of Biped Robot [42]

Robots have the long ancient history, but most histories are in the fiction, legend, and imaginary. For example, Greek has the legend related to the robot which is called “Taros”. It is used to prevent the island from any enemies and restrict the escape of people from the island that not gave permission from the King Minos. In the legend, Taros is made from brass and clothing by magical water, it can move because of this reason. However, the annals not explain some moving mechanism details of the robot; it is only a rough idea about robot and its prototype. According to the record of Leonardo da Vinci, the Italian Renaissance polymath, in 1495, he presents the first humanoid. The humanoid has some moving mechanism inside and its head and arms can move. On the other hand, it cannot prove that the robot, designed by Leonardo da Vinci, is created. The objective of robots manufacturing is serving in human responsibility. For instance, the robots can do arduous and endanger works. In addition, they are produced for amusements etc. The idea of the robots in the early history leads to robot develops in the presence.

The word “robot” comes from “robota” in Czech language. This word, which from “Rossum’s Universal Robots” (R.U.R.) produced by Kalvel

Capek in 1920, means *work as slave or forced worker*. This plot is renowned and the word "*robot*" is very popular all over the world. The performance is related to human's imagination that tries to find something for serving responsibilities. The robot manufacturing originates from this idea. Additionally, the notion may leads to the conflict between robot and human in the future.

In 1942, an American and Russian poet, Isacc Asimov, presents the short scientific poetry deal with robot. There are three rules of robot displayed in his plot. All rules can be listed as:

I. A robot may not harm a human being, or, through inaction, allow a human being to come to harm.

II. A robot must obey the orders given to it by human beings, except where such orders would conflict with the First Law.

III. A robot must protect its own existence, as long as such protection does not conflict with the First or Second Law.

After the poetry is distributed and corrected in the verse name as I-Robot. Because of this lyric, the scientist is familiar with the word "Robot". The ideas of this poetry lead to the notion of robot design and development in the future.

After the Second World War, the inventor and businessman, George C. Devol, and the engineer, Joseph F. Engelberger, are named as "*Father of Robotic*". The first robot is used in the work of metallic melting process. The robot, Unimation, has two duties, bring metal out of the machine and weld the part of product. This is because the work is risk safety for human. Moreover, the robots have reliability and economy then they make the development of industries.

In 1970, Lunokhod 1, which produced by The Union of Soviet Socialist Republics (Russian), is the remote control robot using for the moon surface exploration. This robot composes of 8 wheels and many measuring devices such as camera, X-ray radiation sensing device, and cosmic-ray sensing device. Additionally, the solar energy can be used to drive this robot.

In 1977, The Star Wars is extremely famous because the movie presents the imaginary of automatic moving robot (R2D2) and the robot like human (C3PO). This movie makes the human more interested in robots.

The Honda Company, Japanese company, use 14 years for developing the humanoid robot. The robots, Advanced Step in Innovative Mobility (ASIMO) [31], have 11 versions until now. This originated humanoid robot is studied and developed in 1981.Subsequently, in 1986, the humanoid robot of the Honda Company is initiated. One of the company's organizations is founded for developing the humanoid robots. The seven robots in the model name E-series (E0-E6) are used as experimental robots. After that the 3 P-series robots are progressed until the latest version of the robot name ASIMO.

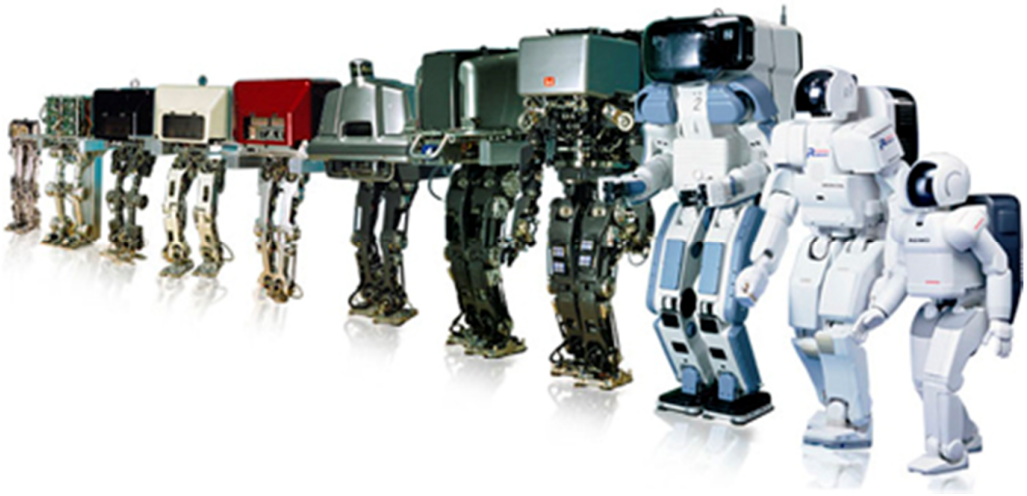

Figure 2.1: Evolution of ASIMO [34]

2.2 Previous Review on Bipedal Walking Robot

The researches of humanoid robot and biped robot have a long history and continuation in two decades. In order that the robot has capable of gestures, expressions, replicates, and decisions human-like. The researches of biped robot have spread extensively and have been extremely favorite topic. On account of, all of these respond to human needs in industries, services and entertainments. Because of these reasons, the studies of robot are popular. One of the important researches and very basic mobility is walking. This is proved by the medical research about the human gait that has been continuously as with the gait of biped robot.

For two decades, the studies of walking biped robot are incessant research topic such as ASIMO, WABIAN-2, WABIAN-2R, HRP2, HRP3, HRP4C, H6 and H7. ASIMO of HONDA [1] is undeniable that the launch of ASIMO cause excitement and increase in the study of biped robot's popularity. ASIMO has been developed from Honda P-series bipedal robot (P1, P2, and P3) until it has small and lightweight. ASIMO has many abilities such as to run, walk smoothly, climb stairs, and communicate human-like. The controller that controls ASIMO's movement is housed in the robot's waist area and can be controlled by a PC or wireless controller. The fact that human has toes for helping our body balance was also taken into consideration. The ASIMO’s posture actually has soft projections on its feet that play a similar role to the one of human toes play when human walk. This soft material also absorbs impact on the joints, just as our soft tissues do when human walk. ASIMO has 34 degrees of freedom totally including six on each leg spread over different points of its body in order to allow it to move freely. The number of degrees of freedom was necessary variable for ASIMO's legs and they were designed by measuring human joint movement while walking on flat ground, climbing stairs and running. ASIMO's engineers had to find a way to work with the inertial forces created while walking. This is called the "zero moment point" (ZMP). ZMP is defined as the point on the ground at which the net moment of the inertial forces and the gravity forces has no component along the horizontal axes [5]. To control ASIMO's posture, engineers worked on three areas of control: First, floor reaction control means regulation the soles of the feet absorb floor unevenness while still maintaining a firm stance. Second, target ZMP control

means the control state that ASIMO can't stand firmly and its body begins to fall forward, the controller maintains position by moving its upper body in the opposite direction to the impending fall. At the same time, it increases walking speeds quickly to counterbalance the fall. Third, Foot-planting location control is used when the target ZMP control has been activated. The controller adjusts the length of the step to regain the right relationship between the position and speed of the body. The successful of the control system is that the ASIMO's posture is widely studied and applied to the walking robot field.

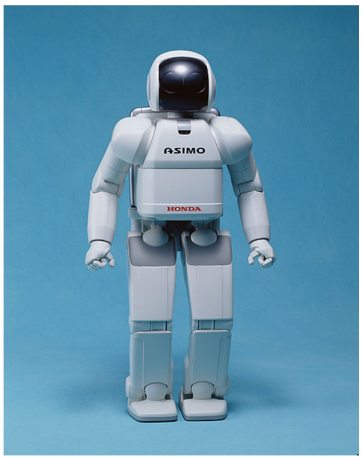

Figure 2.2: ASIMO biped humanoid robot [31]

The studies of bipedal humanoid robot are continuously such as WABIAN-2, WABIAN-2R [2][31] of Waseda University, Waseda University has one of the longest histories on the development of human-like robot. The WABIAN-2 has been designed according to a development of robot having capability of walking like humans walking. WABIAN-2 can obtain data needed for developing medical and rehabilitation instruments by measuring the robot's motions instead of a human, which are difficult to measure quantitatively. WABIAN-2 has capable of walking without the bent knee posture that different from among common bipedal humanoid robots because it has added degrees of freedom in its rocking waist, swiveling knees, and pivoting ankles. In 2006, WABIAN-2R was developed for two purposes. The first one is to develop a robot that would be a human's partner. The second one is to develop a human motion simulator. WABIAN-2R has been designed mimic human movements, the robot has 41 DOFs and the movable range of the joints is designed reference from human. WABIAN-2R used a photo sensor to detect the basing angle. Also, each ankle has a 6-axis

force/torque sensor, which is used for measuring Ground Reaction Force (GRF) and Zero Moment Point (ZMP). In the feet part, WABIAN-2R's foot is designed to be similar to human foot. A Foot with a passive toe joint is applied with WABIAN-2R, this application based on the results of gait analysis with motion capture system. Researchers focus on a walking steady, they offer these main advantages because it lightweight and don't need a necessity complex control structure. In addition, one of the human walk characteristics is heel-contact and toe-off motions in steady walking. From the reasons, the researchers have developed the principle of the pattern generation for stretched knee, heel-contact and toe-off motions. This development based on the ZMP criterion applied with WABIAN-2R. For the pattern generation, some parameters of the foot trajectories of a biped robot were optimized by using a genetic algorithm in order to generate a continuous and smooth motion of leg. The results obtained from WABIAN-2R have the ability to realize more human-like walking styles. The development of the robot's feet is continuous study. In 2009, foot with human-like arch structure was presented. The researchers described a new foot mechanism composed of mimicking the human's foot arch structure and the function of the arch structure. The developed foot mimics the elastic properties of the arch of human's foot and the change of arch height during walking. The foot mechanism consists of a passive joint in the internal toe, a passive joint in the external toe, and joint in the foot arch. The result of arch elasticity shown that it could absorb a foot-landing force at the plantar contact phase and the change of the arch height contributed to a strong trust at the push-off phase. In 2010, WABIAN-2R is capable of two walking styles, one is knee-stretched walking like a human, another one is knee-bend walking. Knee-stretched walking enables fast walking. In contrast, knee-bend walking enables stable walking on uneven terrain. In the real environment, it is preferable that WABIAN-2R change the walking style depending on the ground condition. WABIAN-2R researchers developed a new inverse kinematics method to generate walking motions of robot legs regardless of the walking style and an online walking parameter generation to bend its knees depending on the ground condition. By using the methods and the online pattern generation method above, an adaptive walking process was realized. Design and development capabilities as mention above, these are some of the WABIAN-2R researches.

Figure 2.3: WABIAN-2R biped humanoid robot [32]

Kawada Industries Inc. launched on the development of humanoid robots involved in H6 and H7 [4][32] projects of the University of Tokyo. H6 has 1370 mm height, and its mass is 55 kg including 4 kg of batteries. H6 is designed as a research platform of the humanoid robot that can interact to the complex environment by coupling sensor and behavior. H7 is designed to be a human-sized robot capable of operating autonomously in indoor environments for humans. H7 has 1470 mm height, and the mass is 58 kg. It has 35 DOF totally. Researchers have developed an efficient walking trajectory generation method that follows a given input ZMP trajectory for H7. The key to our method is the modification of the torso horizontal trajectory from a given initial trajectory, by using dynamic trajectory generation and motion planning control software. Therefore, H7 can walk up and down 25 cm high steps.

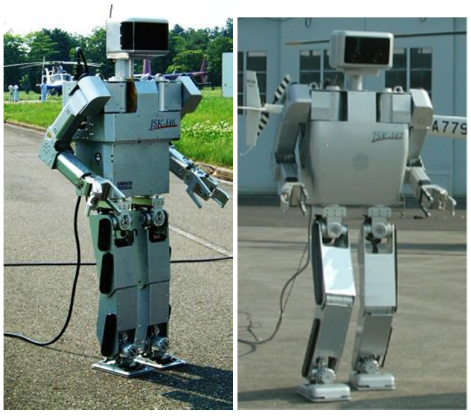

Figure 2.4: H6 (left) and H7 (right) biped humanoid robots [33]

Figure 2.5: HRP-4C biped humanoid robot [34]

In addition, Kawada Industries has attended the Humanoid Robotics Project (HRP) [3][34] of the Ministry of Economy, Trade and Industries of the Japanese Government (METI). They had developed HRP2, HRP3 and HRP4C. The objective of this project is to develop a safe, reliable, and human-friendly robot system. The developed robot has an ability to carry out complicated tasks and supporting humans within human living and working environments. HRP-2 is the final robotic platform for the HRP together with the Humanoid Research Group of National Institute of Advanced Industrial Science and Technology (AIST), and Yaskawa Electric Corporation. HRP-2 has an ability to walk on narrow paths, to cope with uneven surface, to walk at two third level of human speed, to lie down, and to get up by a humanoid robot own self. It has a body similar to human's body by eliminating a backpack for electronics installation. HRP-3, which is developed subsequently, is a model with strong focus on operating under severe outdoor environments. HRP-3 is capable not only of operating in rain, but also of walking on a slippery floor surface. To control of legged locomotion, HRP-3 researchers used ZMP concept, which can be utilized for calculating the stability criterion even if contact points between a humanoid robot and environment doesn’t exist in the same plane. HRP-4C announced in 2009, it is a female humanoid robot with an appearance exactly like a human. She has been named "Miim". This robot has 158 cm height and 46 kg weight. HRP-4C is being developed for the entertainment industry. For characteristics of the legs, HRP-4C’s knees are stretched by up/down motion

of the waist, she mimics the swing motion of human legs, and the single-toe supporting realizes longer strides. The foot of HRP-4C used active toe joint for realizing human-like walking motion. In addition, the hand was redesigned to realize a human-size with realistic skin, also the eye with camera provides visible and useful image for operation and color recognition without deviation from human appearance. HRP-4C became a global focus of interest immediately after its announcement.

These studies are successful and established from the public which mostly in Japan. However, the studies of the biped robot also have many subdivision fields to improve the ability of robots, and to meet the requirements of humans as much as possible. From previous studies of the walking robots, in this research I am classified as follows:

In the gait optimization field, generally, many researches always use Fuzzy logic or Genetic Algorithm (GA) to optimize biped gait, for example, Zhe Tang et al. [6] have proposed Genetic Algorithm (GA) base optimization for humanoid walking. They used GA to optimize walking gait in both the sagittal and frontal plan, simultaneously. The result of their algorithm was verified on the real robot. The GA based optimization for walking planning has improved walking performance quite a lot. However, some researchers have devised a new method for optimization such as; Lingyun H. et al. [7] have presented bipeds gait optimization using spline function based on probability model. They proposed a new type of population-based searching algorithm named Estimation of Distribution Algorithm (EDA) with spline kernel function (EDA_S). They applied this algorithm in humanoid soccer robot. The result is shown that the effective of EDA_S for biped gait optimization has been successfully, which has won several awards in Robocup competitions.

For various surfaces framework, in this case the various surfaces mean different surface shape (uneven terrains, slope, or step etc.) or non-constant friction. There are some studies which related to framework for biped robot locomotion. S. Ali A. Moosavian et al. [8] have proposed the introduction of a Cartesian approach for gate planning and control of biped robots and implementation on various slopes. They used a cartesian approach for gate planning and control of biped robot. The proposed approach constrains have four important points. These four points include the toe of right and left foot,

the hip joint and the total center of mass. The trajectory planning for the toe is designed to reduce the effect of impact force between toe and the ground. Additionally, the trajectory of the hip joint is fashioned such that the robot can walk naturally, while the trajectory of CoM is designed such that stable walking. The obtained result is the Cartesian approach can successfully control tracking on various slopes. Naoya Ito and Hasegawa Hiroshi [9] have presented a robust optimization uncertain factor of environment for simple gait of biped robot to optimize the gait for biped robot. They simulated a robot walking by using Simulated Annealing (SA), robust optimization considered random values as floor's friction and restitution. They obtained result shown that a simulation robot can walk on random values as floor's friction and restitution by using robust optimization. Yu Zheng et al. [10] have proposed a walking pattern generator for biped robots on uneven terrains. They presented an algorithm to compute the feasible acceleration of the robot's CoM for generate biped walking patterns. The approaches were more general and applicable to uneven terrains as compared with previous research methods based on the ZMP criterion. The simulation obtained results exhibited that the robot can walk over terrains with varying slopes.

From abovementioned, most of the biped robot models were used without toes mechanism model. Furthermore, a natural human walking was proposed with toe mechanism for biped robot. The initial studies of biped robot walking with toe component or different foot type have a greater role. This is because, the researchers believed in increasing the flexible feet. This part will support the force from the weight during walking, make robot to walk faster and reduce the energy consumption during walking. Nandha Handharu et al. [11] have proposed gait pattern generation with knee stretch motion for biped robot using toe and heel joints. They reasoned that during walking sequence, human heel act as passive joint that creates some support area which enhances the stability of human walking. They try to replace human-heel like mechanism with a heel joint in the biped robot foot. The obtained result shown a stable knee stretch walking pattern utilizing toe and heel joint generated by using their simulation algorithm, which has some similarity to the human walking pattern. Sven Behnke et al. [12] have proposed human-like walking using toes joint and straight stance leg. They applied an actuated toes joint in robot "*Toni*" to achieve human-like biped walking. The robot dose not shorten the stance leg, but uses the segment

between at the ankle joint and toe joint to over-extend the unloading leg in the double-support phase. They obtained the result that Toni use low energy-consumption in the knee joint, the toe allows walking dynamically with large step and increase walking speed. Cheol Ki Ahn et al. [13] have proposed development of a biped robot with toes to improve gait pattern. They studied the effect of the toe joint in gait pattern generation. The gait pattern of the robot with toes is compared with that of a condensational biped robot which has only sold without toe. The gait pattern is generated by using ZMP. The results of 3D graphical simulation with toes joint shown that the gait of robot is more similar to human's gait than without toes model, the double-support phase was increased walking period, the loads of motors at joints (thigh, knee and ankle) are decreased, and the maximum stride of stable gait is longer than without toe model. Shuuji Kajita et al. [24] have proposed zero of moment point (ZMP) based running pattern generation for a biped robot equipped with toe spring. They applied torsion spring in the toe joint of humanoid robot HRP-2LT. The trajectory of the CoM is designed to realize the specified running motion and the foot trajectories are determined to get proper spring action at lift off phases.They also conducted a preliminary experiment of one time hopping motion with both legs. HRP-2LR could successfully walking and jump by using toe springs. Kenji Hashimoto et al. [2] have proposed a study of function of foot's medial longitudinal arch using biped humanoid robot. They described a new feet mechanism capable of mimicking the human's foot arch structure to fix the function of the arch structure. Especially, the elastic properties were developed by the arch of human's feet. The feet mechanism consists of a passive joint in the internal toe, a passive joint in the external toe and a joint in the foot arch. They conducted various walking experiments by using WABIAN-2R. The arch elasticity could absorb a foot-landing force at the plantar contact phase and the change of the arch height contributed to strong thrust at the push-off phase.

However, the present research of biped robot is still cannot all control human-like walking, which human have flexibility and stability, when walking on the variety of rough ground or easy to step over obstacles. Therefore, the study on robot walking is still continuing. The robot foot design is a topic that I am interested to students. This research presents a study of small biped robots walking by consist passive bigtoe mechanism in

the foot structure. The research has focused on bigtoe mechanism for robot foot because the study of bigtoe foot has narrowly and inexplicitly. I consider the bigtoe size [22]; to make our robot can walk straight forward and stay in walking conditions. Additionally, the research concentrates on a situation that the robot walks on flat ground and friction is assume to be constant.

3

Theories of Walking

In this chapter, the characteristics of biped robot and the basic theory about robot motion including anatomy of biped robots are presented. For example, the walking motions, the supporting parts, and the structure of biped robot foot.

3.1 Anatomy of body [14][35][36]

The production of biped robot always uses the reference characteristic from human such as joints and plane. Therefore, the introduction of the human anatomy is presented first.

The details of human body motion are presented in Cartesian coordinate as shown in Figure 3.1. The figure exhibits the human in the standing motion; the face is straight forward, the arms attaches with the body, the hands turn into front direction, the legs stretch, and the feet place together. The three planes of cartesian coordinate are perpendicular. The positions of each point of the body are specify by X, Y, and Z as shown in the figure.

- Fontal plane is the plane that parallel with YZ plane, the plane is used to separate the body into two parts, anterior and posterior.
- Median plane is the plane that parallel with XZ plane, this plane can be used to separate the body into two parts, right and left body parts.
- Horizontal plane parallel with XY plane, this plane is used to separate the body into two parts, superior and inferior.

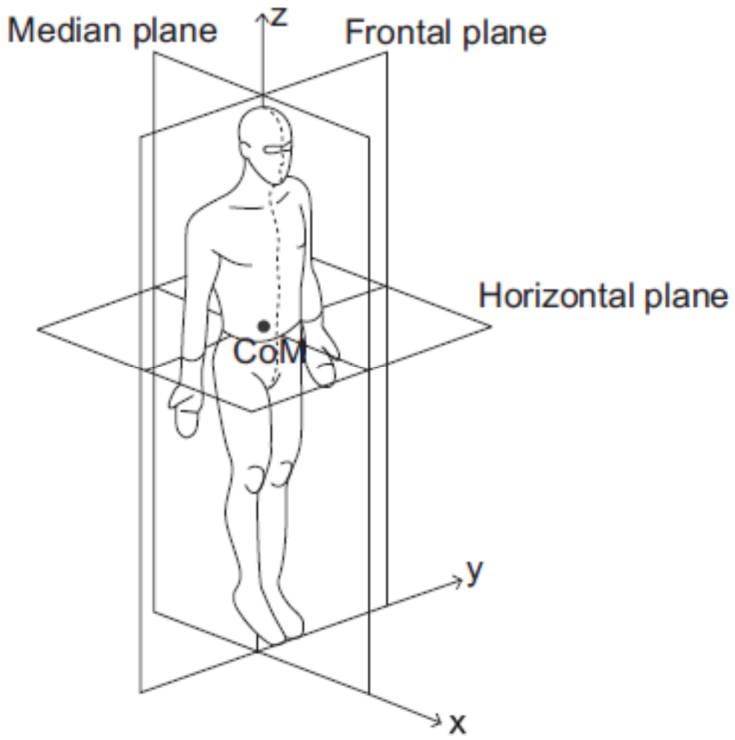

Figure 3.1: The three planes of motion for a human being. The depicted person is standing in anatomical position [35]

The locomotion in each manner of human such as eating, walking, standing, sleeping, and sitting is the motion of bone and muscle structure. The bone structure is very importance because it is the main part that muscle, ligament, and nerve attached. This structure made the body can maintain its shape. The bone structure composes of cartilage, compact bone and joints. The structure includes tendon and ligament. In this research, I interested in joints that are important points in the motion.

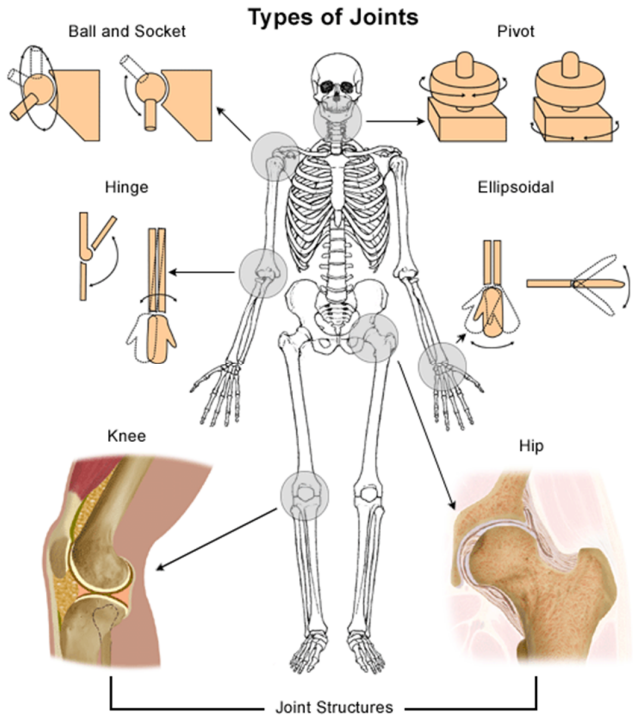

Figure 3.2: Type of joints [36]

Joints are the point that two or more bones are connected. There are two types of joint immovable and movable joint. For example, immovable joint is skull, movable joint are wrist, ankle, brachium and elbow. Some types of joints can move in limiting direction. However, various types of joint can turn around. This is depended on the type of the joints.

- Ball and socket joint are the most flexible joints because they can move in three dimensions. For example, the joints found in shoulder and hip.
- Hinge joint can move in two dimensions that like hinge, found in elbow and knee.
- Pivot joint composes of an extended bond part and another part like curve or ring. This joint can turn along the axis such as the skull bond connecting with neck.
- Ellipsoidal joint has the same feature as socket joint but the motion is limited in one direction such as the joint of wrist.

According to the above mentioned, when I analyze the walking motion, the moving joints compose of hip joints, knee joints, ankle joints, tiptoe joints, and bigtoe joints. The torque and the angle motion during moving of all parts have the relations that make the human walking is stable. When I analyze the structure of moving components in human walking process, the ball joints, reference from Cartesian coordinate, have three degree of freedoms (DOF), the knees that are the hinge joints have only one DOF, and the ankle joints and the hip joints have three DOF. The final parts are tiptoes that have one DOF. Based on the assumption that all tiptoes moving in same direction simultaneously.

Therefore, I can analyze that each leg of human has 8 important and necessary DOF in walking process. In the design walking process of biped robots, the DOF may be increased or decreased depend on the design assumption. The number of degree of freedoms led to the difficulty of controller design. Therefore, the selection of DOF affect to the mechanism design and controller design of the biped robot.

3.2 Foot Structure [14]

“A Foot” is small parts that are critical to human survival. Feet have to support the weight of the body according to the theory of gravity. While the human standing, walking or running weight of the whole body will be sent to both feet. The arch of the feet collapses to reduce the impact. The impact of feet is about 1.4 - 1.6 of body weight and as high as 3-5 of body while running. The structure of the human feet is an architectural fantastic and dramatic. This has unique nature structural design containing exactly 26 bones, 33 joints (20 of which are actively articulated), and more than a hundred muscles, tendons, and ligaments. Feet are very special, they compose of thickness about 4-5 mm final layer by the total for weight distribution, mitigate the impact force to be forwarded to knee and hip.

The feet are important parts of human walking process especially toe. The toes are basic support points received load from body weight. There are five toes in each foot of human, and the details of each toe can be expressed as

- Hallux ("big toe", or "great toe"), the innermost (most proximal) toe and the closest to the toes of the other foot
- Second toe or "long toe"
- Third toe, or "middle toe"
- Fourth toe, or "ring toe"
- Fifth toe ("little toe", "pinky toe", or "baby toe"), the outermost (most distal) toe

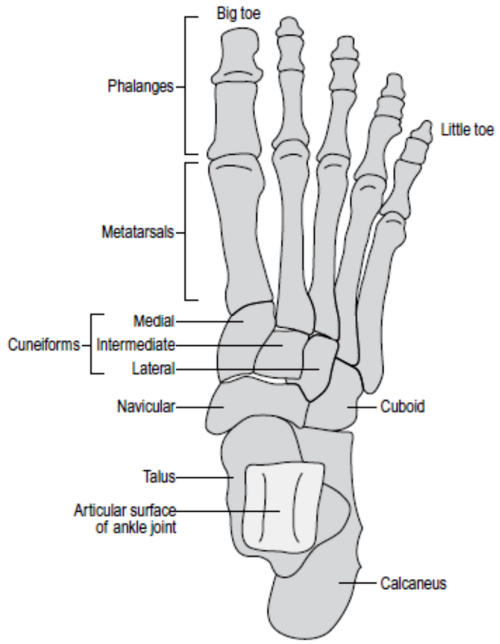

Figure 3.3: Bone of the foot (from above) [14]

The human toes has the natural curve feature that are important parts during walking because these will support the load from body weight and make the walking stable. The researches in the field of clinical have many research papers interested in the force affected to the feet in several situations, for example standing at rest, walking, and running. The results show that the force that affect to bigtoe is more than other toes. On the other hand, the results of researches will be difference when the shape of human foot is changed that may occur from many reasons such as use the improper shoes and the foot be pained by accident. The irregular shape of foot will

affect to the walking process. Other researches focus on the number of toes that are influence during human walking. Hsin-Yi Kathy Cheng et al. [15] presented "the importance of the great toe in balance performance" to evaluate function of the great toe in maintaining human static and dynamic balance. The conclusion of this research shows that the great toe is an important part during human standing and walking. Additionally, this part will make the process stable when human standing by using only one leg and has the effect in the direction control (forward and backward). Consequently, the various types of tiptoe are investigated in robot design and walking process of biped robot.

3.3 Gait Cycle [14][16]

Gait is used to express the human locomotion and the walking method in the medicine. The gait pattern of human is difference from other animals and unique. The gait pattern of human uses two legs working together in different sequence (alternating and rhythmic). Additionally, the body motion will make the center of gravity of body move forward. The walking process has cycle or gait cycle that can be presented as

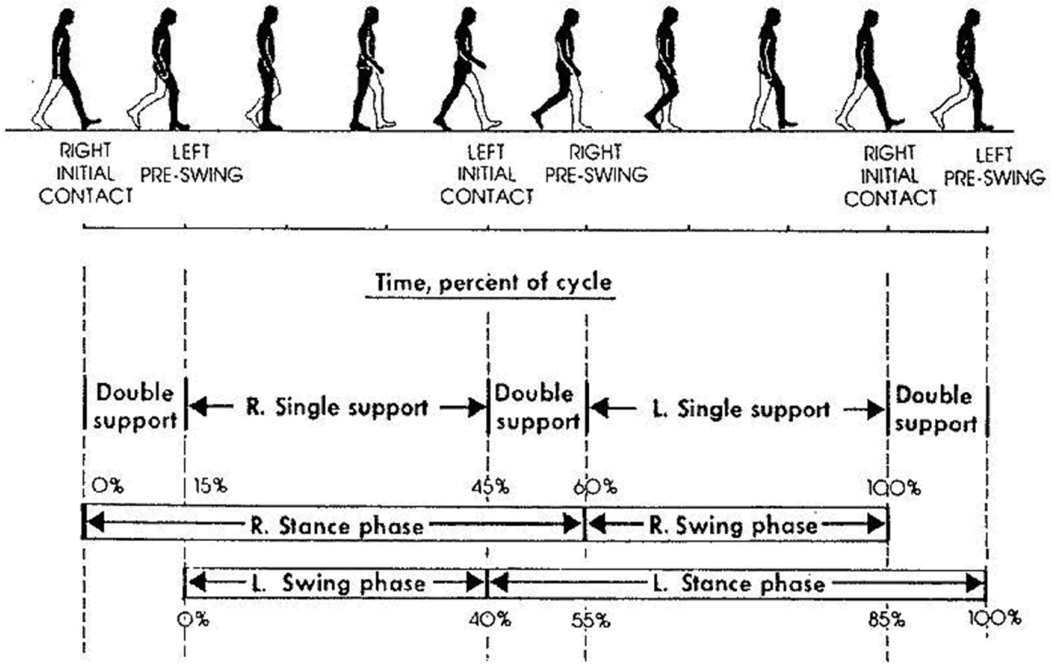

Figure 3.4: The normal gait cycle [36]

Stance Phase: defined as the interval in which the foot is on the ground (60% of the gait cycle). Stance is divided into four phases:

I. "Heel strike" to "Foot flat" is the period that the beginning of the gait cycle is marked by the heel contacting the ground.

II. "Foot flat" through "Midstance" is the period that the forefoot contacts the ground, stabilizing the foot and the body.

III. "Midstance" through "Heel off" is the period when the weight of the body is directly over the foot. The opposite foot is swinging from the rear of the body towards the front of the body.

IV. "Heel off" to "Toe off" is the period when the heel starts to lift from the ground, the weight shifts to the front of the foot. The opposite foot has made contact with the ground. This phase is the terminal stance phase of the gait cycle, which means that the foot is pushing off the ground and will be entering the swing phase (swinging from the rear of the body to the front of the body).

Swing Phase: defined as the interval in which the foot is not in contact with the ground (40% of the gait cycle). Swing is divided into two phases:

V. **"**Acceleration" to "Mid-swing" is the process after pass the stance phase and go to the initial of the swing phase. This phase the toe will separate from the ground and the distance is increased.

VI. "Mid-swing" to "Deceleration" is the process from the swing phase; the toe has maximum distance, and goes to the deceleration phase that is the final process of swing phase. Subsequently, the foot will go down and reach the stance phase of the next cycle.

In Figure 3.5, W. Whittle shows the joint angles (degrees) during a single gait cycle of right leg at hip, knee and ankle. Since, these joint patterns, I will take to compare with our result.

IC = initial contact

OT = opposite toe off

HR = heel rise

OI = opposite initial contact

TO = toe off

FA = feet adjacent

TV = tibia vertical.

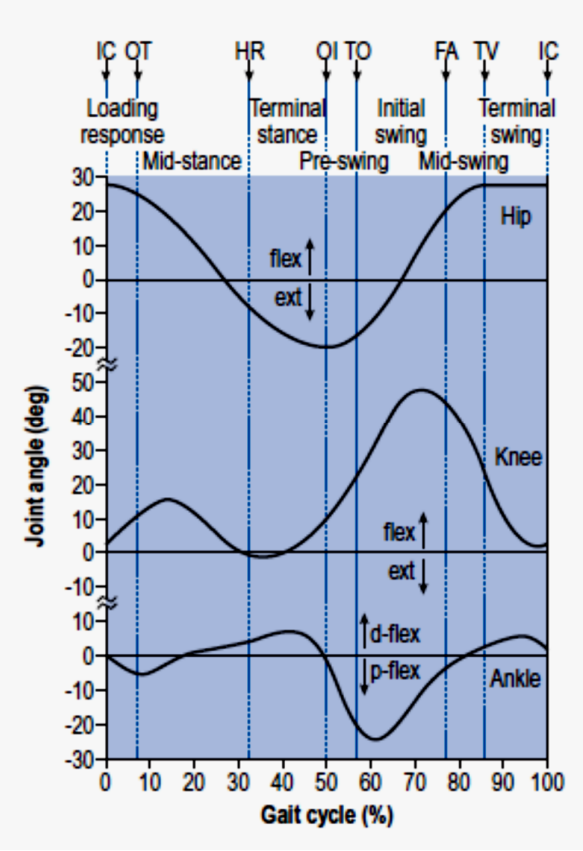

Figure 3.5: The joint angles (degrees) during a single gait cycle [14]

Figure 3.6: CoM trajectory (bold line) in horizontal plane during straight ahead walking. [43]

Michael S. Orendurff et al. [43] presented "the kinematics and kinetics of turning: limb asymmetries associated with walking a circular path". In their research studied about the biomechanics of changing direction while walking. Since, they had shown the CoM trajectory during straight ahead walking compare between CoM trajectories of walking in circular path. Therefore, I used CoM trajectory during straight as shown in Figure 3.6 for referenced in this research. In Figure 3.6, the shape of trajectory like a continue *cosine function*.

3.4 Foot Contact [16]

In this section I discuss about "Foot support pattern". The difference between heel and forefoot that attach to the ground of walking duration can be separated into three parts (three foot-support pattern). The sequence can be arranged as heel, foot flat, and forefoot respectively. The last area of foot flour that reaches the ground is metatarsal. After that the weight of the body will change to another foot. The distance that attaches the ground of each foot is difference. Moreover, the form of forefoot loading depends on foot shape.

- **Heel Support (Calcaneograde):** The stance period normally is initiated by just the heel contacting the floor. Rapidity of this action has led to the term heel strike. This persists for approximately6 to 15% of the gait cycle.
- **Foot Flat Support (Plantigrade):** Forefoot contact terminates the heel only support period and introduces a plantigrade or foot flat

posture. This persists for approximately 20% of the gait cycle. The manner of forefoot contact varies among individuals. Most commonly (71%) the fifth metatarsal head is the first to touch the floor.

- **Forefoot Support (Digigrade):** Heel rise changes the mode of foot support from flat to forefoot. This occurs at the 30% point in the gait cycle and persists until the end of stance. All the metatarsal heads are involved, though the simplified foot switch indicates on1y the metatarsals.

- **Toe tips (Unguligrade):** Toe contact with the floor is quite variable. Scranton identified very early onset, while Barnett found the onset of toe involvement followed isolated forefoot support by 10% of the stance period.

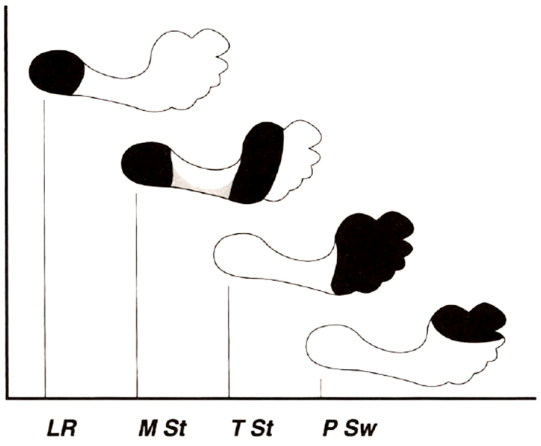

Figure 3.7: Human sequence of foot support areas during stance phase [16]

In Figure 3.7, Perry J. [16] shows the sequence of foot support areas during stance phase. The black area is the position where supports forces areas. Wherewith, LR is heel only in loading response, MSt is foot flat in mid stance, TSt is forefoot and toes in terminal stance, and PSw is medial forefoot in pre-swing.

When the load from body sends to the foot [16], the force will goes through plantar tissues. The force has the stability related to the intensity of the loading force and the area of the foot in contact with the floor.

- Heel pressure shows two patterns. Initial loading occurs on a small posterior lateral area, and body weight is dropped rapidly. All total force, ranging between 70% and 100% of body weight.

- Advancement of body weight onto the center of the heel reduces the pressures to a third (33% of body weight)

- Lateral mid foot contact with the floor is moderately common but of low intensity. The pressure in this area averages 10% of body weight.

- Metatarsal head pressure differs among the individual bones. Generally the highest pressures are registered under the second and third metatarsal heads. Whether the forces are equal or one is slightly greater than the other is highly variable among individuals. Compared to the posterior heel value, the metatarsal head pressures varied between 60% and 100% of body weight.

- Toe pressures differ markedly. The hallux (bigtoe) has the greatest pressure. It ranged between 30% and 55% of that at the heel. The fifth metatarsal head always registered the least pressure within the forefoot.

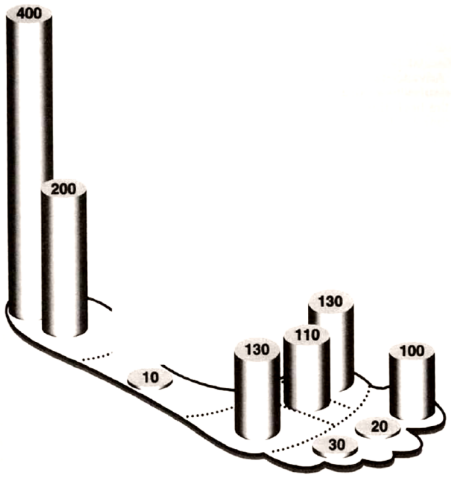

Figure 3.8: Sequence of weight-bearing pressure (KPa) form initial impact at the heel to toe roll off [16]

4

Methodology

4.1 Overview of Robot Models

In this research, I used a small biped robot for creating a model for simulation study of walking robot. Currently, a study in the field of robot is widespread and very popular. Therefore, the product of tool kit set was produced in many types such as humanoid robot, biped robot, robot arm, quadruped robot, and hexapod robot. These robots have been produced to meet human requirements both education and entertainment. The small biped robot used in the simulation responds more rapidly and it is popular. As a result, there is a great demand for these devices in the market, but their cost will be reduced every year. Meanwhile, their capabilities and performance are increased. Consequently, I used the small biped robot for making simple simulation models. The models KHR-2HV and KHR-3HV of KONDO Company were used in this study.

4.1.1 KONDO KHR-2HV[38]

Kondo's KHR-2 is the second version of Kondo's KHR-1 (the first humanoid kit robot in the world). The upgraded robot features more controls,

gears, servos, and software. Besides, more tricks and skills are added. For the design, this robot is designed to have a well-balanced body with bigger chest for a muscular look. With ultra-light weight aluminum alloy frames of the body, Kondo KHR-2HV is faster and lighter for jumping. Adopting 17 adjustable joints, it is capable of doing back flips and cartwheels, and its motions look more human-like.

Size:	340(H) x 180(W) mm
Weight:	1270 gram
Number of servo :	17 Digital servo motors
Digital servo motor:	KRS-788HV, 0.14sec/60deg, 9-12V power

Figure 4.1: KONDO KHR-2HV model [38]

4.1.2 KONDO KHR-3HV [37]

The KHR-3HV is the third generation of humanoid robots developed by KONDO KAGAKU Co. Ltd. This is possibly made by up to 22 degrees of freedom with 17 actual servos and 5 dummy servos. The new micro controller board RCB-4 can control up to 35 serial servos. It is compatible with ICS3.0 (serial) servo protocol and a wide range of options parts. The board also includes several extension ports (10xA/D and 10xPIO) which can be applied to a wide range of sensors and extension options.

Size:	401.05(H) x 194.4(W) mm
Weight:	1500 gram

Number of servo	17 Digital servo motors
Digital servo motor:	KRS-2555HV Servo Specks Maximum Operating Angle 270º Maximum Holding Torque 14kgf.cm (11.1V) Speed 0.14s/60º (11.1V, under no load) Size 41x21x30.55 mm Weight 41.5gram Operating Voltage 9V~12V

Figure 4.2: KONDO KHR-3HV model [37]

4.2 Simulation Based Design Tools

In this section, I will discuss the software which is used in the simulation study. The software that I used is MSC.Visual Nastran Desktop 4D for the first part of the research and ODE (Open Dynamics Engine) for the next part. These programs are dynamic simulation software for analyzing the locomotion and the movement in the gait of the robot.

4.2.1 MSC.Visual Nastran Desktop 4D

MSC.Visual Nastran Desktop 4D is MSC. Software's three-dimensional viewing, authoring, and simulation product line for CAD engineering and marketing environments (Microsoft Windows

operating systems). Each of the Desktop products MSC.Visual Nastran Desktop 4D is designed to suit your engineering design needs, from annotating CAD files and authoring professional presentations to building prototypes and running real world simulations with functional modeling capabilities.

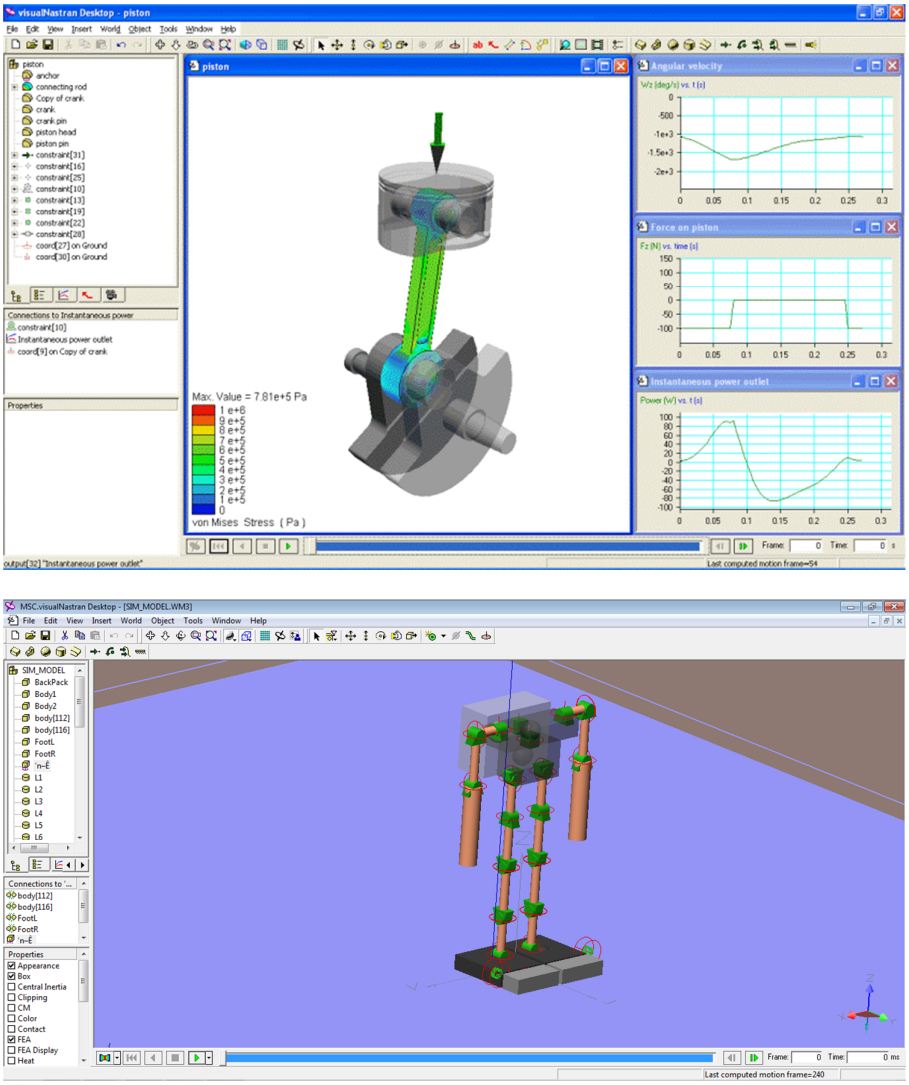

Figure 4.3: The simulations by using MSC.Visual Nastran Desktop 4D [41]

MSC.Visual Nastran Desktop 4D is the ultimate mechanical simulation platform for the integration of motion and stress simulation into a single functional modeling system. It can perform integrated

dynamic motion and stress simulations on your assemblies in one program, without intermediate files or links to third-party programs. Calculated loads are automatically transferred from assembly mates and joints of the model parts for more accurate stress simulation.

4.2.2 Open Dynamics Engine (ODE)

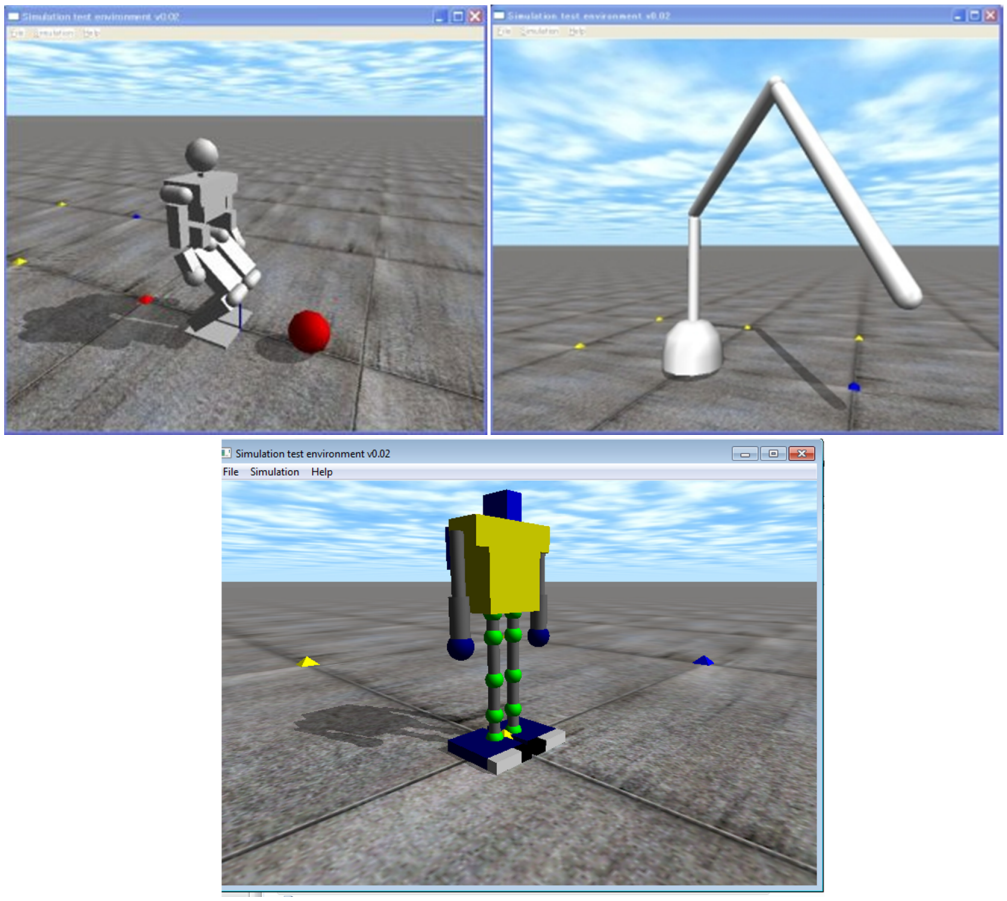

Figure 4.4: The simulations by using the Open Dynamics Engine (ODE) [17]

The Open Dynamics Engine (ODE) [39][40], which has been developed by Russell Smith since 2001, is an open source physics engine written in C/C++. Its two main components are a rigid body dynamics simulation engine and a collision detection engine. It is free licensed software. Due to its scenarios such as mobile robot locomotion and simple grasping, ODE becomes a popular choice for robotics simulation applications. However, ODE has some drawbacks in this field, for

example, the method of approximating friction and poor support for joint-damping, inadequate solver robustness, and friction approximation via linearization.

4.3 Gait Generation Method

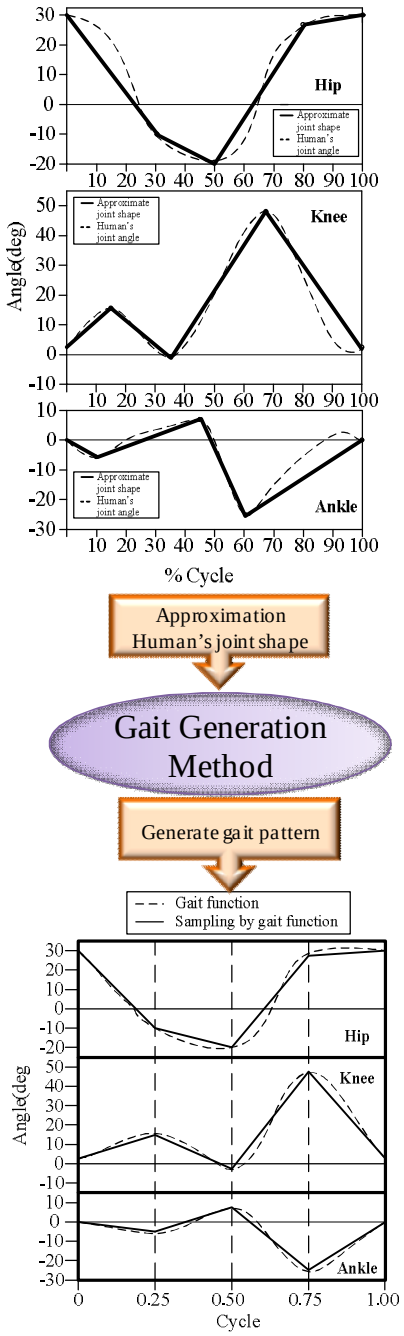

Figure 4.5: Comparison of gait function and human's joint angle pattern [18]

The human walking pattern is caused by a cycle of both legs. A single sequence of limb functions is called a gait cycle. It is essential for the functional unit of gait. The gait cycle has two basic components: the swing phase and the stance phase. This study assumes that the robot's walk is based on the gait function. The principle to create gait function will be presented as follows. Firstly, I estimated that the gait pattern would be based on the human walking cycle. From human's joint angle motion (dot line in Figure 4.5 on the top graph), I approximated the shape at multi-peak point as shown in dot line on the top graph. Secondly, from human's joint angle motion, when I observed the waveform, I can approximate the waveform by using trigonometric function. Therefore, I offered the gait generations function as shown in Eq. 4.1 to generate gait pattern of each joint. Finally, Eq. 4.1 is used by changing these coefficients to generate various waveforms for robot's joints. A sampling time for gait function is a quarter of gait cycle as shown in Figure 4.5 on the bottom graph, and the generated angle data is allocated a joint for position control value.

$$\theta_i(t) = a_i + b_i \cos(\omega t) + c_i \sin(\omega t) + d_i \cos(2\omega t) + e_i \sin(2\omega t) \quad (4.1)$$

Where t is time (sec), ω is angular velocity (rad/sec), i is number of each joint. a, b, c, d and e are coefficients of generating the gait pattern for various waves. In Eq. 4.1, sometime I can eliminate term $e_i \sin(2\omega t)$ because this term has a bit effect on the equation. The gait for biped robot is changed by operating these coefficients.

$$\omega = \frac{2\pi}{t} = \frac{2\pi}{1.2} \quad (4.2)$$

The sampling time of the function to generate the gait pattern is a quarter of gait cycle. The generated angle data is allocated by the joint for position control value. Each joint moves by using a constant velocity between initial point and control point. In this simulation, *one* cycle of walking is limited to

1.2 sec. Thus, angular velocity in Eq. 4.2 is as follows: three cycles of walking time is *3.6 sec* and the total time is *7.0 sec*, then take *3.4 sec* in order to check after walking stability. In this simulation, *one step* takes *0.001 sec*, thus the number of total step is *7000 steps*. In KHR robot, joint is controlled by position control but in this research, I use constant angular velocity because I would like to simplify the calculation in these parameters. It can impact the practical term, however, it may probably have little effect. Because in the simulation, I set angular velocity at *2π per 1.2 sec (5.235 rad/sec*, or *300 deg/sec*) which is sudden speed. One quarter of my simulation takes 0.3 sec, when I consider changing angle to the minimum at 0.1 deg. The angular velocity is at (*0.1 deg / 0.3 sec*.) when it is compared with the constant speed control (*300 deg/sec*). This changing result is difficult to observe its occurrence.

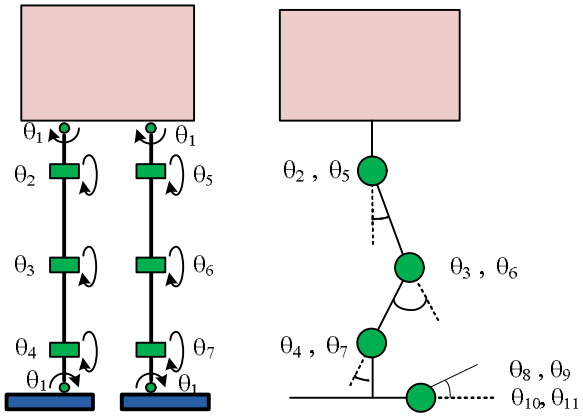

Front side view Right side view

Figure 4.6: The link of model for ODE

The position of the joint is shown in Figure 4.6. In addition, because of the servomotor of the biped robot joint, its joint can rotate *60 degree per 0.14* sec. The rotation directions for each joint are shown in Table 4.1. Knee joints do not rotate to backward direction from standing. Thus, these joints are stricter to rotate to minus. The horizontal surface is applied for the ground surface of the simulation. Moreover, for the ground surface, friction and restitution coefficients are defined as *1.0* and *0.0* respectively. This is the most ideal for no-slip and no deformation.

Table 4.1: Parameter and rotation direction for ODE

Parameter	Leg	Joint	Rotation	Lower limit rotation(deg)	Upper limit rotation(deg)
θ_1	Both	Hip and Ankle	SS	-15	15
θ_2	Right	Hip	BF	-60	60
θ_3	Right	Knee	BF	0	60
θ_4	Right	Ankle	BF	-30	30
θ_5	Left	Hip	BF	-60	60
θ_6	Left	Knee	BF	0	60
θ_7	Left	Ankle	BF	-30	30
θ_8	Right	Bigtoe	BF	-30	0
θ_9	Right	Tiptoe	BF	-30	0
θ_{10}	Left	Bigtoe	BF	-30	0
θ_{11}	Left	Tiptoe	BF	-30	0

Note SS - Side to Side
BF - Backward and Forward

4.4 Design of Simulation Experiments

This research will analyze the trajectory simulation which is typically considered at the Center of Mass (CoM). The result can be calculated from:

$$x_{CoM} = \frac{\sum_{j=1}^{N} m_j x_j}{M} \tag{4.3}$$

$$y_{CoM} = \frac{\sum_{j=1}^{N} m_j y_j}{M} \tag{4.4}$$

$$z_{CoM} = \frac{\sum_{j=1}^{N} m_j z_j}{M} \tag{4.5}$$

where;

$$M = \sum_{j=1}^{N} m_j \tag{4.6}$$

where *j* is a part number of robot simulation parts, m_j is a mass of each part, (x_j,y_j,z_j) is a position of each part, M is a total mass of simulation robot and $(x_{CoM}, y_{CoM}, z_{CoM})$ is a position of simulation robot.

This procedure used ODE (Open Dynamics Engine) [39][40] in windows platform for simulation. The ODE is a physical engine in C/C++. Its two main components are a rigid body dynamics simulation engine and a collision detection engine. It has advanced joint types and integrated collision detection with friction.

In order to set spring and damper which are important components of the toe mechanism for ODE, I introduced Error Reduction Parameter (ERP) and Constraint Force Mixing (CFM). ERP is a parameter which corrects joint error. The simulation will be repeated and the joint error increases due to various internal approximations. ERP can fix the error. Firstly, the value must be set between 0 and 1. Zero does not fix the error and one fixes the error by the next step. Next, to set the constraints, ODE uses CFM parameters. There are two types of constraints: hard constraint and soft constraint. Hard constraint is the constraint which must be obeyed. Meanwhile, soft constraint is the constraint which is not so hard. Some violations can be permitted. If I set CFM at 0, the hard constraint which is applied the greater value of CFM will be more soft constraint. I can simulate a spring and damper system by using ERP and CFM as follows:

$$ERP = \frac{hk_p}{hk_p+k_d} \tag{4.7}$$

$$CFM = \frac{1}{hk_p+k_d} \tag{4.8}$$

Where *h (second)* is the step size, k_p *(N/m)* is a spring constant and k_d (N/ms) is a damping constant. In order to simulate, I defined *h= 0.001 seconds*, k_p*= 0.033 N/mm* and k_d*=0 (N/ms*) (because I design toe joints as hinge-spring) as a result I often set *CFM = 30.*

There are three periods in the simulation design: starting, gait generation, and standing period. Firstly, the time of starting period is from *0* to *0.3 sec*. In this period, the robot model pauses for preparing to the next step. The system parameters as shown in Table 4.1 are setting. Secondly, gait

generation period (*0.3 < t < 3.2 sec*), the gait cycle works for driving each joint of robot model. Finally, the standing period (*3.2 ≤t ≤3.6 sec*), the model will prepare to stop and stay in the standing posture. Then the parameters in Table 4.2 are implemented.

$$\theta_i = [a_i, b_i, c_i, d_i]; \qquad (i = 1, 2,3,4,5,6,7) \qquad (4.9)$$

$$\theta_{\text{all}} = [\theta_1, \theta_2, \theta_3, \theta_4,\theta_5, \theta_6, \theta_7]$$

The gait generation method is the process used for designing the variable vectors (waveform). They are generated from gait function as shown in Eq. 4.1 by eliminating the term $e_i\, sin(2\omega t)$ because this term has less effect on the equation. This process is not applied to the part of big toe and tiptoe because from these parts, I determined the passive toe mechanism and the design coefficient of variable vectors as shown in Eq. 4.9. Also, this model has 28 degrees of freedom.

Table 4.2: Starting and Standing period times setting

Joint	Starting Period		Standing Period	
	t = 0 sec	t = 0.3 sec	t = 3.2 sec	t = 3.6 sec
θ_1	0	0.3	-1.5	0
θ_2	0	-30	-15	0
θ_3	0	60	15	0
θ_4	0	30	5	0
θ_5	0	20	-15	0
θ_6	0	0	15	0
θ_7	0	-15	-15	0

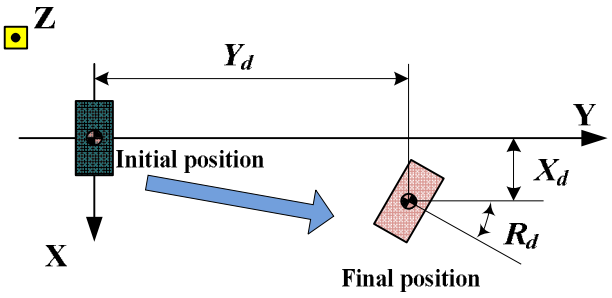

Figure 4.7: Overview of the simulation at final position

$$-30 \leq X_d \leq 30 \quad (mm) \quad if \quad t = 7.0\ (sec) \tag{4.10}$$

$$-10.0 \leq R_d \leq 10.0\ (deg) \quad if \quad t = 7.0\ (\text{sec}) \tag{4.11}$$

$$Y_d \leq 200 \quad (mm) \quad if \quad t = 7.0\ (\text{sec}) \tag{4.12}$$

I define the following conditions for verification and setting the criteria to move the simulation model forward and go straight on the path until the end of the simulation as shown in Eq. 4.10 and Eq. 4.11. When X_d is the distance at the side under $\pm 30\ mm$ in Eq. 4.10 and in Eq. 4.11. R_d is the angle to the rotation direction under $\pm 10\ (deg)$ and distance Y_d does not exceed $200\ mm$ to prevent the slip. When X_d, Y_d and R_d are denoting the distance and rotation of model's CoM at final position as shown in Figure 4.7.

5

Design of Robot's Foot

In this chapter, I will discuss a design of robot's foot. The design will be explained in the following experiments.

- Experiment I: Robot's foot with toe mechanism
- Experiment II: Robot's foot with different types of toe mechanism
- Experiment III: Robot's foot with big toe sizing mechanism

5.1 Experiment I: Robot's Foot with Toe Mechanism

This experiment is the first step to study a small biped robot's walking behaviors. I design and create a robot model by consisting of toes component based on KHR-2HV model, then simulate on flat ground (FG) and rough ground (RG). I simulated robot model by using MSC.Visual Nastran Desktop 4D robot model. The simulation model is shown in Figure 5.1 and Figure 5.2. It can move by servo motors from hip downward. The simulation model has 10 servo motors and same DOF on these joints. Adaptive Plan system with Genetic Algorithm (APGA) has been implemented to gait pattern optimization. In this section, I also describe the methodology for

determining the conditions and optimization because the different software are used.

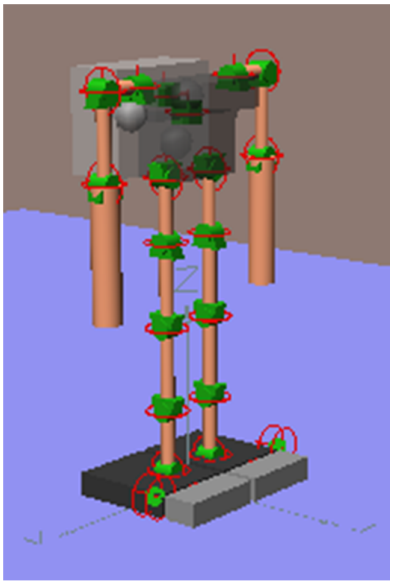

Figure 5.1: The simulation model is made from MSC. Visual Nastran Desktop 4D on flat grounds (FG)

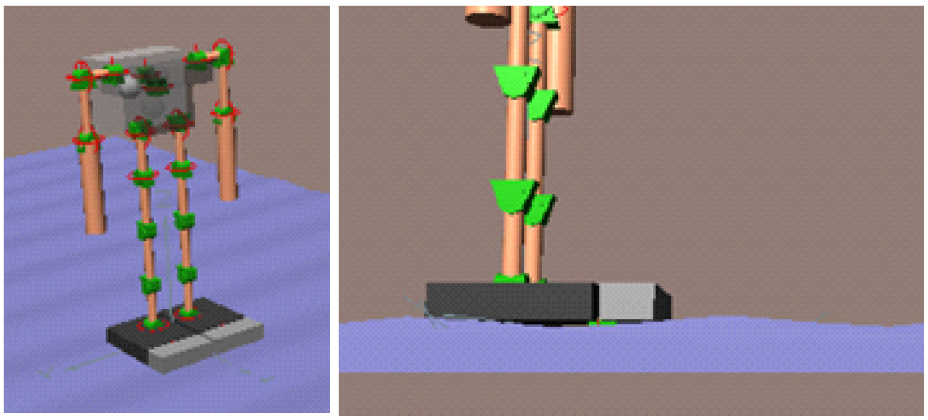

Figure 5.2: The simulation model is made from MSC.Visual Nastran Desktop 4D on rough grounds (RG)

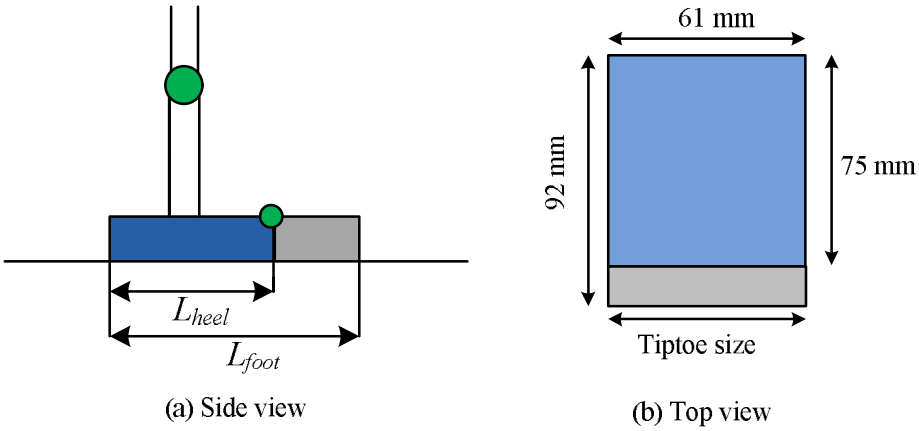

Figure 5.3: Model of robot's foot

The robot's foot is designed in this experiment. I have designed toe component for robot's foot. I defined toe component as "tiptoe". A model of robot's foot is shown in Figure. 5.3. A parameter L_{foot} is a length of foot limited *to 92 mm* and L_{foot} is a length of heel limited to *75 mm*. The foot-heel length ratio which is obtained from Eq. 5.1 is *1.227*. The range of ratio has the value from *1.196 to 1.426* [19].

$$L_{foot-heel} = \frac{L_{foot}}{L_{heel}} \tag{5.1}$$

5.1.1. Methodology for Simulation by Using MSC.Visual Nastran Desktop 4D

5.1.1.1. Adaptation to Simulation

Gait pattern created by gait function is shown in Eq. 4.1. However, the time steps and the environment values are different. In this simulation, one cycle of walking is limited to *1.2 sec*. *Three cycles* of walking time is *3.6 sec* and the *total time* is *4.8 sec*, then take *1.2 seconds* in order to check after walking stability. In this simulation, *one* step takes *0.2 sec*, thus the number of total step is *240 steps*. Moreover, for the ground surface, *Friction* and *Restitution*

coefficients are limited to *0.3* and *0.0* respectively. Gait Functions of model are defined as follows:

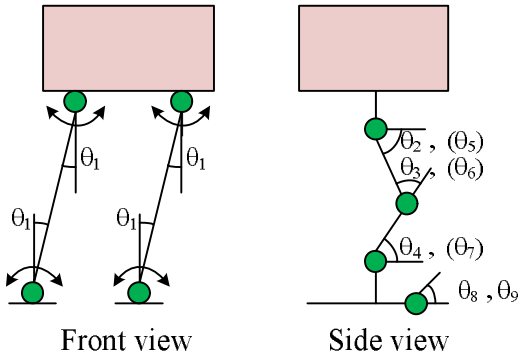

Figure 5.4: The links of robot's model for MSC.Visual Nastran Desktop 4D

$$\theta_1 = \begin{cases} 0 & if\, t = 0 \ or\ t > 3.3 \\ \theta_1(t) if & 0 < t \leq 3.3 \end{cases}, \tag{5.2}$$

$$\theta_2 = \begin{cases} 0 & if\ t = 0 \ or\ t > 3.3 \\ -20 & if\ t = 0.3 \\ 30 & if\ t = 3.3 \\ \theta_2\,(t) & if\ t = 0 \ < t < 3.3 \end{cases}, \tag{5.3}$$

$$\theta_3 = \begin{cases} 0 & if\ t = 0 \ or\ t > 3.3 \\ 0 & if\ t = 0.3 \\ 60 & if\ t = 3.3 \\ \theta_3\,(t) & if\ t = 0 \ < t < 3.3 \end{cases}, \tag{5.4}$$

$$\theta_4 = \begin{cases} 0 & if\ t = 0 \ or\ t > 3.3 \\ 20 & if\ t = 0.3 \\ 30 & if\ t = 3.3 \\ \theta_4\,(t) & if\ t = 0 \ < t < 3.3 \end{cases}, \tag{5.5}$$

$$\theta_5 = \begin{cases} 0 & if\ t = 0 \ or\ t > 3.3 \\ 30 & if\ t = 0.3 \\ -20 & if\ t = 3.3 \\ \theta_2\,(t + 0.6) & if\ t = 0 \ < t < 3.3 \end{cases}, \tag{5.6}$$

$$\theta_6 = \begin{cases} 0 & if\ t = 0\ or\ t > 3.3 \\ 60 & if\ t = 0.3 \\ 0 & if\ t = 3.3 \\ \theta_3\,(t + 0.6) & if\ t = 0 < t < 3.3 \end{cases}, \quad (5.7)$$

$$\theta_7 = \begin{cases} 0 & if\ t = 0\ or\ t > 3.3 \\ 30 & if\ t = 0.3 \\ 20 & if\ t = 3.3 \\ \theta_4\,(t + 0.6) & if\ t = 0 < t < 3.3 \end{cases}, \quad (5.8)$$

$$\theta_8 = \begin{cases} 0 & if\ t = 0 \\ 0 < \theta_8 < 30 & if\ 0 < t \end{cases}, \quad (5.9)$$

$$\theta_9 = \begin{cases} 0 & if\ t = 0 \\ 0 < \theta_9 < 30 & if\ 0 < t \end{cases}, \quad (5.10)$$

5.1.1.2. Formulation of the Optimization

APGA is used to perform optimization process. The objective function is obtained from the RSM as shown on the flow chart in Figure 5.5. In addition, penalty function and constraints are determined. In this optimization process, the appropriate coefficients are obtained for gait function in order to get the angle of the each joint. There are 20 variables which are coefficients of this experiment for control all joints. For the design variable vectors, an objective function, a penalty function and constraints are defined as shown in Eq. 5.11 to Eq. 5.17.

Design variable vector (DVs):

$$\theta_i = [a_i, b_i, c_i, d_i, e_i]; \qquad (i = 1,2,3,4) \quad (5.11)$$

$$\theta_i = [a_i, b_i, c_i, d_i, e_i];$$

Objective function:

$$F = -Y_d + \gamma P \rightarrow Min. \quad (5.12)$$

Penalty function:

$$P = \sum_{j=1}^{3} max(g_j, 0) + h_1 \quad (5.13)$$

Constraint functions:

$$g_1 = \begin{cases} 30.0 - X_d \leq 0 & if \quad X_d > 0 \\ 30.0 + X_d \leq 0 & Otherwise \end{cases}, \quad (5.14)$$

$$g_2 = \begin{cases} 5.0 - R_d \leq 0 & if \quad R_d > 0 \\ 5.0 + R_d \leq 0 & Otherwise \end{cases}, \quad (5.15)$$

$$g_3 = 200.0 - Z_h \leq 0 \quad (5.16)$$

$$h_1 = 240.0 - N_s \quad (5.17)$$

The objective function is minimized. In Eq. 5.12, Y_d denotes the distance between centers of the biped robot model as shown in Figure. 4.6. The penalty coefficient is the value of γ that is equal to *1.0*. The penalty function includes four constraint functions. In Eq. 5.14, g_1 and X_d are the distances at the side under *±30 mm.* In Eq. 5.15, g_2 and R_d are the angles to the direction under *±5 degree*. In Eq. 5.16, g_3 and Z_h are the heights from the ground to the hip. The distance is over *200 mm* in order to check the slip at the end of the simulation. In Eq. 5.17, N_s is the number of steps should be *240* to indicate the success of the simulation. Approximated optimization process shown in Figure 5.5 is as the following steps.

I. Initial design is initialized by specifying the simple analysis.

II. For making a response surface model (RSM), θ_{all} to generate the angle of each joint is defined. Moreover, random sampling is performed to get the results of simulation.

III. Then, random sampling is simulated to obtain the results for making the RSM.

IV. Using APGA for optimization, the design variables are optimized by APGA based on RSM.

V. The design variables from APGA in step IV are used for verifying the result by simulation.

VI. Verification process is conducted to check the convergence of the solutions. If the convergence is achieved, the optimal design will be stopped. Otherwise, the repetition of this process from step III will be carried out.

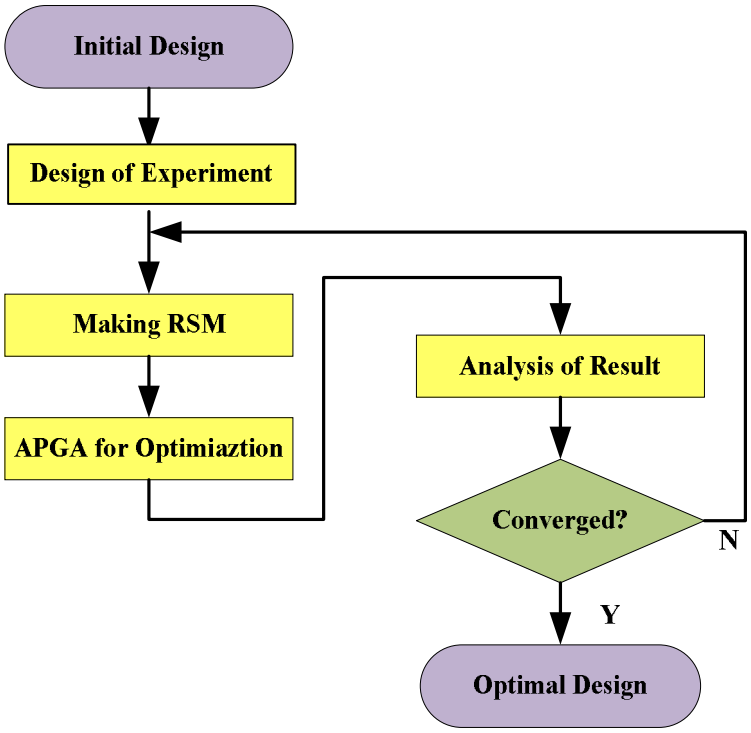

Figure 5.5: Approximated optimization process

5.1.2. Response Surface Model (RSM) [21]

In the optimization process of gait pattern for the robot, the system used a lot of calculation times. A large portion of this time cost can use RSM by approximating more cost analysis. Therefore, various

optimization problems with this cost are applied by this method. In the experiment, I used Response Surface Model (RSM) of 3rd orders (Cubic polynomial) for approximating response of an actual analysis code. A number of exact analyses using the simulation code(s) have to be performed initially to construct a model with a set of analyzed design point that can be used. The 3rd order (Cubic) model is represented by a polynomial as follows:

$$\tilde{F}(x) = a_0 + \sum_{i=1}^{N} b_i x_i + \sum_{i=1}^{N} c_{ii} x_{\mathrm{i}}^2 + \sum_{ij(i<j)} c_{ij} x_i x_j + \sum_{i=1}^{N} d_i x_{\mathrm{i}}^3 \quad (5.18)$$

N is number of model inputs or number of variable

X_i is the set of model inputs

a, b, c, d are the polynomial coefficients

The number of sampling for initialization equals the number of polynomial coefficients which is for a cubic polynomial as follows:

$$\frac{(N+1)(N+2)}{2} + N \quad (5.19)$$

The number of sampling is calculated using the equation Eq. 5.19 and $N = 20$ (number of design variables), and obtains *215* of data for the calculation of all polynomial coefficients. *251* samples, which are obtained from the simulation results of robot, can walk forward and do not fall down by using Eq. 4.1. The random process of 20 design variables for creating RSMs uses the method of uniform random variables and upper/lower bounds of each variable are predefined. The process of uniform random variables is the uniform distribution process in which random variables with probability density function obtain from the pre-specified boundary of each variable, for example, it is set to be equal to 1/(upper bound-lower bound). The values of lower and upper bounds related to predefined bounds of joint angle rotational limit. In this case, three RSMs are created for application in

optimization process. There are three RSMs that are defined in the process: RSM of go straight distance (RSM - Y_d), RSM of side distance (RSM - X_d) and RSM of rotation (RSM - R_d). All three RSMs are shown in Appendix A.

5.1.3. Adaptive Plan System with Genetic Algorithm (APGA) [20]

This section describes optimization method to generate suitable gait pattern. In this process, Eq.5.19 from RSM is used in order to set objective function. Therefore, I will discuss simple APGA.

APGA has been proposed to solve the multi-peak optimization problems with multi dimensions by H. Hasegawa [20]. The proposed algorithm is a stochastic global search heuristics in which EAs based approaches are combined with local search method. APGA uses the Adaptive Plan (AP) in order to control its optimization process for the local search process. APGA differs in handing design variable vectors (DVs) from genetic algorithm (GA) encode DVs into genes, and handle them through GA operator. However, APGA encodes control variable vectors (CVs) of AP, which searches to local minima, into its genes. CVs decide on global behavior of AP, and DVs are handled by AP in the optimization process of APGA. APGA has been confirmed to improve the calculation cost and the stability of convergence towards the optimal solution.

5.1.3.1. Formulation of the Simple APGA

APGA is developed to overcome the difficulty in controlling switching, choosing and steering a combination of global and local search method. On the other hand, natural and artificial system adapt the behavior of themselves to the changing global and social environments over generations. These systems have been defined as an Adaptive System (AS) and AS has an adaptive plan (AP) which decides on its behavior through response to environment (ENV).

APGA is introduced its concept to new evolution algorithm (EA) strategy for multi-peak optimization problems. Hence, this study considers a global search method as AS, a local search

method as AP and an optimization space of DVs as ENV respectively. The conceptual strategy of APGA is shown in Figure 5.6. APGA differs in handing DVs from general EAs based on GAs to overcome these difficult problems. EAs generally encode DVs into genes of chromosome, and them through GA operator. However, APGA separates DVs of global search and local search methods completely. It encodes control variable vector (CVs) of AP, which searches to local minima into its genes on AS. CVs decide on a global behavior of AP, and DVs are handled by AP in the optimization process of APGA. The generation process of DVs is shown in Figure 5.7. This process generates a new DVs X_{t+1} from current search point X_t according to the following formula:

$$X_{t+1} = X_t + AP(C_t, R_t) \tag{5.20}$$

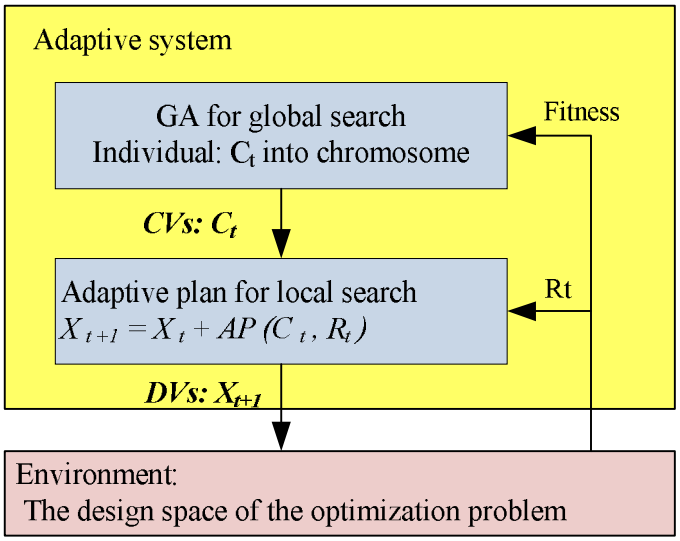

Figure 5.6: Conceptual strategy of APGA

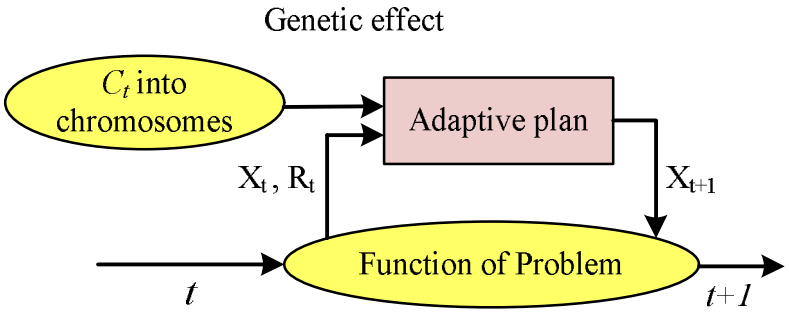

Figure 5.7: Generation process of DVs

Where AP, C, R and t denote a function of AP, CVs, response value (RVs) and generation respectively. AS is controlled by the behavior of AP via feedback on loop of fitness value f, or by a function of problem (ENV) during the global search process. Moreover, C can be renewed by estimating f by suing the GA operators within this process, and their trends are believed to make optimal behaviors like a cooling temperature of Simulate Annealing (SA).

5.1.3.2. Adaptive Plan (AP) : Sensitivity Plan (SP)

In this study, the plan introduces a *DV* generation formula using a sensitivity analysis, which is effective in the convex function problem as a heuristic rule, because a multi-peak problem is combined of convex functions. This plan uses the following equation.

$$AP(C_t, R_t) = -Scale \cdot SP \cdot sign(\nabla R_t) \quad (5.21)$$

$$SP = 2C_t - 1, \; 0.0 \le c_{i,j} \le 1.0, \quad (5.22)$$

Where scale and ∇R are denoted the scale factor and sensitivity of the *RVs*, respectively. A step size *SP* is defined by *CVs* for controlling a global behavior to prevent it from falling into the local optimum. $C = [c_{i,j}, \ldots, c_{i,p}]$ is used by Eq. (5.22) so that it can change the direction to improve or worsen the objective function, and C is encoded into a chromosome. In

addition, i, j, and p are the individual number, design variable number, and its size.

5.1.3.3. Ingenuities for DVs and CVs

- **Handing of significant figures**

In the optimal design of the product design, a dimension of products can be mainly dealt with as DVs. These are always assigned dimensional accuracies on a mechanical drawing. Therefore, a value of DVs is done well to use a number of significant figures of assigned dimensional accuracy in its drawing in the optimal process. In APGA, a number of significant figures of DVs are defined, and DVs truncated to it within optimal process.

- **Handling of DVs's out of range**

DVs are renewed by AP, and when their values exceed the range of them, returns by Eq. (5.23) into the range of them.

$$\left.\begin{array}{llll} if & X_t < X^{LB} & then & X_i = X^{LB} \\ if & X_t < X^{UB} & then & X_i = X^{UB} \end{array}\right\} \quad (5.23)$$

- **Coding into chromosome for CVs**

This ten bit string with two values 0 and 1 represents a real value of CVs by using procedure of Figure 5.8. In addition, Figure 5.8 has shown DVs and CVs of two dimensional cases.

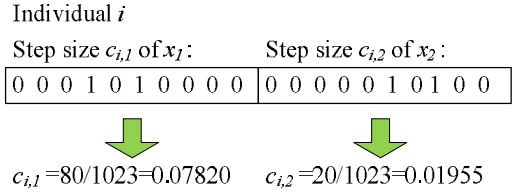

Figure 5.8: Encoding into genes

5.1.3.4. GA Operators

- **Selection**

Selection is performed using tournament strategy to keep a diverseness of individuals at early generations. The tournament size of two is used.

- **Elite strategy**

An elite strategy, where the best individual survives in the next generation, is adopted during each generation process. It is necessary to assume that the best individual, i.e., as for the elite individual, generates two global behaviors of AP by updating DVs with AP, not GA. Therefore, its strategy replicates the best individual to two elite individuals, and keeps them to the next generation. As shown in Figure. 5.9, DVs of one of them (▲ Symbol) is renewed by AP, and its CVs which are coded into chromosome are not changed by GA operators. Another one (• Symbol) means that both DVs and CVs are not renewed, and are kept to next generation as an elite individual at the same search point.

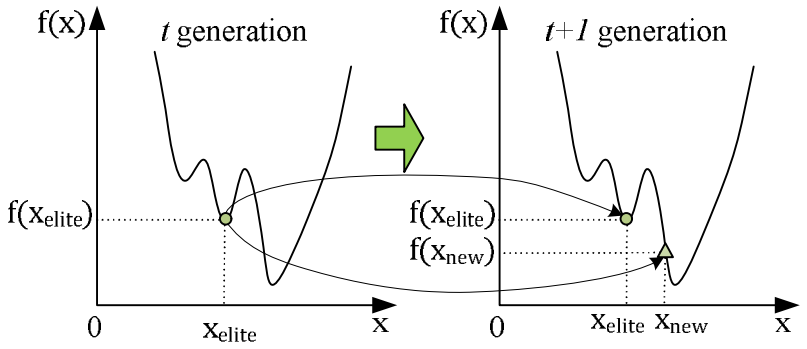

Figure 5.9: Elite Strategy

- **Crossover and mutation**

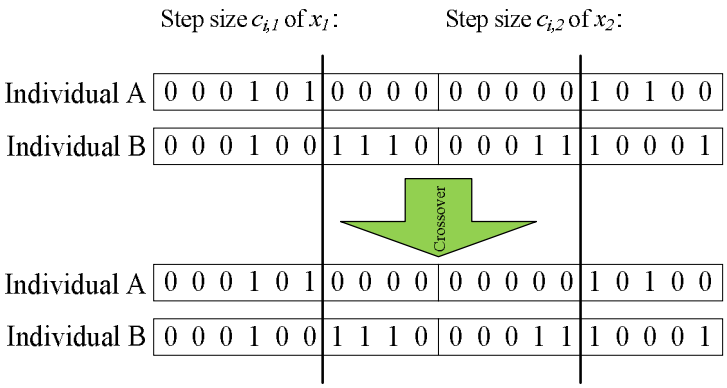

Figure 5.10: Example of crossover

In order to pick up the values of each CV, a single point crossover is used for string of each CV. This can be considered to be a uniform crossover for the string of chromosome as show in Figure. 5.10. The mutation is adapted for string of each CV, and its method reverses the one bit in its string.

- **Recombination of gene**

As following conditions, the genetic information on chromosome of individual is recombined by a uniform random function.

- One fitness value occupies 80% of the fitness of all individuals.
- One chromosome occupies 80% of the population.

If this manipulation is applied for general GAs, improved chromosome which DVs have been encoded into is broken down. However, in APGA, genetic information is only CVs to make a decision of a decision of a behavior of AP. Therefore, to prevent from falling into a local optima,

and to get out from the condition converged with a local optimal search process can recalculate by recombination gene of CVs into chromosome. This strategy is believed to make behavior like a reannealing of SA.

For the gait equation in Eq. 4.1 is used for optimization by using APGA. When I try to find the optimal value of gait, this experiment is same scenario as the first experiment, which is very difficult and consumes a lot of time to collect the samples. For example, from the first experiment, making RSM need 251 samples from 20 variables (Eq. 5.19). In addition, from the second experiment, numbers of variables were increased to 28, so we need 463 samples for experiment. From this reason, creating RSM is more difficult. Therefore, I used the optimization by APGA only in the first experiment.

5.2 Experiment II: Robot's Foot with Different Types of Toe Mechanism

In this experiment, I have designed different types of toe mechanism. Since I have presented four models, the simulation models have been created by using ODE based on KHR-3HV robot model. The foot designs are based on human foot structure and support areas during normal human walking (Figure 3.3 and 3.7), as I have discussed in chapter three. In addition, the toe's stature is designed based on foot supporting research [22] by using the Novel Win Mask software program. Schematic representation of the plantar surface area is shown in Figure 5.11.

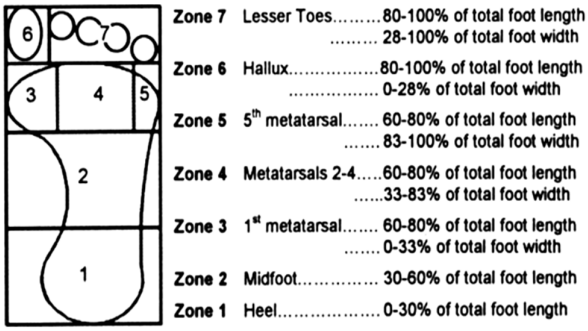

Figure 5.11: Schematic representation of the seven plantar surface areas [22]

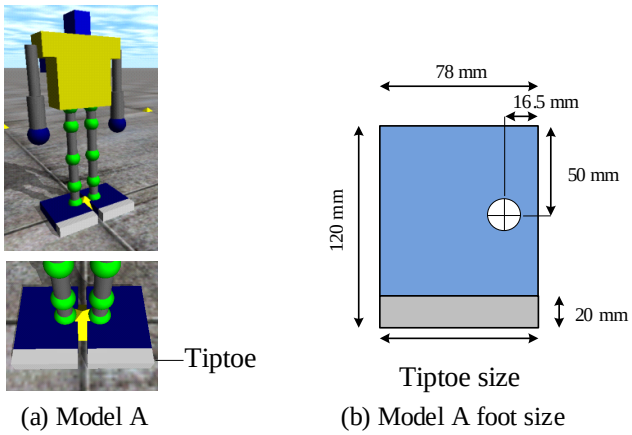

(a) Model A (b) Model A foot size

Figure 5.12: Model A, The simulation model with tiptoe

The foot of model A has the same design as robot model of the first experiment but different sizes because the base model has changed model. The simulation model A is shown in Figure 5.13(a) and the foot size is shown in Figure 5.13(b). The foot size of model A is 78(width) x 100(length) x 20(height) mm. This tiptoe is designed from a combination of zone 6 (hallux) and zone 7 (lesser toes) from Figure 5.11, which other research has also presented this type of toe. The tiptoe size of model A is 78(width) x 20(length) x 20(height) mm. For the tiptoe length, it is equal to maximum length (20 percent of foot length).

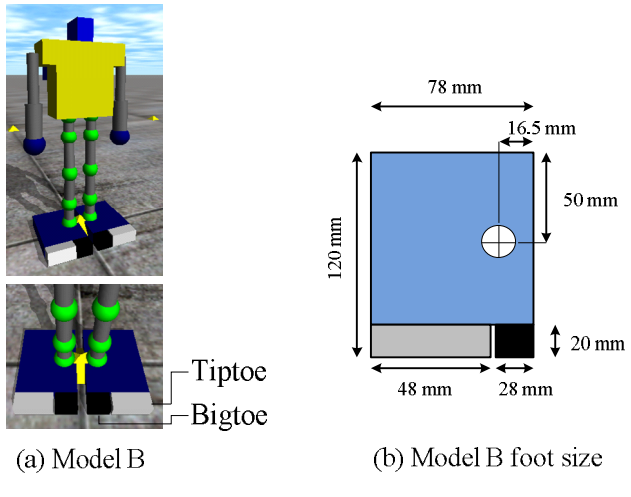

(a) Model B (b) Model B foot size

Figure 5.13: Model B, The simulation model with big toe and tiptoe

The foot of model B has been designed by composing of big toe and tiptoe. The simulation model B is shown in Figure 5.13(a) and the foot size is shown in Figure 5.13(b). Since the big toe is designed like a hallux (zone 6) and the tiptoe is designed like a lesser toes (zone 7), the big toe size of model B is 28(width) x 20(length) x 20(height) mm and the tiptoe size of model B is 48(width) x 20(length) x 20(height) mm. However, at first I take into consideration the model foot size which is relatively small size. Although, the tiptoe width size of model B is equal to 36 percent of foot width which it over maximum width of zone 6. Therefore, I set the big toe width to be equal to 28 mm for this experiment.

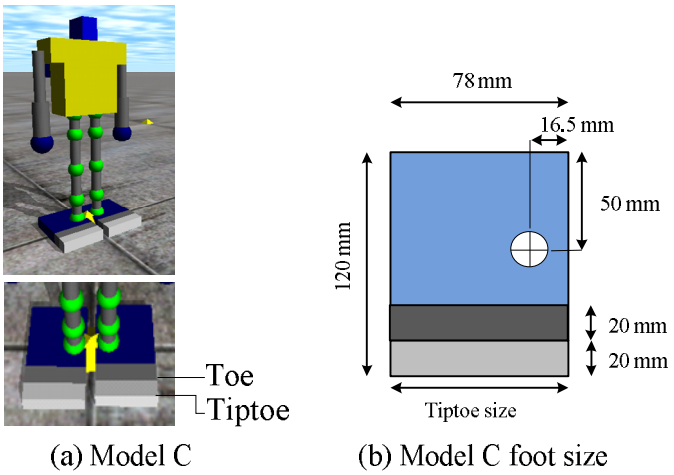

(a) Model C (b) Model C foot size

Figure 5.14: Model C, The simulation model with toe and tiptoe

The foot of model C has been designed by composing of toe and tiptoe. The simulation model C is shown in Figure 5.14(a) and the foot size is shown in Figure 5.14(b). The tiptoe has the same size as model A. The toe size of model C is 78 (width) x 20 (length) x 20 (height) mm. since the toe is designed from a combination of zone 3, zone 4 and zone 5 as in Figure 5.11.

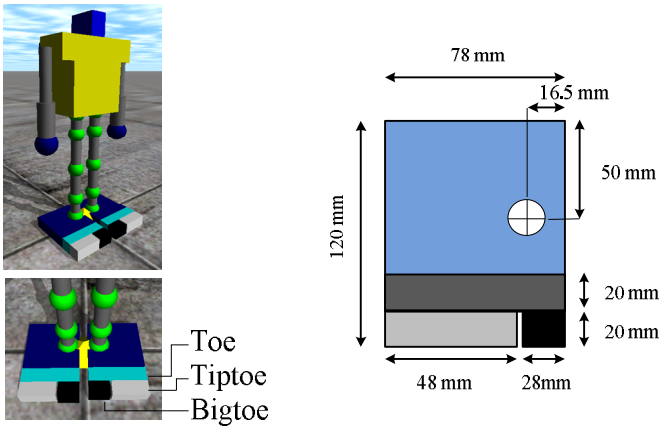

(a) Model D (b) Model D foot size

Figure 5.15: Model D, The simulation model with big toe, tiptoe and toe

The foot of model D has been designed by composing of big toe, tiptoe and toe. This model is the most complex model when it is compared to previous models. The simulation model D is shown in Figure 5.15(a) and the

foot size is shown in Figure 5.15(b). The big toe and tiptoe have the same size as model C. In addition, the toe has the same size as model B.

5.3 Experiment III: Robot's Foot With Big toe sizing Mechanism

The design of robot's tiptoe uses reference structure from the second experiment because model B has shown the best result in our specified condition (the detail of this experiment will be presented in next chapter). The design structure of robot's feet in model B composes of big toe and tiptoe. The study of big toe is not widely, therefore, I will focus on the robot model with this component. The optimal size of big toe is considered in this experiment and is applied in the experimental robot model. Moreover, the robot model must be walking in accordance with our specified conditions.

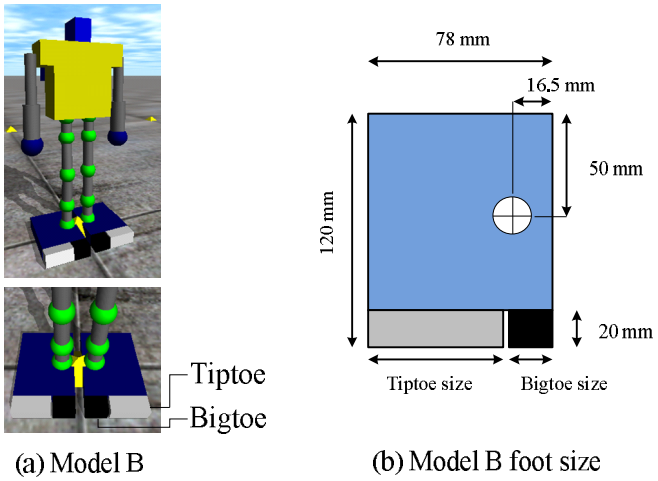

(a) Model B (b) Model B foot size

Figure 5.16: Model B, The simulation model with big toe and tiptoe, for bigtoe sizing

In this experiment, there are ten robot models having different foot sizes. The models in this simulation have the different big toe and tiptoe sizes. The details are shown in Table 5.1. The maximum big toe size must be less than or equal to a half of foot width because I refer to normal size of big

toe. On the other hand, the minimum big toe size is considered from the support area of foot components that will be used to install a device. Therefore, I set the minimum value of big toe size at 20 mm.

For joints of the heel and toe, I design by using torsion spring. I applied torsion spring in form of a hinge joint that is spring hinge. A torsion spring is a spring that works by torsion or twisting, in the direction perpendicular to the spring axis. The spring constant (K_p) is multiplied by the angular displacement of the hinge. For the simulation, I have to set the constant value. Therefore, I set K_p to be equal to 0.033 and 0.037 N/deg. This value is selected from a range of test spring hinge, by bending test of the three values as shown in Table 5.2. According to the size that I have designed, a size of spring testing is 10x20 mm. Moreover, the K_p values are slightly different because I want to check the trend of the results, when I changed the value of the spring constant in the range of about 10%.

Table 5.1: The robot foot size of model B1-B10

Model	Bigtoe size (mm)	Tiptoe size (mm)	Ratio (Bigtoe width\Foot width)
B1	20	56	0.26
B2	22	54	0.28
B3	24	52	0.31
B4	26	50	0.33
B5	28	48	0.36
B6	30	46	0.38
B7	32	44	0.41
B8	34	42	0.44
B9	36	40	0.46
B10	38	38	0.49

Table 5.2: The spring constant (K_p)

N =15	Degrees of bending(deg)		
	10	20	30
Average (N/deg)	0.046	0.029	0.019
SD	0.0072	0.0035	0.0026

6

Experimental Results

In this chapter, I will present the walking simulation results of robot with toe mechanism. In order to achieve the research aim at studying big toe size, I have divided the results into three experiments. I will discuss the results of the experiment I, II, and III respectively.

- The result of Experiment I: Robot's foot with toe mechanism
- The result of Experiment II: Robot's foot with different types of toe mechanism
- The result of Experiment III: Robot's foot with big toe sizing mechanism

I considered the robot gait pattern comparing with human gait pattern, such as trajectory of CoM and joint angle pattern (waveform) etc. The aims of robot walking were to obtain a long distance and go straight within conditions. The results were as follows.

6.1 The Result of Experiment I: Robot's Foot with Toe Mechanism

6.1.1 The Result of Experiment I

The robot models with passive tiptoe (as shown in Figure 5.1 and Figure 5.2) were used in this simulation. The model in Figure 5.1 was called simulation model on flat ground (FG), and the model in Figure 5.2 was called simulation model on rough ground (RD). The FG model, I could make RSMs from *251* sampling models by using APGA method. The three RSMs were shown in appendix A. The results were presented in Table 6.1. I set the number of iterations to *500*. Maximum distance was *116 mm*, side distance X_d was *24.8 mm* in the case of *24 times* (FG-24).

On the rough ground (RG), the results were not good because robots could not walk or could walk but fell down. As a result, I could not make RSM by using APGA method. However, the trajectory of the robot's CoM, which could walk, was shown in Figure 6.1.

Table 6.1: The simulation results at final position of experiment I

No. Iteration	X_d	Y_d	R_d	Z	N_s
4	-22.7	120.2	7.0	244.0	240.0
7	-28.8	114.9	9.1	244.0	240.0
11	-27.9	119.4	10.6	244.0	240.0
14	-24.5	119.1	5.9	244.0	240.0
16	-20.6	119.5	5.4	244.0	240.0
18	-22.7	121.1	6.1	244.0	240.0
20	-22.4	122.5	7.1	244.0	240.0
22	-24.9	119.0	5.9	244.0	240.0
23	-24.9	119.0	5.9	244.0	240.0
24	***-24.8***	***116.0***	***4.8***	***244.0***	***240.0***
25	19.5	121.8	7.2	244.0	240.0

The trajectory of the robot's CoM was FG-24 when I compared with RG as shown in Figure 6.1. On RG, trajectory was small and walking was awkward. The other sides, the trajectory of FG-24 was larger and similar to a

human walking trajectory [43], which was a shape of trajectory like a cosine function.

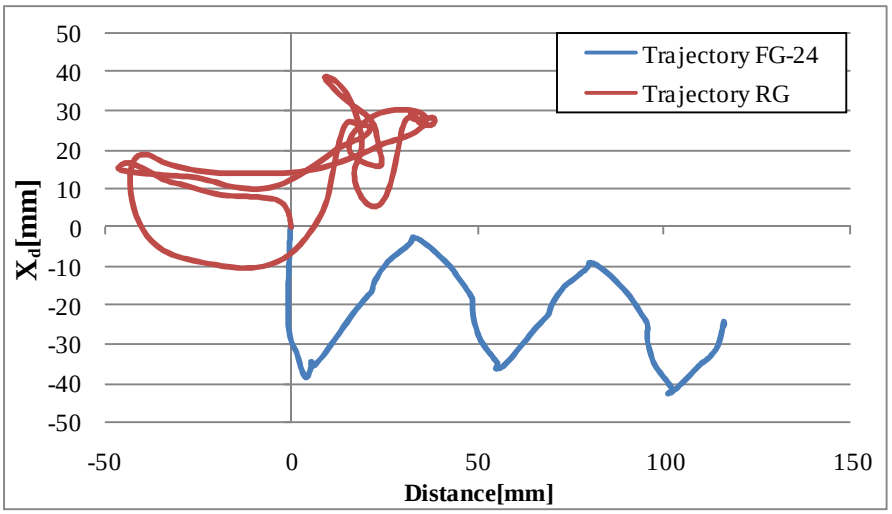

Figure 6.1: CoM trajectory of the simulation model

Gait pattern of the gait functions was assigned to joints FG4. FG24 and RG were compared as shown in Figure 6.2 - 6.5. The width of waveform has less change. Moreover, $\theta_1(t)$ (hip and ankle joints, rotating side to side) and $\theta_4(t)$ were similar to cosine function. Moreover, the gait patterns of knee joint ($\theta_3(t)$ and$\theta_6(t)$) were similar to a link of human's knee joint angle pattern as shown in Figure 4.5. In Figure 6.2, the waveforms indicated relation with CoM trajectory of FG24 in Figure 6.1. Their shapes look like cosine function in both figures because the position of the θ_1 at hip point on vertical or Z axis is close to the position of CoM in same plane. This is one of the key points for transferring weight from one foot to the other side in order that simulation models move forward. I consider this relation from the walking models only on the flat ground. In case of rough ground walking simulations, I also cannot observe this relationship. Due to the simulation on the rough ground, the result was not satisfactory. To walk on uneven ground, the joints were controlled by passive control which might inappropriate because walking on a rough surface required high stability. When I compared between FG4 and FG24 in Figure 6.2, the gait cycle peak points of FG24 was greater than FG4. I guess that is one reason. The FG24 can walk in longer distance but if the distance is too far, the stability of walking may decrease and lead to falling or rotation of the simulation model.

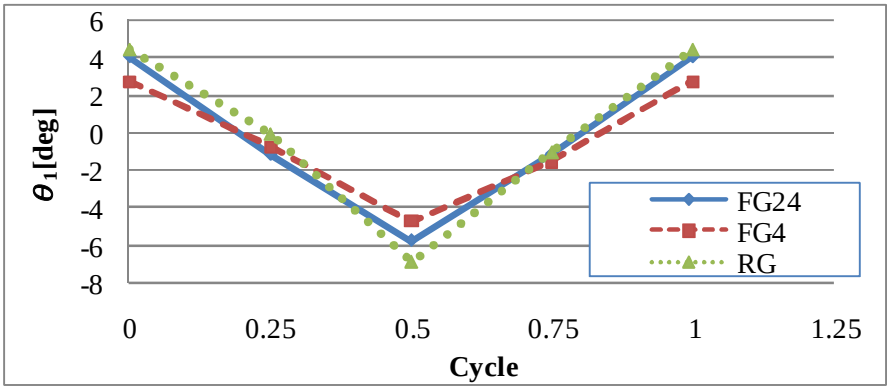

Figure 6.2: A cycle of gait function θ_1 (t) @ (hip and ankle, side to side)

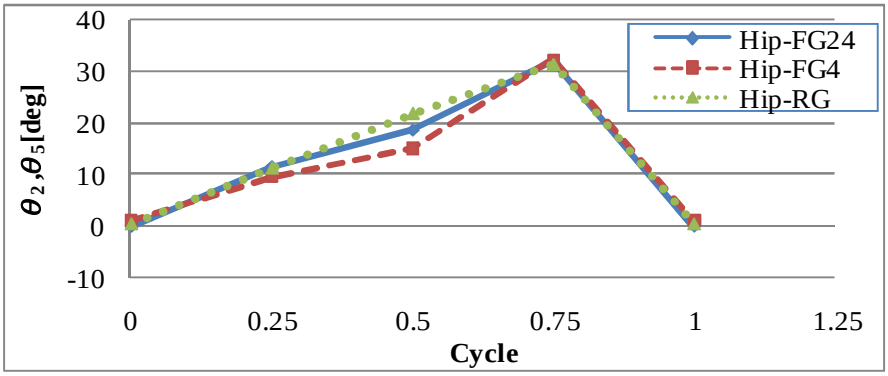

Figure 6.3: A cycle of gait function θ_2 (t) & θ_5 (t) @ hip

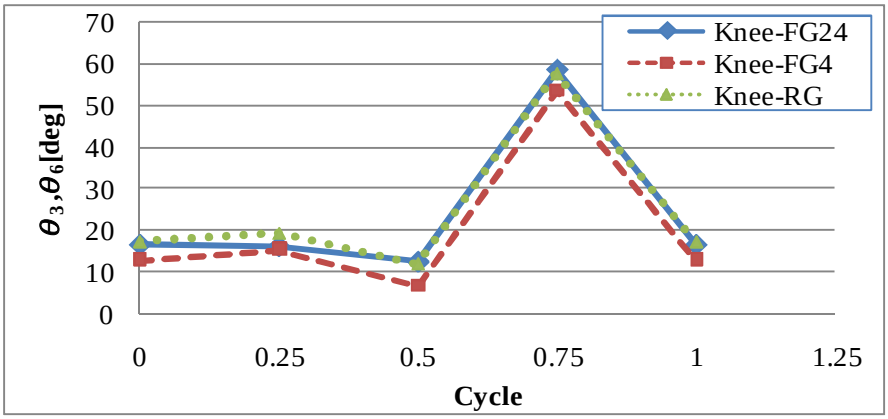

Figure 6.4: A cycle of gait function θ_3 (t) & θ_6 (t) @ knee

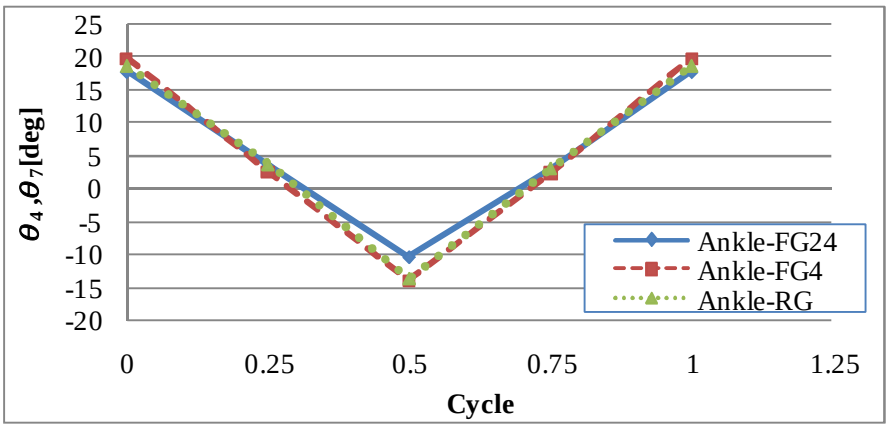

Figure 6.5: A cycle of gait function θ_4 (t) & θ_7 (t) @ ankle

6.1.2 Conclusion of Experiment I

In this section, the robot model with passive tiptoe was analyzed by walking on a rough and a flat surface, when the friction coefficient of both surfaces was assumed to be constant. The results of the simulation were as follows:

- The robot simulation model with passive control mechanism could be applicable to walk on a flat surface. On the other hand, this model was not proper for walking on a rough surface. This was because, in this simulation, the robot model could walk on flat surface quite well; it could maintain the walking stability and continuous movement. However, a walking on rough surface was quite difficult because it needed more control walking stability.

- The walking of robot with tiptoe mechanism on flat ground showed the effect of a flexible tiptoe mechanism. In an application, this part of robot composed of hinge spring joint that was used for supporting a body load of the robot.

- The movement behavior of spring was similar to a human's toe during a stance phase from heel off to toe off.

- The robot model simulated on flat ground showed a satisfied performance. It had a trajectory on XY-plane which looked like human's walking trajectory.

- APGA that I used for analyzing the robot model had high calculation performance because it could converge to an objective function within 24-iterrations.

- From the format of gait pattern as shown in Figure 6.2 - 6.5, all graphs had the same trend but their gait patterns were different, and these affected the walking distance of robot model.

6.2 The Result of Experiment II: Robot's Foot with Different Types of Toe Mechanism

6.2.1 The Results of Experiment II

This experiment proposed various toe mechanisms. The simulation model A, B, C, and D were used in this experiment. All simulation models of small biped robot with passive toe mechanism can walk. The results were shown in Table 6.2. The results of model A and model B satisfied the conditions. The maximum distance Y_d was exhibited in model *B (119 mm)*, minimum side distance X_d was *-5 mm* and rotation R_d was *3.1 deg*. The latter was the model A whose distance Y_d was *86 mm*, side distance X_d was *-25 mm* and rotation R_d was *4.2 deg*. On the other hand, the results of model C and model D were not as good as expected. The trajectories of the robot's CoM model A, B, C, and D were compared as shown in Figure 6.6-6.8.

Table 6.2: The Simulation results at final position of experiment II

	Distance		Rotation
Model	**Y_d (mm)**	**X_d (mm)**	**R_d(deg)**
A	86	-25	4.2
B	119	-5	3.1
C	49	-11	12.0
D	0	-64	23.2

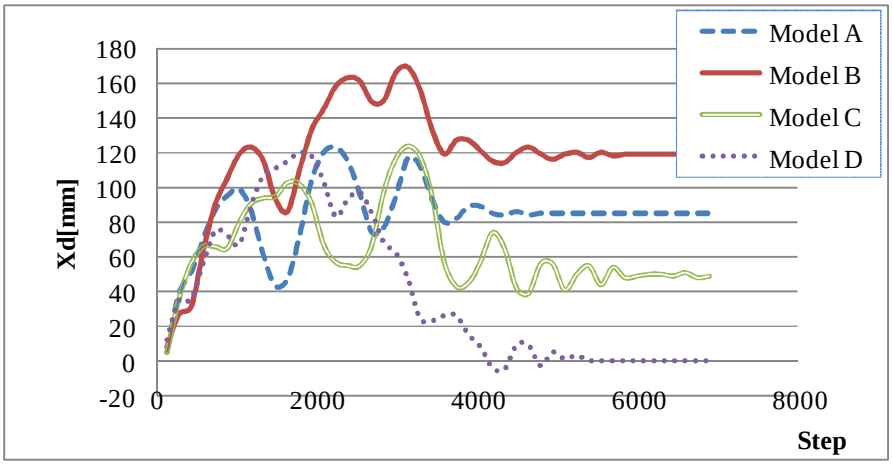

Figure 6.6: The distance trajectory (Y_d) of the robot's CoM

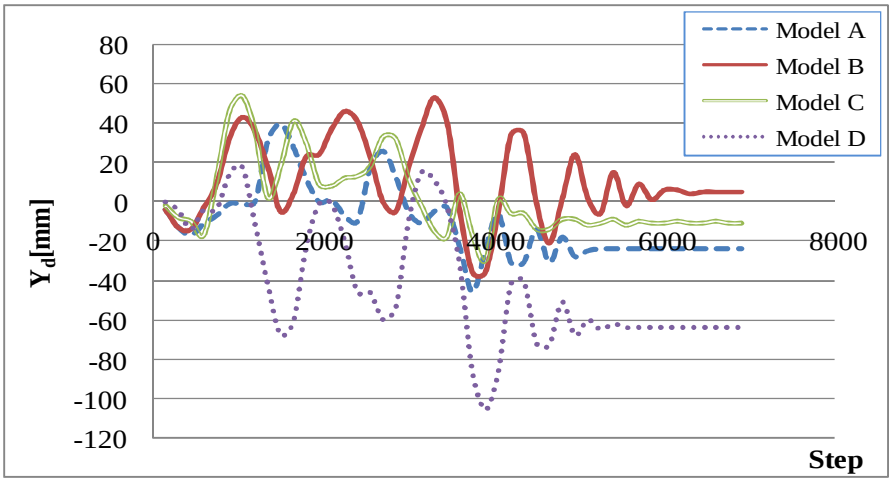

Figure 6.7: The side trajectory (X_d) of the robot's CoM

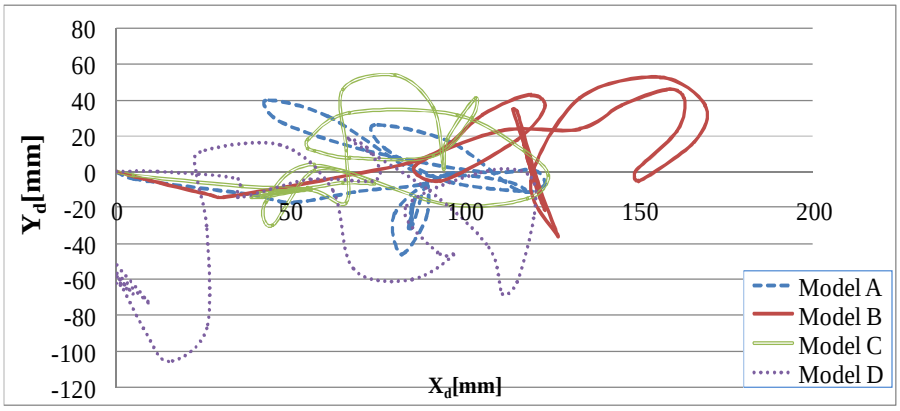

Figure 6.8: The trajectory of the robot's CoM

The trajectory of the robot's CoM was shown in Figure 6.6, 6.7 and 6.8. In model A, when I considered the walking step, I found that the trajectory of model B was long distance and similar to human walking trajectory [43] and shape of trajectory like a cosine function. But at the beginning of stance phase, the trajectory would swing a lot before entering to stable phase. The other side, the trajectories of model C and model D were small and walking was awkward. Waveforms of the gait functions of model A, model B, model C and model D assigned to joints were compared as shown in Figure 6.9 - 6.15. The width of waveform of hip and ankle roll-joints $\theta_1(t)$ had less change. However, the values of the other joints (Figure 6.10 - 6.15) were distributed to adapt walking ability without falling. This

was one thing from the effects on the difference of toe mechanisms in this study.

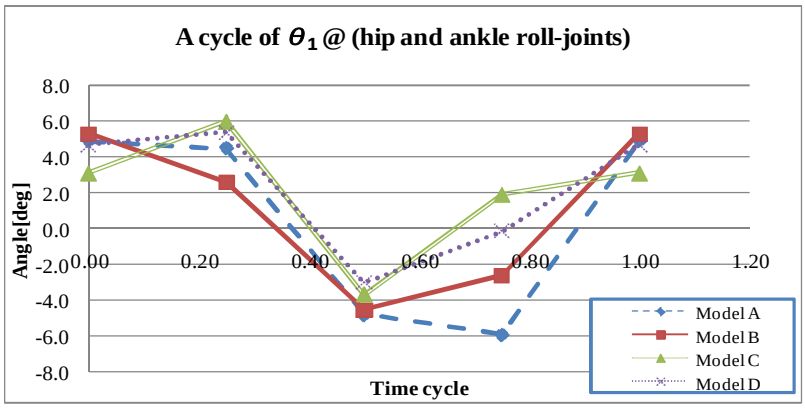

Figure 6.9: A cycle of gait function θ_1(t) @ (hip and ankle)

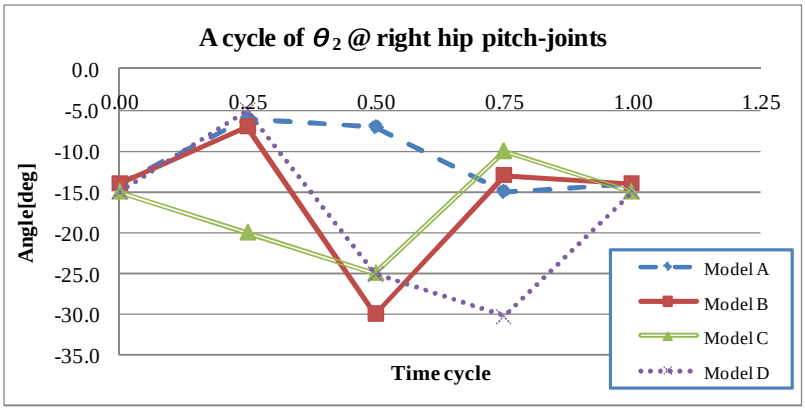

Figure 6.10: A cycle of gait function θ_2(t) @ (right hip pitch-joint)

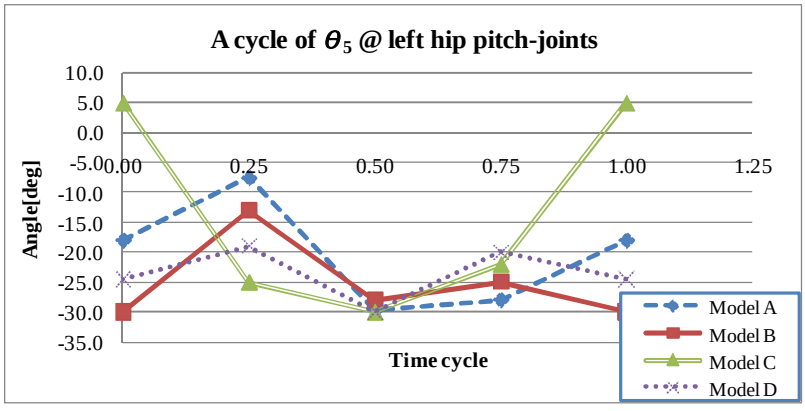

Figure 6.11: A cycle of gait function θ_5(t) @ (left hip pitch-joint)

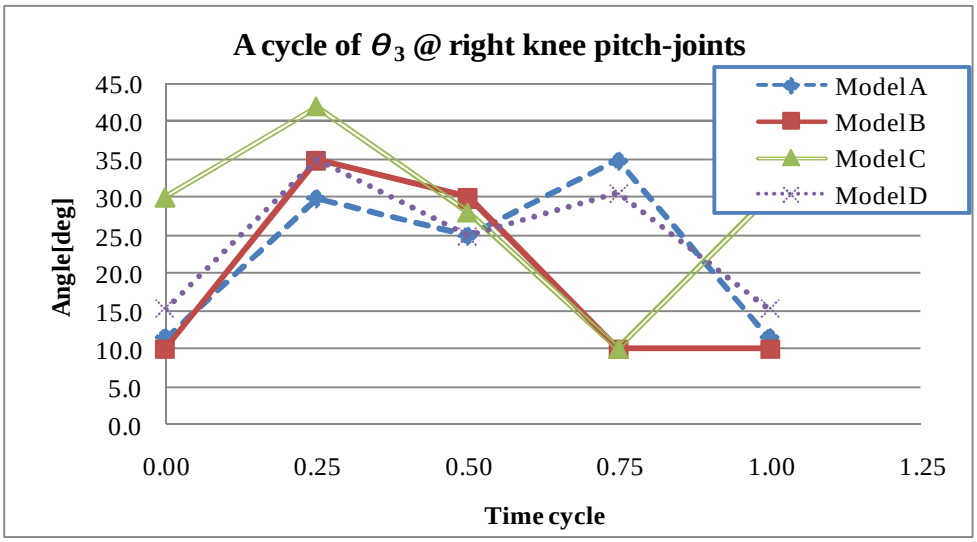

Figure 6.12: A cycle of gait function θ_3(t) @ (right knee pitch-joint)

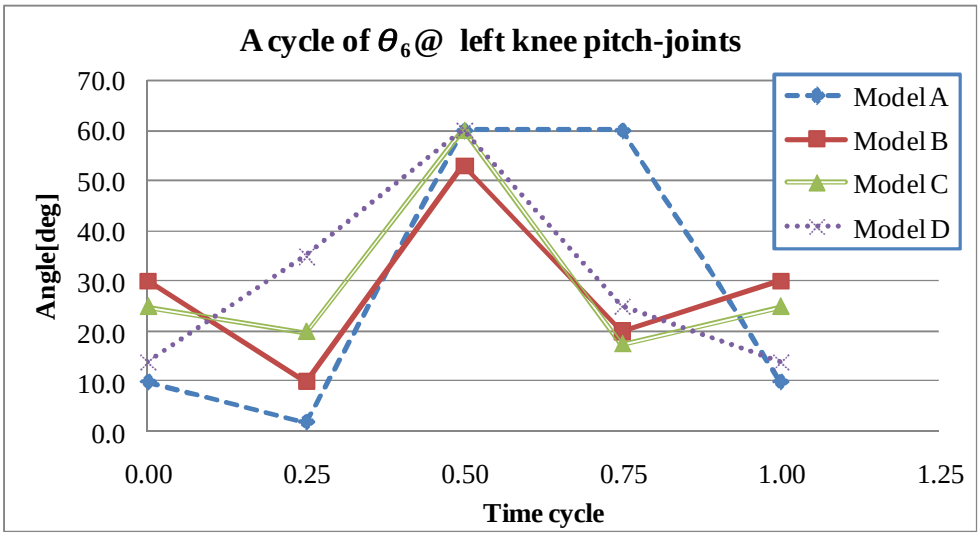

Figure 6.13: A cycle of gait function θ_6(t) @ (left knee pitch-joint)

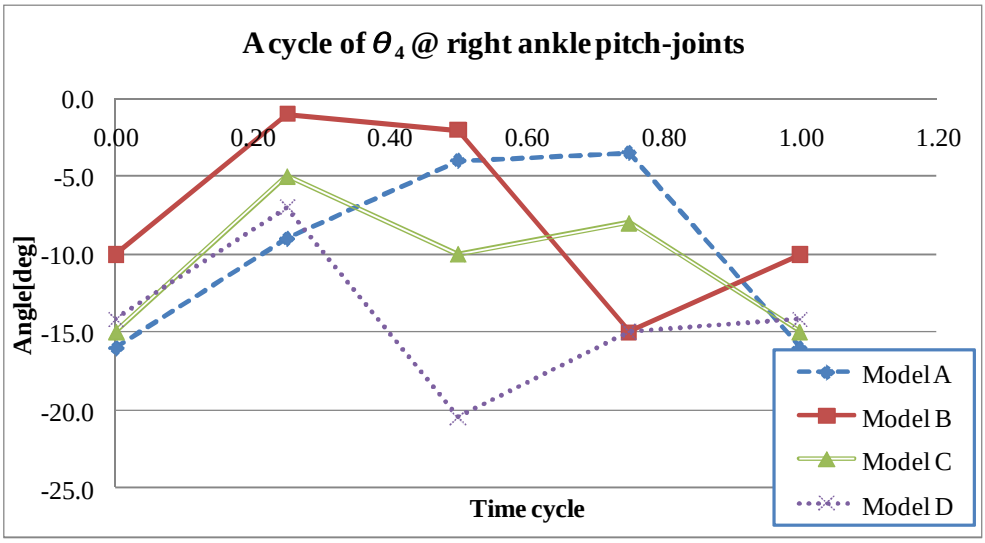

Figure 6.14: A cycle of gait function θ_4(t) @ (right ankle pitch-joint)

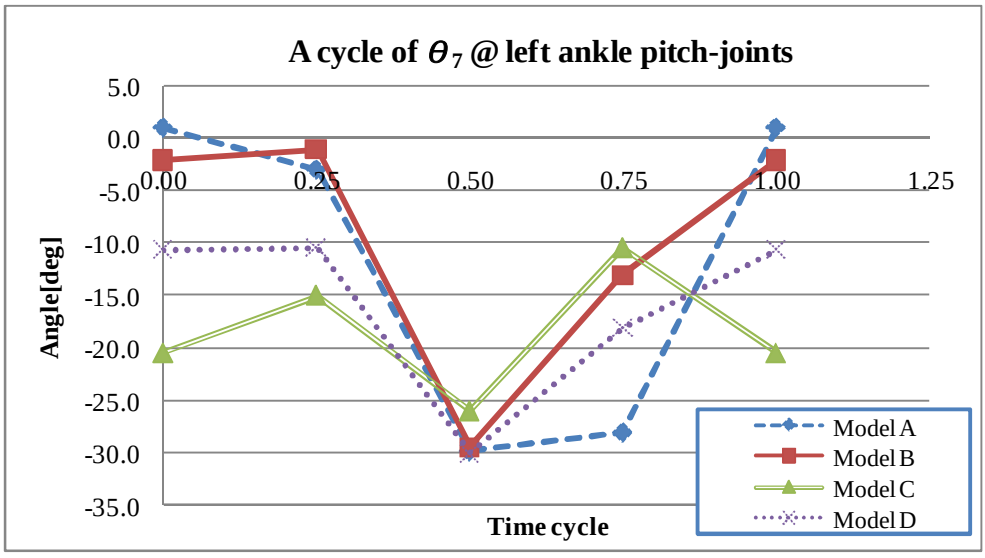

Figure 6.15: A cycle of gait function θ_7(t) @ (left ankle pitch-joint)

6.2.2 Conclusion of Experiment II

The results of previous section led to insight of the effect of a toe in robot walking behavior. This part can improve the robot walking behavior like human walking behavior. In this section, I designed various types of toe and investigated the appropriate passive toe for the robot model. This study was based on our specified condition (long walking distance and stable). The results of this section can be concluded as:

- The model B with big toe and tiptoe showed a long walking distance. The simulation exhibited the movement of big toe and tiptoe evidently.

- The model C and model D had less walking stability and got short walking distance. Tuning of these models was quite difficult because the improper properties of additional toe. A total area of foot was constant but the size of toe was increased, so a support loading area of heel was reduced. Therefore, the walking of these robots had less stability than other models. This was because the result from the movement of robot's forefoot was not suitable and the passive joint was inapplicable for these models.

- The joint pattern, which received from simulation results, showed the same trend only in the part of hip-roll. The joint pattern of others parts showed the various results.

6.3 The Result of Experiment III: Robot's Foot with Big toe Sizing Mechanism

6.3.1 The Result of Experiment III

This section proposed a design on property of toe mechanism with bigtoe. The simulation model B1 - B10 with big toe and tiptoe mechanism were used in this experiment. All simulation models of small biped robot with changed passive big toe size mechanism can walk and go straight as the criteria in gait generation method. In this experiment, I performed the simulation by using two stiffness values of hinge spring (K_p= 0.033 N/deg , 0.037 N/deg) as joint toes part and heel. The results of robot position and rotation angle position are shown in Table 6.3. For the gait coefficients of ten models, look at Appendix C.

Table 6.3: The simulation results at final position of experiment III

Model	k_p= 0.033 N/deg			k_p= 0.037 N/deg			Yd Distance Trend
	Distance (mm)		Rotation	Distance (mm)		Rotation	
	Y_d	X_d	R_d(deg)	Y_d	X_d	R_d(deg)	
B1	150	7	7.3	151	9	0	⇗
B2	***188***	***2***	***8.5***	***192***	***10***	***7.3***	⇗
B3	163	7	3.6	165	10	5.1	⇗
B4	159	7	0	172	9	4.4	⇗
B5	156	4	6.3	174	18	6.8	⇗
B6	175	3	9.6	163	16	4.4	⇘
B7	175	-1	6.3	152	17	3.6	⇘
B8	174	-3	6.3	166	3	0	⇘
B9	159	10	2.6	167	5	0	⇗
B10	150	6	2.6	154	14	4.4	⇗

In Figure 6.16 - 6.17, the distance of Y_d and R_d have some relationship when K_p is constant. If the distance Y_d is extended, the degree of rotation angle R_d will increase. The results showed the dependent relation of Y_d and X_d. If the distance X_d is short, the distance Y_d is extended. However, R_d is increased into the allowable rotation angle $|R_d| \leq 10.0$. In case of same test model by changing K_p value from 0.033 to 0.037 (N/deg), the distance Y_d tends to extend and X_d is also increased.

For model B6 to B8, walking distances are decreased when K_p is used at 0.037 (N/deg), I expect that these ranges may change along with the toe

ranges because experimental results showed that walking distance had some relation with side distance and rotation of robot. I obtained a good result of big toe size as shown in model B2 which obtained longer distance than other models. This model's sizing ratio is equal to 0.28 (bigtoe width = 22 mm/foot width = 78 mm/foot width) when the gait posture of model B2 and human are compared in Figure 6.18. In Figure 6.18, the simulation at time 1.5 (sec) gait likes a "Initial contact period" of human gait , at time 1.8 (sec) likes "Midstance period", at time 2.1 (sec) likes "Pre Swing period" which it can be observed the bending of the big toe and tiptoe, and at time 2.4 (sec) likes "Terminal swing period". In addition, the gait posture of model B2 is similar to human gait posture. The differences of gait are expected to occur as a consequence of the physical model structure with human's structure.

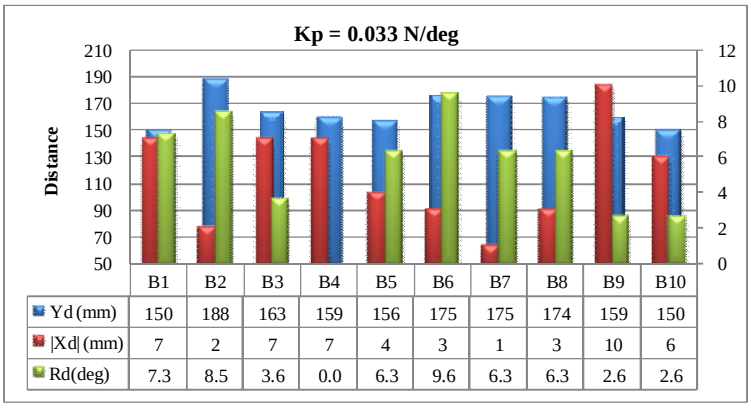

	B1	B2	B3	B4	B5	B6	B7	B8	B9	B10
Yd (mm)	150	188	163	159	156	175	175	174	159	150
|Xd| (mm)	7	2	7	7	4	3	1	3	10	6
Rd(deg)	7.3	8.5	3.6	0.0	6.3	9.6	6.3	6.3	2.6	2.6

Figure 6.16: The simulation results at final position when K_p= 0.033 N/deg

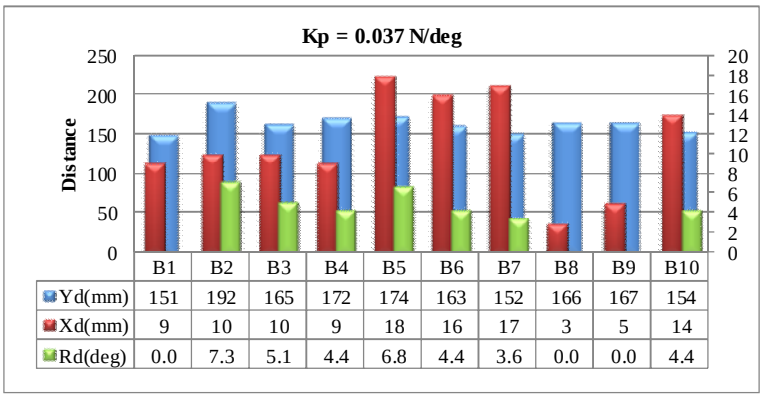

	B1	B2	B3	B4	B5	B6	B7	B8	B9	B10
Yd(mm)	151	192	165	172	174	163	152	166	167	154
Xd(mm)	9	10	10	9	18	16	17	3	5	14
Rd(deg)	0.0	7.3	5.1	4.4	6.8	4.4	3.6	0.0	0.0	4.4

Figure 6.17: The simulation results at final position when K_p= 0.037 N/deg

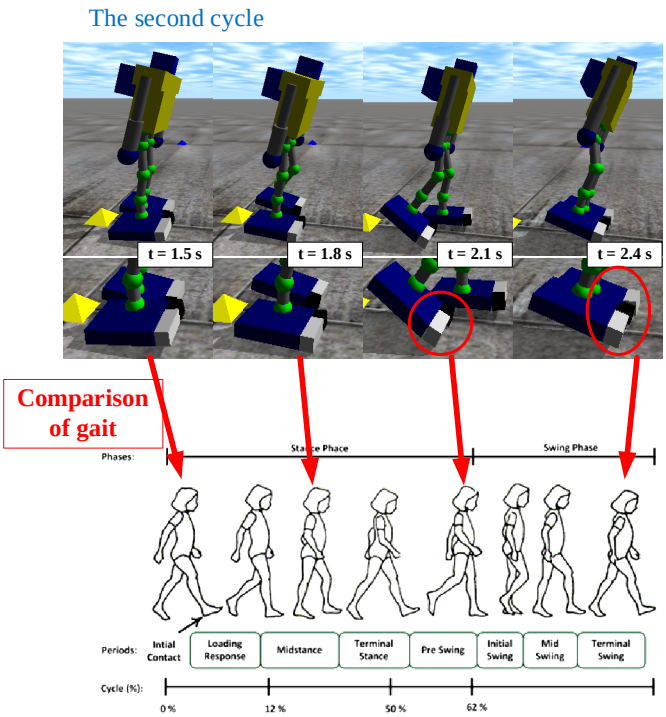

Figure 6.18: Comparison of gait between model B2 (K_p = 0.037 N/deg) and human

Figure 6.19-6.20 showed the side distance trajectory (X_d) of the robot's CoM from starting point to about 3000 steps, all of model trajectory showed a similar trend. Afterwards, there will be different swings before going into steady stage. The trajectory of X_d showed that the value of our models does not exceed |±70| (mm) to stabilize the simulation model and not to fall down.

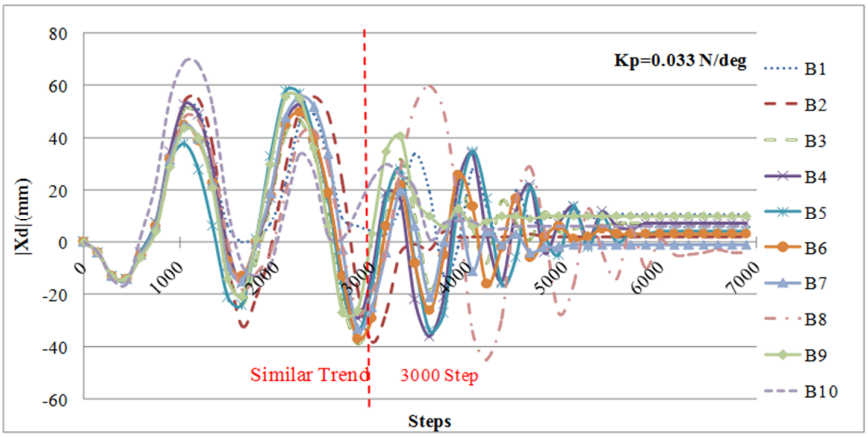

Figure 6.19: The side trajectory (X_d) of the robot's center of mass (CoM) when K_p= 0.033 N/deg

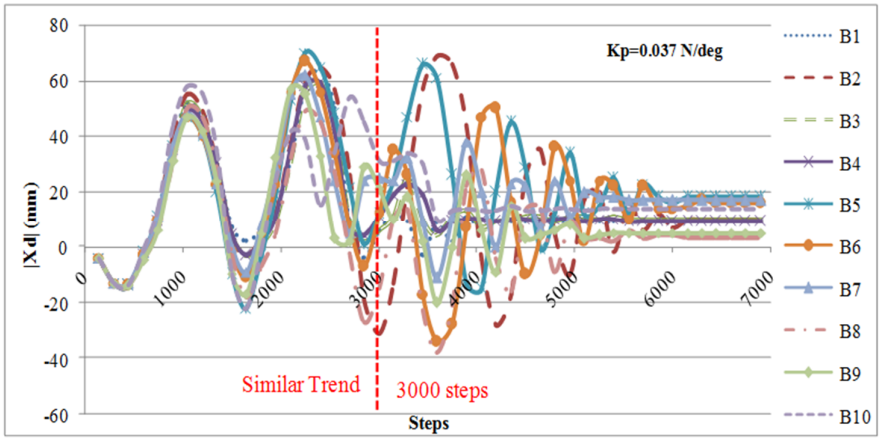

Figure 6.20: The side trajectory (X_d) of the robot's center of mass (CoM) when K_p= 0.037 N/deg

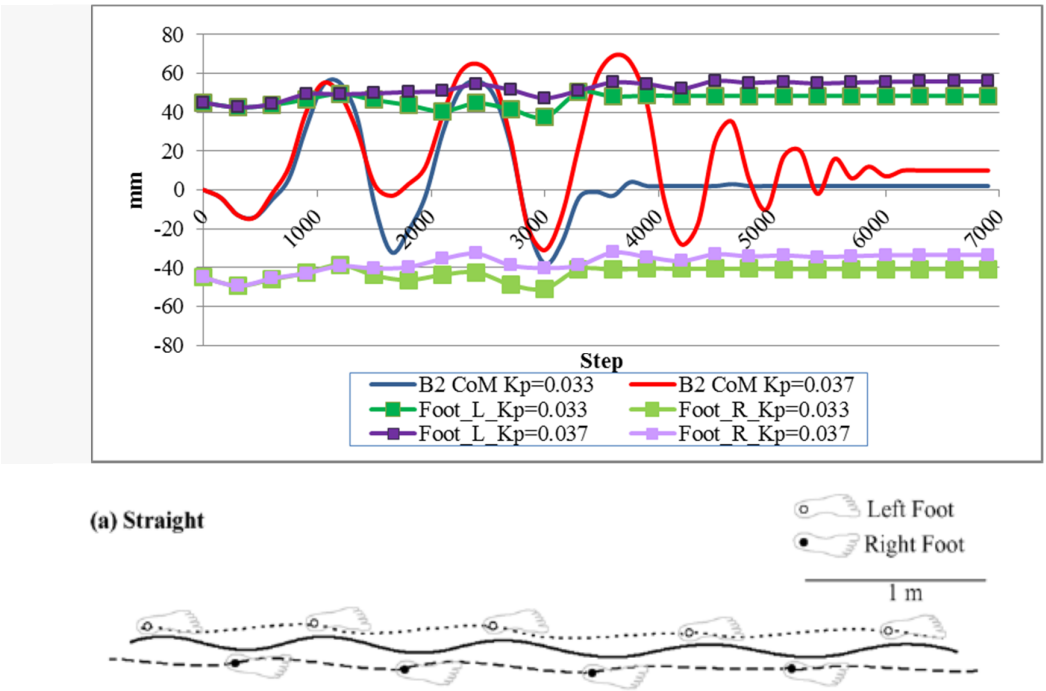

Figure 6.21: The distance trajectory (X_d) and foot of model B2 compare with human [43]

In Figure 6.21, distance trajectory from both B2 models is similar to cosine function same as human for walking period (start to 3600 steps). For standing period, B2 model which K_p equals 0.037 N/deg has high swing. This may be a result of side swing of the model which has the swing more than the other models. Additionally, a lot of side swing will affect the plane

of the model when it rests on the ground. Furthermore, the foot trajectories of both models have a curve tread like a human foot trajectories. In addition, the differences relate to the side swing of the CoM.

Table 6.4: The gait function of model B2

The gait function of model B2					
k_p	θ_i	**t=0.0 cycle**	**t=0.25 cycle**	**t=0.50 cycle**	**t=0.75 cycle**
0.0333 N/deg	θ_1	4.0	1.5	-4.5	-0.2
	θ_2	-14.0	-8.0	-30.0	-16.0
	θ_3	10.0	35	30.0	10.0
	θ_4	-10.0	-2.2	-5.0	-15.0
	θ_5	-30.0	-13	-27.0	-25.0
	θ_6	30.0	10	53.0	19.8
	θ_7	-2.0	-1.5	-30.0	-13.2
0.0337 N/deg	θ_1	5.5	2.0	-4.4	-0.1
	θ_2	-14.0	-8.0	-30.0	-15.8
	θ_3	10.0	35.0	30.0	10.0
	θ_4	-10.0	-2.0	-5.0	-15.0
	θ_5	-30.0	-13.0	-27.0	-25.0
	θ_6	30.0	10.0	53.0	19.8
	θ_7	-3.2	-1.2	-30.0	-13.0

Waveforms of the gait function that were assigned to joints of model B2 were compared as shown in Figure 6.22-6.25. In Figure 6.22, the waveforms at hip and ankle roll-joints differ slightly, but the shapes of waveforms like a cosine function. Moreover, this position is consistent with the characteristics of X_d trajectory and human's CoM trajectory. For another joint (Table 6.4, Figure 6.23-6.25), the same angle position is a little different. On the other side, the waveforms shapes are different for each leg, and different from human's joint angle. The differences of waveforms shapes occur, I expect a consequence of differences in the physical structure of the model and humans. However, the waveform can make our models walk. The walking simulation results of model B2, bending of the bigtoe and tiptoe position, are shown in Figure 6.26. Moreover, this figure has shown bending flexibility function of spring joint, which bending value of bigtoe and tiptoe are different and depend on the load of each part.

When I consider the gait cycle characteristics of the model B2 in Figure 6.22, model B in Figure 6.9 and model FG24 in Figure 6.2, they have similar waveform shape which look like the cosine function. It can be

assumed that the model will obtain long distance that depends on gait cycle of the θ_1. When I consider maximum value of gait cycle which has higher value, it will obtain long distance such as in Figure 6.2 when K_p = 0.037 N/deg and Figure 6.2 for FG24. On the other hand, gait cycle which its peak points are too high will affect stability as presented in Figure 6.21. The model B2 of K_p =0.037 N/deg had to swing in the stand action than another one.

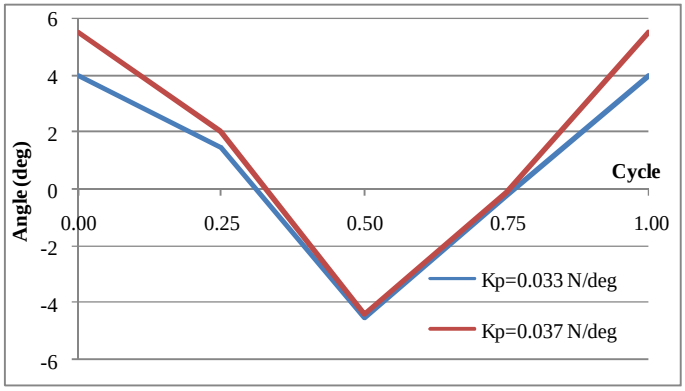

Figure 6.22: The cycle of gait functions $\theta_1(t)$ @ (B2 model's hip and ankle roll joints)

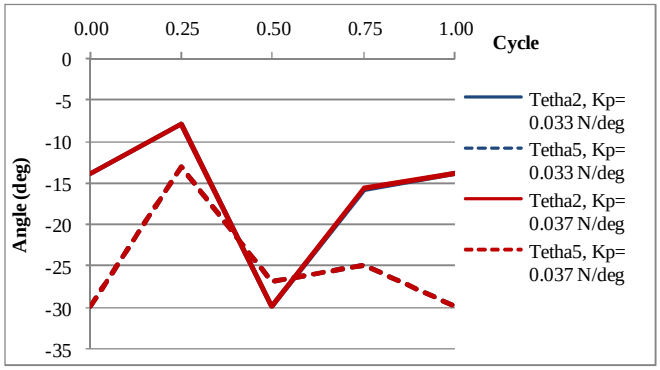

Figure 6.23: The cycle of gait functions $\theta_2(t)$ and $\theta_5(t)$ @ (B2 model's hip pitch joints)

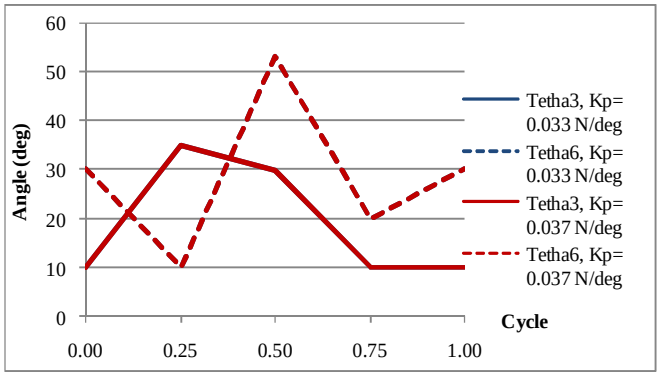

Figure 6.24: The cycle of gait functions $\theta_3(t)$ and $\theta_6(t)$ @ (B2 model's knee pitch joints)

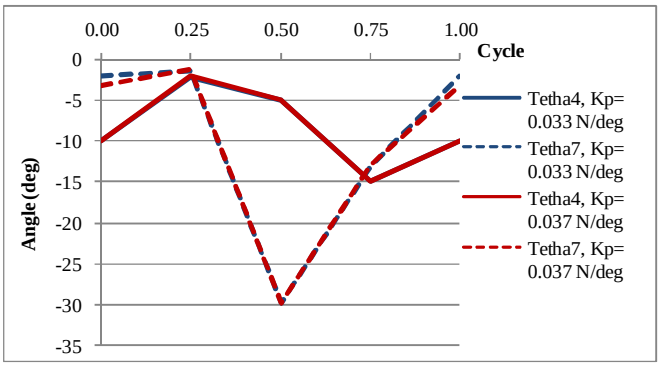

Figure 6.25: The cycle of gait functions $\theta_4(t)$ and $\theta_7(t)$ @ (B2 model's ankle pitch joints)

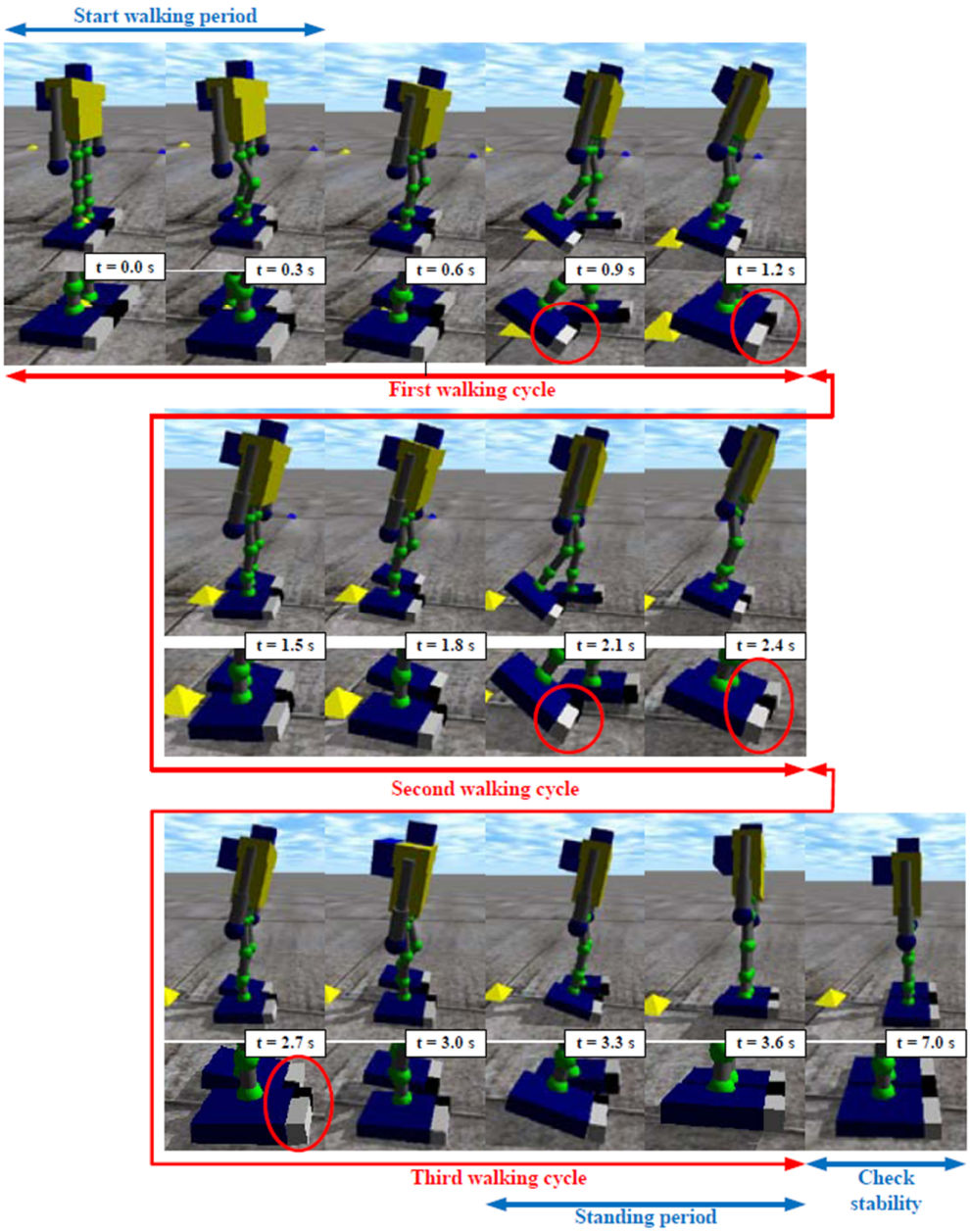

Figure 6.26: The simulation of walking (model B2, K_p = 0.037 N/deg)

6.3.2 Conclusion of Experiment III

From the results of the second experiment, the model B with big toe, tiptoe, and heel can walk in a long distance when it was compared to the model A. The movement of bigtoe and tiptoe affected the walking distance of robot model. The effect of bigtoe in walking behavior of robot model was the obstacle then I focused on the analysis of bigtoe size that made our robot model walk in pre-specified conditions.

- For the model B2, big toe width per foot width *ratio equals 0.28* (28% of foot width) like the ratio of human foot. Besides, this model had the longest walking distance when I fixed toe length per foot length ratio which was equal to 0.20 (20% of foot length). Although the experiments performed by changing the spring constant in narrow range, the models B2 still obtained a long distance.
- The movement behavior of CoM trajectory during walking of robot had the same trend but different while it was approaching the stop.
- The gait pattern of the joints, that made the robot model walk in specified conditions of each model, was not much different except in the area of ankle-pitch. Therefore, I can conclude that this area was important point for our simulation model. Additionally, the gait pattern in this area was altered when the size of bigtoe was changed.
- The walking behavior of the model B2 was like the walking behavior of human because the walking cycle had the period of heel contact, foot flat, heel off, and toe off as presented in Figure 6.18.

From experiments, model B2 can obtain the longest walking distance. This was driven by many variables. In addition, the direct part that I have studied was size of toe and big toe which support and transfer body weight. Furthermore, the stiffness of spring could show that it also affect walking distance.

7

Discussions and Conclusions

This research studied the walking behavior of biped robot and focused on the design of robot's foot having big toe component. The main objective is to determine the optimal size of big toe that can make robot go straight and has the maximum distance within our specified conditions. In previous investigations, some researchers have presented the research related to bigtoe but they are not widely spread. The purpose of toe is to increase robot's walking abilities such as stability and posture. Additionally, the robot posture looks like human posture and it can walk on rough surface. The results from simulation have the same trend as our assumption because the bigtoe can increase robot's walking. However, these results do not cover whole abilities development of robot walking process. Therefore, the study about robot foot design is continuous.

In this research, the study concentrated on the size of big toe because I had the assumption that this component was one of important components in human walking process. The design of robot's tiptoe is not obvious in previous research. In this study, there were three experimental sections to achieve our purpose as shown in previous chapter. This section will demonstrate the experimental results and conclude the work. Additionally, the future work will be also presented in this chapter.

7.1. Discussion of Experiment I: Robot's Foot with Toe Mechanism

In this experiment, the simple robot model with tiptoe was designed; some details were presented in previous chapter 5.1. There were two types of surface used in the experiment: flat ground (FG) and rough ground (RG). The APGA method was applied to determine optimal walking parameters. The results of this experiment can be presented as follows:

Walking simulation on flat ground

- The simulation robot with tiptoe can walk in specified conditions by using gait generation method. The result showed that this method can be applied to create gait pattern for a real robot.
- The best result that had been received was shown in model FG-24. Robot CoM trajectory and human CoM Trajectory were alike.
- The gait pattern behavior of simulation robot looked like human knee angle pattern manner.
- The walking behavior of simulation robot with big toe was almost the same as human manner. Both tiptoes showed the bending motion when they received the effect from body load.
- The APGA method exhibited high efficiency in optimization and the speed of convergence depended on predicted initial condition.

Walking simulation on rough ground

Because of the limit of sampling model, the simulation robot with passive tiptoe could not be optimized in the desired process. Moreover, the walking on rough ground needed high stability but the passive toe did not have sensor so it was difficult to control the stability. Therefore, the robot with the passive toe was not proper for walking on rough ground. The use of MSC.Visual Nastran program in robot simulation took quite long time because the program needed more calculation time.

7.2. Discussion of Experiment II: Robot's Foot with Different Types of Toe Mechanism

This section will present the study of the robot walking process with four different foot types. The walking on flat ground with constant friction coefficient was investigated. The simulation used ODE method for solving the problem. The gait cycle of joint in hip pitch, knee pitch and ankle pitch were independent because I considered that the human walking process might use different gait cycles in each leg. The leg was flexible in each walking state because of this reason. In this experiment, the gait pattern was tuning referred to the results of previous experiment. The results of the experiment are as follows:

- The model A and the model B showed the long walking distance in the desired condition and the robot's CoM trajectory before stop walking like human behavior. The model B showed a maximum walking distance.

- The model C and The model D exhibited a short walking distance and they could not walk in specified conditions. From the simulation results, I expected that this was because the support area on the heel was reduced. In addition, the simulation conditions might limit the motion of toe's joint that made robot cannot walk well.

- The results might not be absolutely true but the interesting point was the effect of bigtoe in robot walking process.

The basic experimental results showed that there were some interesting behaviors of bigtoe in the model B in the first experiment. The effect of the bigtoe in the robot's walking behavior was satisfactory. Moreover, when I considered human foot, I found that the size of big toe was an important factor. The optimal size of big toe will be investigated in the next section.

7.3. Discussion of experiment III: Robot's Foot with Bigtoe Sizing Mechanism

In this section, the optimal size of bigtoe and the effect on walking process were studied. The model B in the second experiment showed the best results and it could walk almost like human behavior (Figure 6.25). The responsibility of heel, bigtoe, and tiptoe of model B was considered. The big toe width size of model was varied and each value of big toe size was used by simulation model. Ten models of simulation robots were investigated. All simulation parameters were referred to the model B. Although the experiments were performed by changing the spring constant in narrow range, the models B2 still obtained a long distance. The simulation results showed that the model B2, which had the ratio between bigtoe width size and foot width size *equal 0.28 (28% of foot width)*, had a maximum walking distance. Additionally, the trajectory of CoM had the same trend as model B. The gait pattern of all models (B1-B10) was almost the same when the size of big toe was changed. The different gait patterns occurred in area of ankle pitch of both legs. I can conclude that if the foot size is changed, the ankle pitch of robot will alter. The changing of the ankle pitch of robot will affect the gait of robot. The best result of this experiment shown in model B was the ratio between bigtoe width size and foot width size *equal 0.28*. However, I expected this bigtoe ratio size to be the appropriate size for our model size, which had weight, height and properties as I defined. *This did not mean that this ratio would be appropriate with all robot size, but it showed that robot with big toe could walk similarly to human walking*. *The big toe size had effect on walking distance when the size was changed*. Therefore, if I can define appropriate size of bigtoe, I hope it will improve the ability of robot's walking. The simulation result showed that when the size of bigtoe varied, gait patterns were changed. However, to find the appropriate bigtoe size is needed to study more. The results that I obtained now are interesting because they are consistent with the bigtoe ratio of the human.

7.4. Conclusions

The study of walking behavior of robot with bigtoe can be concluded as follows:

In the first experiment, the walking behavior of robot with tiptoe was investigated. The result from this experiment showed that the gait generation method could generate the gait for simulation robot and APGA method had high efficiency in optimization process. The convergence rate of APGA was very fast and the rate depended on expected initial value. The robot with passive toe was not proper for walking on rough surface.

From the study of gait generation method, I have known that the gait generation method can generate gait pattern for simulation robot walking process. The simulation robot had almost the same walking behavior as human. Subsequently, the effect of different toe sizes in robot walking behavior was studied. The robot model B that had tiptoe and big toe component showed the simulation results in CoM trajectory trend like a human, and obtained a long distance. The simulation model B showed that the bending functions of big toe and tiptoe were flexible for the foot. Additionally, the simulation that shows an evident effect of tiptoe and bigtoe will be investigated in next section.

The results from the second experiment, model B obtained a good result. The model B consisted of heel big toe and tiptoe, which assumed that a big toe was an important part like a human's bigtoe. A robot's bigtoe has not been studied explicitly in the present. Therefore, I am interested in the study of bigtoe size affected in simulation robot. The simulation used a flat ground with constant friction coefficient and the robot model had constant spring stiffness in each joint. The robot model B2 showed the greatest walking ability according to the desired conditions. Moreover, the ratio of bigtoe (bigtoe width size/ foot width size) was equal to *0.28* that was almost the same as human foot. However, I expected this bigtoe ratio size to be the appropriate size for our model size, which had weight, height and properties as I defined. This did not mean that this ratio would be appropriate with all robot size, but it showed that robot with big toe could walk similarly to human walking. The big toe size had effect on walking distance when the size was changed. Therefore, if I can define appropriate size of bigtoe, I will

improve ability of robot's walking. The simulation result showed that when the size of bigtoe varied, gait patterns were changed. However, to find the appropriate bigtoe size is needed to study more. The results that I obtained now are interesting because they are consistent with the bigtoe ratio of the human. The result of bigtoe size may be coincident to be the same with human's bigtoe ratio. This also cannot be guaranteed. Therefore, the other interesting variables still have to be studied and verified our results.

7.5. Future work

The result in this paper is the first study to find the appropriate bigtoe size. Since I have determined that the bigtoe is another one important to support weight of human. The results I obtained now are interesting because they are consistent with the bigtoe ratio of the human. However, there are many variables that I have to try to adjust the value or placement in order to learn more and to verify our results. For future work, I will make and apply foot of the model B to real small biped robot. Furthermore, I suggest to study the behavior of a robot's walking with the toe components, and to compare the results of simulation and real robots. I am interested in the Close-loop control which collaborates with the CoM control. They used for increase stability and balance in walking process. This system is considered to use for walking experiment on uneven surface, which is challenge for walking robots.

Bibliography

[1] M. Hirose, Y. Haikawa, T. Takenaka, and K. Hirai, Development of humanoid Robot ASIMO, *Proc. Of IEEE/RSJ International Conference on Intelligent Robots and Systems*, Workshop2, 2001.

[2] Kenji Hashimoto, Yuki Takazaki, Kentaro Hattori, Hideki Kondo, Takamichi Takashima, Hun-ok Lim, and Atsuo Takanishi, A study of Function of Foot's Medial Longitudinal Arch Using Biped Humanoid Robot, *The 2010 IEEE/RSJ International Conference on Intelligent Robots and Systems*, pp. 2206-2211, October 18-22, Taipei, Taiwan.

[3] Kenji Kaneko, Fumio Kanehiro, Mitsuharu Morisawa, Takuo Tsuji, Kanako Miura, Shin ichiro kanaoka, Shuuji Kanjita and Kanzuhito Yokoi, Hardware Improvement of Cybernetic Human HRP-4C for Entertainment Use, *The 2011 IEEE/RSJ International Conference on Intelligent Robots and Systems*, pp. 4392-4399, San Francisco, CA, USA.

[4] Koichi Nishiwaki, Satoshi Kagami, Yasuo Kuniyoshi, Masayuki Inaba, Korichika Inoue, Toe Joint that Enhance Bipedal and Full body Motion of Humanoid Robots, *Proceedings of the 2002 IEEE International Conference on Robotics & Automation*, May 2002, Washington DC.

[5] Vukobratovic, M., and Juricic,. Contribution to the synthesis of biped gait, in *Proc. IFAC Symp. Technical and Biological Problem on Control*, Erevan, USSR, 1968.

[6] Zhe, T., Zengqi, S., and Changji Z., GA Based Optimization for Humanoid Walking, *ICGST-ARAS journal, 5(2), pp.1-10,* June 2006.

[7] Lingyun, H., Changjiu, Z., and Zengqi S., Biped Gait Optimization Using Spline Function Based Probability Model, *Proceeding of the 2006 IEEE International Conference on Robotics and Automation*, pp. 830-835, Orlando, Florida

[8] Moosavian, S.A.A., Alghooneh, M. Takhmar, A., Introducing a Cartesian Approach for Gate Planning and Control of Biped Robots and Implementing on Various Slopes, *Proceedings of the 2007 7th IEEE-RAS International Conference on Humanoid Robots*, pp. 545-550, Pittsburgh, United States of America.

[9] Naoya Ito, Hiroshi Hasegawa, Robust optimization under uncertain factors of environment for simple gait of biped robots, *Proceedings of the 6th EUROSIM Congress on Modeling and Simulation*, Ljubljana, Slovenia, 2007.

[10] Yu, Z., Ming, C.L., Dinesh, Manocha, Albertus, Hengrawan, Adiwahono., Chee-Meng, C., A Walking Pattern Generator for Biped Robots on Uneven Terrains**,** *IEEE/RSJ International Conference on Intelligent Robots and Systems*, October 18-22, 2010, Taipei, Taiwan.

[11] Nandha, H., Jungwon, Y., Gabsoon, K., Gait Pattern Generation with Knee Stretch Motion for Biped Robot using Toe and Heel Joints, *International Conference on Humanoid Robots*, pp. 265-270, Daejeon, Korea, 2008.

[12] Sven Behnke, Member, IEEE, Human-Like walking using Toes Joint and Straight Stance Leg, *3rd International Symposium on Adaptive Motion in Animals and Machines(AMAM 2005)*, Ilmenau, Germany.

[13] Cheol. K.A., Min, Cheol, L., and Seok, J.G., Development of a biped robot with toes to improve gait pattern Advanced Intelligent Mechatronics, *IEEE/ASME International Conference on Advance Intelligent Mechatronics*, AIM 2003, vol. 2, pp. 729-734.

[14] Whittle, M. W. An Introduction to Gait Analysis, 4th ed., Oxford,, 2007.

[15] Hsin-Yi Kathy Cheng, Chun-Li Lin, Shih-Wei Chou, Yan-Ying Ju, Yin-Chou Lin, May-Kuen Wong, The importance of the great toe in balance performance. *Proceedings of the Fifth IASTED International Conference on Biomechanics*, BioMech, Vol. 59-63, 2007.

[16] Perry J., Gait Analysis: Normal and Pathological Function, Slack Inc., N.J., 1992.

[17] Kosei Demura, Robot Simulation , Robot programming with Open Dynamics Engine , Morikita Publishing Co. Ltd., Tokyo, 2007.

[18] Naoya Ito, Hiroshi Hasegawa, The Robust Design to Generate the Gait Pattern of a Small Biped Robot, *Journal of Japan Society for Design Engineering* . Vol.45(6), pp. 304-311, 2010.

[19] Chockalingam, N., Ashford, RL., Selected foot length ratios in a non-pathological sample. *Revista Internacional de Ciencias Podologícas*, Vol. 1(2), pp. 25-30. 2007.

[20] Hiroshi Hasegawa, Adaptive Plan System with Genetic Algorithm based on Synthesis of Local and Global Search Method for Multi-Peak Optimization Problems, *Proceedings of the 6th EUROSIM Congress on Modeling and Simulation*, Ljubljana, Slovenia, 2007.

[21] iSIGHT is a trademark of Engineous Software Inc., *iSIGHT version 9.0*, pp. 321-327, United States of America, 2004.

[22] Scott Cameron Wearing, Stephen Urry, James E Smeathers, Diana Battistutta, A comparison of gait initiation and termination methods for obtaining plantar foot pressures, *Gait and Posture 10 (1999)*, pp. 255-263

[23] The Clinical Gait Analysis Forum of Japan,, *Gait Analysis Based on Joint Moment. Ishiyaku publisher, pp. 19-22*, Japan, 1997.

[24] Shuuji Kajita, Kenji Kaneko, Mitsuhasu Morisawa, Shinichiro Nakaoka and Hirohisa Hirukawa, ZMP-based Biped Running Enhanced by Toe Springs, *IEEE International Conference on Robotics and Automation Roma*, pp. 3963-3969, Italy, 2007.

[25] Kemji Hashimoto, Yusuke Sugahara, Hun-Ok Lim, Atsuo Takanishi, Biped Landing Pattern Modification Method and Walking Experiments in Outdoor Environment, *Journal of Robotic and Mechatronics*, Vol.20, No.5, pp.775-784, 2008.

[26] Kensuke Harada, Mitsuhara Morisawa, Shin-ichiro Nakaoka, Kenji Kaneko, Shuuji Kajita, Kinodynamic Planning for Humanoid Robots Walking on Uneven Terrain, *Journal of Robotic and Mechatronics*, Vol.21(3), pp.311-316, 2009.

[27] Astushi Yamashita, Masaaki Kitaoka, Toru Kaneko, Motion Planning of Biped Robot Equipped with Stereo Camera Using grid Map, *Journal of Robotic and Mechatronics*, Vol.5(5), pp.639-647, 2011.

[28] Xiang, Y., Chung, H.J, Mathai. A., Rahmatalla, S., Kim, J., Marler, T., Beck, S., Yang, J., Arora, J.S., Abdel-malek, K., Optimization-based Dynamic Human Walking Prediction, *SAE Human Modeling for Design and Engineering Conference*, June 12-14, Seattle, Washington, 2007.

[29] Krissana Nerakae., Hiroshi Hasegawa., The Effect of Toe Mechanism for Simulation of Small Biped Walking Robot by Gait Generation, *The 11th International Conference on Modeling and Applied Simulation*, pp. 80-85, Sep 19-21, Vienna, Austria, 2012.

[30] ASIMO, The World's Most Advance Humanoid Robot, http://asimo.honda.com/, (Accessed: 20 March 2013)

[31] WABIAN, Biped humanoid robot group, http://www.takanishi.mech.waseda.ac.jp/top/research/wabian/index.htm, ,(Accessed: 20 March 2013)

[32] H6 & H7, Perception-Action Integrated Humanoid Robot, http://www.jsk.t.u-tokyo.ac.jp/research/h6/, (Accessed: 20 March 2013)

[33] HRP-4C, Human-like Humanoid Robot, http://www.aist.go.jp/aist_j/press_release/pr2009/pr20090316/pr20090316.html, (Accessed: 20 March 2013)

[34] Coronal plane, http://en.wikipedia.org/wiki/Coronal_plane, (Accessed: 20 March 2013)

[35] Columbia University Medical Center, Anatomy of a joint http://www.cumc.columbia.edu/dept/rehab/musculoskeletal_health/anatomy.html, (Accessed: 20 March 2013)

[36] Walking in graph, http://atec.utdallas.edu/midori/Handouts/walkingGraphs.htm, (Accessed: 20 March 2013)

[37] KHR-3HV biped robot, http://kondo-robot.com/sys/khr-3hv_detail1, (Accessed: 20 March 2013)

[38] KHR-2HV biped robot, http://www.kondo-robot.com/EN/product/khr-2hv.html, (Accessed: 20 March 2013)

[39] Russell Smith, Open Dynamic Engine, http://www.ode.org/. (Accessed: 20 March 2013)

[40] Open Dynamic Engine, http://en.wikipedia.org/wiki/Open_Dynamics_Engine, (Accessed: 20 March 2013)

[41] Multi-body Dynamic modeling, Visual Nastran Desktop 4D http://www.pieroagostinetti.eu/knowledges.htm, (Accessed: 20 March 2013)

[42] A Brief History of Robotics, http://robotics.megagiant.com/history.html, (Accessed: 20 March 2013)

[43] Michael S. Orendurff, Ava D. Segal, Jocelyn S. Berge, Kevin C. Flick, David Spanier, Glenn K. Klute, The kinematics and kinetics of turning: limb asymmetries associated with walking a circular path, Center of Excellence for Limb Loss Prevention and Prosthetic Engineering, *Motion Analysis Laboratory Rehabilitation Research and Development, Veterans Administration Puget Sound Health Care System,* Seattle, WA 98108, vol. 23, pp. 106-111, USA, 2006.

Appendix A

In the first experiment, I presented the process to make three 3rd order RSMs equations (Cubic polynomial) from 20 variables (N=20) and 251 sampling. These are RSM of go straight distance (RSM - Y_d), RSM of side distance (RSM - X_d) and RSM of rotation (RSM - R_d) using 3rd order equation (Cubic polynomial) as shown below.

The 3rd orders RSM equation (Cubic polynomial) can be written as

$$\tilde{F}(x) = a_0 + \sum_{i=1}^{N} b_i x_i + \sum_{i=1}^{N} c_{ii} x_i^2 + \sum_{ij(i<j)} c_{ij} x_i x_j + \sum_{i=1}^{N} d_i x_i^3$$

N is number of model inputs or number of variable

X_i is the set of model inputs

a, b, c, d are the polynomial coefficients

The polynomial coefficients are presented in the term 0 to 250 (251 terms). I obtained the three RSM function coefficients as presented in the following Table A:

Table A: Polynomial Coefficients of RSMs

Term		Polynomial Coefficients		
		Y_d	X_d	R_d
0	a_0	6157.79000	90746.20000	-73214.30000
1	b_1	278.43400	-2729.15000	1708.13000
2	b_2	142.20900	43.98890	-103.75800
3	b_3	48.06850	-108.28500	38.40630
4	b_4	-40.38870	-36.50570	62.89560
5	b_5	73.04030	30.27470	32.44040
6	b_6	79.85860	-22.43990	13.34650
7	b_7	72.26260	-255.17600	208.37700
8	b_8	-268.15800	181.92000	-396.06400
9	b_9	-71.15490	-80.98510	-74.46010
10	b_{10}	-14.41880	63.51420	-36.06630
11	b_{11}	263.05100	-251.60900	308.65300
12	b_{12}	8.90679	-81.79120	0.33680
13	b_{13}	72.34250	355.08700	-406.46200
14	b_{14}	715.98800	1548.89000	-702.12300
15	b_{15}	-48.42560	-18.02940	14.59660
16	b_{16}	30.63760	3.45123	17.63720
17	b_{17}	-144.08300	51.16370	-143.61900
18	b_{18}	-11.41640	40.55260	-9.38225
19	b_{19}	35.00960	165.23300	-74.53710
20	b_{20}	25.69310	-8.91461	8.22611
21	$c_{1,1}$	51.33110	-279.94300	182.73000
22	$c_{2,2}$	-2.60136	-1.03179	2.34693
23	$c_{3,3}$	-0.55343	0.16507	-0.23381
24	$c_{4,4}$	0.39604	0.36604	-0.41034
25	$c_{5,5}$	0.04157	0.55284	-0.38680
26	$c_{6,6}$	-0.55040	-0.00858	0.07165
27	$c_{7,7}$	0.58969	-2.27600	1.91144
28	$c_{8,8}$	-2.35741	1.62147	-3.59276
29	$c_{9,9}$	-0.72529	-0.93906	-1.33808
30	$c_{10,10}$	0.03918	-0.38899	0.66831
31	$c_{11,11}$	-1.05124	1.13737	-1.35958
32	$c_{12,12}$	-0.46932	2.49475	0.67818
33	$c_{13,13}$	0.34001	1.81410	-2.07548
34	$c_{14,14}$	5.82864	12.80060	-6.05799
35	$c_{15,15}$	0.34818	0.20149	-0.14163
36	$c_{16,16}$	-0.46999	-0.58568	0.20373
37	$c_{17,17}$	0.92946	-0.19114	0.86318

Term		Polynomial Coefficients		
		Y_d	X_d	R_d
38	$c_{18,18}$	-0.26330	0.66710	-0.23331
39	$c_{19,19}$	0.55374	-0.45711	0.73125
40	$c_{20,20}$	-0.14018	-0.46196	0.51280
41	$c_{1,2}$	-0.09234	-0.37803	0.29667
42	$c_{1,3}$	0.31567	0.55289	-0.61041
43	$c_{1,4}$	-0.69067	-0.41480	0.88399
44	$c_{1,5}$	0.32487	1.08388	-1.32009
45	$c_{1,6}$	0.42150	0.09293	-0.15394
46	$c_{1,7}$	-0.70085	0.47802	-0.51975
47	$c_{1,8}$	-0.14693	-0.17186	0.17847
48	$c_{1,9}$	0.08739	1.12137	-0.82904
49	$c_{1,10}$	-0.23681	-0.20043	-0.00017
50	$c_{1,11}$	0.16377	0.01357	-0.01574
51	$c_{1,12}$	0.68448	0.10847	-0.00661
52	$c_{1,13}$	-0.15971	-0.73664	0.16762
53	$c_{1,14}$	-0.11854	0.36940	-0.18627
54	$c_{1,15}$	0.11391	-0.07905	0.27658
55	$c_{1,16}$	-0.10352	-0.27364	0.35735
56	$c_{1,17}$	-0.07675	0.25554	-0.18023
57	$c_{1,18}$	-0.57806	0.37128	-0.38429
58	$c_{1,19}$	-0.50996	-0.77729	0.14558
59	$c_{1,20}$	-1.22421	-1.35346	0.88303
60	$c_{2,3}$	0.01609	0.17717	-0.18248
61	$c_{2,4}$	-0.11870	0.35969	-0.33233
62	$c_{2,5}$	-0.16938	0.02934	0.01161
63	$c_{2,6}$	-0.07556	-0.08396	0.02986
64	$c_{2,7}$	-0.04271	-0.06839	0.07618
65	$c_{2,8}$	-0.03775	-0.04370	0.01240
66	$c_{2,9}$	-0.00425	0.07283	-0.00744
67	$c_{2,10}$	-0.04015	-0.01705	-0.02314
68	$c_{2,11}$	0.00778	0.03979	-0.04358
69	$c_{2,12}$	-0.14180	0.01879	-0.09191
70	$c_{2,13}$	-0.06607	-0.01775	0.02681
71	$c_{2,14}$	0.00312	-0.00642	0.00282
72	$c_{2,15}$	0.00368	-0.00652	-0.00346
73	$c_{2,16}$	0.01903	-0.01084	0.05947
74	$c_{2,17}$	0.02524	0.01379	-0.01001
75	$c_{2,18}$	-0.01453	0.13178	-0.25942
76	$c_{2,19}$	0.15863	-0.06822	0.00852

Term		Polynomial Coefficients		
		Y_d	X_d	R_d
77	$c_{2,20}$	-0.05873	-0.04120	-0.06216
78	$c_{3,4}$	0.17550	0.04559	-0.46372
79	$c_{3,5}$	0.34773	0.57319	-0.39007
80	$c_{3,6}$	-0.02758	-0.13796	-0.03380
81	$c_{3,7}$	-0.02826	0.21462	-0.12575
82	$c_{3,8}$	0.06654	-0.12176	0.04788
83	$c_{3,9}$	-0.05742	0.01144	-0.11606
84	$c_{3,10}$	-0.11195	-0.05838	-0.00536
85	$c_{3,11}$	-0.04909	0.24901	-0.14927
86	$c_{3,12}$	0.05034	0.15293	-0.09132
87	$c_{3,13}$	0.10697	0.08951	-0.07526
88	$c_{3,14}$	-0.10160	-0.60783	0.15985
89	$c_{3,15}$	-0.06214	-0.08598	0.00745
90	$c_{3,16}$	-0.14828	0.01622	0.07380
91	$c_{3,17}$	-0.06243	0.17135	-0.03720
92	$c_{3,18}$	0.35111	-0.28607	0.37268
93	$c_{3,19}$	0.56416	0.90472	-0.22228
94	$c_{3,20}$	0.16248	0.22495	-0.30314
95	$c_{4,5}$	-0.28243	-0.06240	0.03458
96	$c_{4,6}$	0.03849	0.18515	-0.06380
97	$c_{4,7}$	-0.10250	-0.05906	0.15058
98	$c_{4,8}$	-0.06410	0.20519	-0.14367
99	$c_{4,9}$	0.15806	-0.12798	0.09397
100	$c_{4,10}$	-0.05812	-0.05429	0.13214
101	$c_{4,11}$	0.14432	-0.10817	0.08141
102	$c_{4,12}$	0.01379	-0.00509	-0.05074
103	$c_{4,13}$	0.05434	-0.07481	0.09410
104	$c_{4,14}$	0.10622	0.10049	0.13650
105	$c_{4,15}$	0.11143	-0.03794	0.00007
106	$c_{4,16}$	0.07701	0.33828	-0.35360
107	$c_{4,17}$	-0.02671	0.05844	0.02867
108	$c_{4,18}$	-0.83538	0.35084	-0.33127
109	$c_{4,19}$	-0.05149	0.22191	0.19882
110	$c_{4,20}$	-0.29089	0.11319	-0.36595
111	$c_{5,6}$	0.10495	0.19228	-0.09792
112	$c_{5,7}$	0.16048	0.00755	0.00809
113	$c_{5,8}$	-0.11036	0.17335	-0.05993
114	$c_{5,9}$	-0.13216	0.08189	0.00294
115	$c_{5,10}$	0.09185	0.04905	0.08084

Term		Polynomial Coefficients		
		Y_d	X_d	R_d
116	$c_{5,11}$	-0.15733	-0.21868	0.03610
117	$c_{5,12}$	-0.09504	0.06857	-0.01874
118	$c_{5,13}$	0.01872	-0.13214	0.10597
119	$c_{5,14}$	0.26864	-0.18818	0.22419
120	$c_{5,15}$	0.05177	0.04193	-0.09845
121	$c_{5,16}$	0.00652	-0.17610	0.03965
122	$c_{5,17}$	-0.05207	-0.19847	0.08383
123	$c_{5,18}$	0.04339	1.26142	-0.74545
124	$c_{5,19}$	-0.09257	0.76697	-0.35903
125	$c_{5,20}$	0.20074	0.34621	-0.21164
126	$c_{6,7}$	-0.09069	-0.04579	0.03752
127	$c_{6,8}$	0.03920	0.05616	-0.02603
128	$c_{6,9}$	0.06176	-0.05980	0.03114
129	$c_{6,10}$	0.02902	-0.02352	-0.02420
130	$c_{6,11}$	0.00214	0.09835	-0.07611
131	$c_{6,12}$	-0.00026	-0.02775	0.00232
132	$c_{6,13}$	-0.01805	-0.00548	-0.00860
133	$c_{6,14}$	-0.00070	-0.02894	0.05263
134	$c_{6,15}$	0.03558	-0.02101	-0.00425
135	$c_{6,16}$	0.00373	-0.04967	-0.02343
136	$c_{6,17}$	-0.02295	0.07152	-0.06884
137	$c_{6,18}$	-0.01766	-0.16825	-0.04054
138	$c_{6,19}$	-0.06061	-0.07996	-0.02638
139	$c_{6,20}$	-0.10119	-0.04548	-0.05999
140	$c_{7,8}$	-0.00483	0.00508	-0.00651
141	$c_{7,9}$	-0.02269	0.04849	-0.02700
142	$c_{7,10}$	0.03004	-0.02711	0.04162
143	$c_{7,11}$	0.02195	0.07751	-0.07120
144	$c_{7,12}$	-0.15719	0.04897	-0.05202
145	$c_{7,13}$	0.05052	-0.06031	0.05222
146	$c_{7,14}$	0.02242	-0.02061	-0.02919
147	$c_{7,15}$	-0.05506	-0.01285	0.01617
148	$c_{7,16}$	0.03302	0.02426	0.04330
149	$c_{7,17}$	0.12552	-0.00326	-0.00313
150	$c_{7,18}$	0.00291	-0.04952	0.15828
151	$c_{7,19}$	0.11006	0.11552	0.06642
152	$c_{7,20}$	0.05831	-0.06000	-0.05419
153	$c_{8,9}$	-0.11036	-0.04671	-0.04407
154	$c_{8,10}$	0.02261	0.17684	-0.10901

Term		Polynomial Coefficients		
		Y_d	X_d	R_d
155	$c_{8,11}$	-0.01622	-0.07629	0.06997
156	$c_{8,12}$	0.13947	-0.10815	0.12987
157	$c_{8,13}$	-0.03126	0.00995	-0.01594
158	$c_{8,14}$	-0.03028	0.02683	-0.01839
159	$c_{8,15}$	0.03351	0.12157	-0.08168
160	$c_{8,16}$	-0.02797	-0.09406	0.04300
161	$c_{8,17}$	-0.02760	0.03301	-0.01647
162	$c_{8,18}$	-0.03120	0.08616	-0.13354
163	$c_{8,19}$	0.05252	0.03268	-0.08069
164	$c_{8,20}$	0.10495	0.12335	-0.09607
165	$c_{9,10}$	-0.02197	0.04333	-0.03758
166	$c_{9,11}$	0.03192	0.16510	-0.09825
167	$c_{9,12}$	-0.11233	-0.02538	-0.01006
168	$c_{9,13}$	-0.02263	-0.05757	0.02170
169	$c_{9,14}$	0.01597	0.01285	-0.07487
170	$c_{9,15}$	0.00957	-0.07394	0.04156
171	$c_{9,16}$	0.07665	-0.04729	-0.00905
172	$c_{9,17}$	-0.05274	0.05668	-0.06092
173	$c_{9,18}$	-0.20796	-0.18934	0.16717
174	$c_{9,19}$	-0.30484	-0.15987	0.12992
175	$c_{9,20}$	-0.05383	-0.30746	0.17505
176	$c_{10,11}$	0.03346	-0.08674	0.05906
177	$c_{10,12}$	0.05105	0.06448	-0.01180
178	$c_{10,13}$	0.00200	-0.02341	0.03173
179	$c_{10,14}$	-0.00879	0.01835	-0.01502
180	$c_{10,15}$	-0.01231	-0.04525	-0.00934
181	$c_{10,16}$	0.00280	0.01549	-0.01737
182	$c_{10,17}$	0.02355	-0.08636	0.05245
183	$c_{10,18}$	-0.01072	0.07349	-0.07680
184	$c_{10,19}$	0.00503	0.11735	-0.09361
185	$c_{10,20}$	-0.05102	-0.40387	0.16913
186	$c_{11,12}$	0.02676	0.10878	-0.06838
187	$c_{11,13}$	0.01086	0.02363	-0.01492
188	$c_{11,14}$	-0.05609	0.11868	-0.12364
189	$c_{11,15}$	0.00261	0.02483	-0.02288
190	$c_{11,16}$	-0.04890	0.01769	-0.03790
191	$c_{11,17}$	0.03776	-0.09997	0.08452
192	$c_{11,18}$	-0.04272	-0.13367	0.09841
193	$c_{11,19}$	-0.08466	-0.11335	0.05319

Term		Polynomial Coefficients		
		Y_d	X_d	R_d
194	$c_{11,20}$	-0.04735	0.08827	0.07726
195	$c_{12,13}$	-0.04397	-0.05151	0.01217
196	$c_{12,14}$	0.06973	0.10267	-0.09594
197	$c_{12,15}$	0.02585	0.00652	0.03739
198	$c_{12,16}$	0.02932	0.02875	-0.01911
199	$c_{12,17}$	-0.00870	0.06395	-0.00251
200	$c_{12,18}$	-0.01590	0.09926	-0.08479
201	$c_{12,19}$	-0.19386	-0.23069	0.19005
202	$c_{12,20}$	-0.00027	0.23733	-0.12921
203	$c_{13,14}$	-0.01059	0.03981	-0.01066
204	$c_{13,15}$	0.01448	-0.01841	-0.00359
205	$c_{13,16}$	0.05626	0.03463	-0.02095
206	$c_{13,17}$	0.00801	-0.00369	0.00631
207	$c_{13,18}$	0.09016	0.03886	-0.02154
208	$c_{13,19}$	-0.00258	0.33136	-0.16308
209	$c_{13,20}$	0.16719	0.29606	-0.12208
210	$c_{14,15}$	-0.06898	-0.03859	-0.00633
211	$c_{14,16}$	-0.01756	-0.08922	0.01164
212	$c_{14,17}$	-0.00051	0.02427	-0.00648
213	$c_{14,18}$	-0.05022	-0.41727	0.16886
214	$c_{14,19}$	-0.00554	0.26241	-0.25158
215	$c_{14,20}$	-0.31025	-0.21970	0.24702
216	$c_{15,16}$	0.02437	-0.10284	0.03018
217	$c_{15,17}$	0.02316	0.00690	-0.01902
218	$c_{15,18}$	0.06388	-0.18768	0.10069
219	$c_{15,19}$	-0.01676	-0.10577	-0.00599
220	$c_{15,20}$	-0.02288	-0.05077	-0.00604
221	$c_{16,17}$	0.00218	0.05025	-0.04270
222	$c_{16,18}$	0.15053	-0.23161	0.20518
223	$c_{16,19}$	0.11171	0.14904	-0.09579
224	$c_{16,20}$	-0.13235	0.09829	-0.08312
225	$c_{17,18}$	0.04581	-0.12798	0.11812
226	$c_{17,19}$	-0.11080	-0.07167	0.03269
227	$c_{17,20}$	0.06963	0.10642	-0.04679
228	$c_{18,19}$	0.15666	-0.20082	0.45213
229	$c_{18,20}$	0.36563	-0.67427	-0.07990
230	$c_{19,20}$	0.23041	0.49391	-0.59158
231	d_1	1.69646	-9.59163	6.22971
232	d_2	0.01435	0.00606	-0.01391

Term		Polynomial Coefficients		
		Y_d	X_d	R_d
233	d_3	0.04242	-0.06368	0.04589
234	d_4	0.40045	0.03075	-0.02920
235	d_5	0.02261	0.16003	-0.10323
236	d_6	0.00126	-0.00009	-0.00001
237	d_7	0.00164	-0.00715	0.00597
238	d_8	-0.00744	0.00479	-0.01118
239	d_9	-0.00385	-0.00631	-0.00730
240	d_{10}	-0.00003	0.00498	-0.00876
241	d_{11}	0.00137	-0.00157	0.00188
242	d_{12}	0.00529	-0.04657	-0.00754
243	d_{13}	0.00053	0.00298	-0.00346
244	d_{14}	0.01616	0.03496	-0.01711
245	d_{15}	-0.00122	-0.00082	0.00066
246	d_{16}	0.00644	0.00668	-0.00242
247	d_{17}	-0.00198	0.00042	-0.00191
248	d_{18}	0.00708	0.06870	0.21538
249	d_{19}	-0.01964	-0.36702	0.30353
250	d_{20}	-0.12265	-0.15883	0.07384

Appendix B

Linking diagram of simulation model B

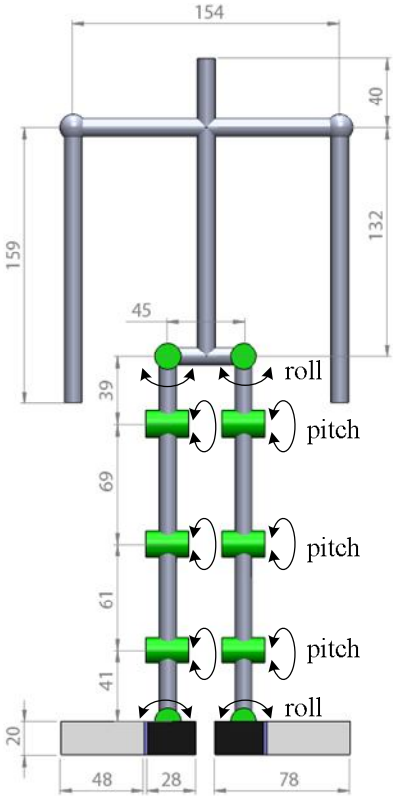

Front view

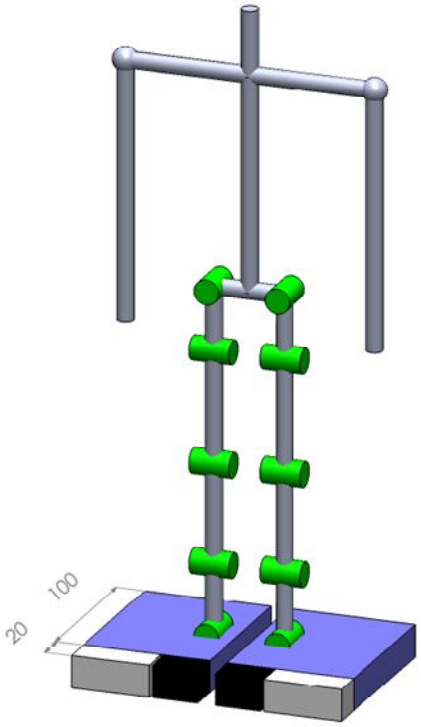

Isometric view

Robot feet diagram

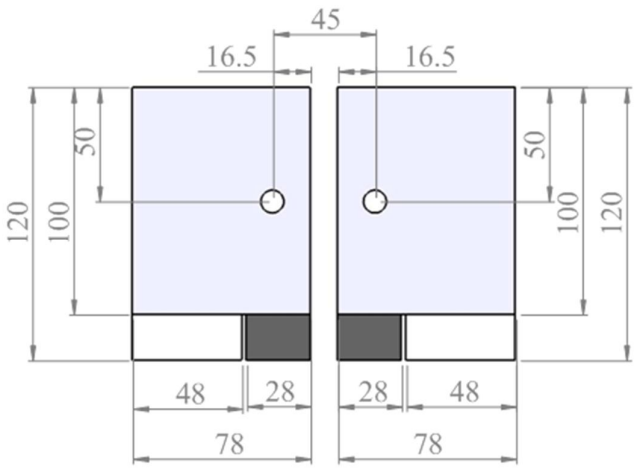

Right foot Left foot

Appendix C

In this part, I presented the gait coefficients of Experiment III. The gait cycles which appeared in Experiment III were generated by gait generation function (Eq. 4.1) as performed below.

$$\theta_i(t) = a_i + b_i \cos(\omega t) + c_i \sin(\omega t) + d_i \cos(2\omega t)$$

Table C-1 and Table C-2 indicated coefficient values which used in Eq. 4.1 for generating gait cycle of model B1-B10's joints. These coefficients drove each joint of robot model to walk as shown in table 6.3. The sets of coefficients were different because the different size of big toe affected several load supporting and load transferring. In spite of using same set of coefficient, several spring stiffness affected different results too.

Table C-1: Coefficients of model B2 , *Kp* = 0.033 N/deg

Coefficients of model B2 , *Kp* = 0.033 N/deg																
	B1				B2				B3				B4			
	a_i	b_i	c_i	d_i	a_i	b_i	c_i	d_i	a_i	b_i	c_i	d_i	a_i	b_i	c_i	d_i
θ_1	0.250	4.900	2.600	0.150	0.200	4.250	0.850	-0.450	0.400	4.900	0.600	0.000	0.425	4.800	0.950	-0.125
θ_2	-16.000	8.000	3.000	-6.000	-17.000	8.000	4.000	-5.000	-17.000	8.000	4.000	-5.000	-17.025	8.000	3.950	-4.975
θ_3	21.250	-10.000	12.500	-1.250	21.250	-10.000	12.500	-1.250	21.250	-10.000	12.500	-1.250	21.250	-10.000	12.500	-1.250
θ_4	-7.000	-4.050	6.950	1.050	-8.050	-2.500	6.400	0.550	-8.100	-2.400	6.400	0.500	-7.900	-2.450	6.750	0.350
θ_5	-24.000	-1.000	6.000	-5.000	-23.750	-1.500	6.000	-4.750	-23.750	-1.500	6.000	-4.750	-24.000	-1.000	6.000	-5.000
θ_6	28.125	-11.500	-5.250	13.375	28.200	-11.500	-4.900	13.300	28.200	-11.500	-4.900	13.300	28.250	-11.500	-5.000	13.250
θ_7	-11.375	13.750	6.000	-4.375	-11.675	14.000	5.850	-4.325	-11.775	14.050	5.600	-4.175	-11.500	13.750	5.750	-4.250
	B5				B6				B7				B8			
	a_i	b_i	c_i	d_i	a_i	b_i	c_i	d_i	a_i	b_i	c_i	d_i	a_i	b_i	c_i	d_i
θ_1	-0.050	4.850	1.950	0.400	0.325	4.750	1.100	-0.075	0.500	4.850	0.850	-0.150	0.475	4.850	0.800	-0.125
θ_2	-17.000	8.000	4.000	-5.000	-17.050	8.000	3.900	-4.950	-17.000	8.000	4.000	-5.000	-16.775	8.000	3.450	-5.225
θ_3	21.250	-10.000	12.500	-1.250	21.250	-10.000	12.500	-1.250	21.250	-10.000	12.500	-1.250	21.250	-10.000	12.500	-1.250
θ_4	-8.100	-2.500	6.500	0.600	-7.875	-3.000	6.250	0.875	-8.050	-2.500	6.400	0.550	-7.275	-3.500	6.950	0.775
θ_5	-23.875	-1.500	5.750	-4.625	-23.750	-1.500	6.000	-4.750	-23.750	-1.500	6.000	-4.750	-23.750	-1.500	6.000	-4.750
θ_6	28.200	-11.500	-4.900	13.300	28.200	-11.500	-4.900	13.300	28.200	-11.500	-4.900	13.300	28.200	-11.500	-4.900	13.300
θ_7	-11.800	14.100	5.300	-4.100	-11.625	14.000	5.750	-4.375	-11.750	14.100	5.600	-4.150	-11.700	14.100	5.500	-4.200
	B9				B10											
	a_i	b_i	c_i	d_i	a_i	b_i	c_i	d_i								
θ_1	0.425	4.750	0.800	-0.175	-0.600	2.750	2.450	-1.150								
θ_2	-17.000	8.000	4.000	-5.000	-21.000	10.000	8.000	-4.000								
θ_3	21.250	-10.000	12.500	-1.250	20.775	-6.500	14.950	-4.275								
θ_4	-8.250	-2.500	6.000	0.750	-7.950	0.500	0.200	-2.550								
θ_5	-23.825	-1.500	5.850	-4.675	-26.350	-0.100	2.200	-3.550								
θ_6	28.850	-11.500	-3.800	12.650	31.400	-12.500	0.300	11.100								
θ_7	-13.550	12.500	2.600	-3.950	-14.575	11.900	-1.250	-3.325								

Table C-2: Coefficients of model B2 , *Kp* = 0.037 N/deg

Coefficients of model B2 , *Kp* = 0.037 N/deg																
	B1				B2				B3				B4			
	a_i	b_i	c_i	d_i	a_i	b_i	c_i	d_i	a_i	b_i	c_i	d_i	a_i	b_i	c_i	d_i
θ_1	0.425	4.950	2.600	0.225	3.250	4.950	6.050	-2.700	0.800	5.100	1.400	-0.100	0.775	5.100	1.350	-0.075
θ_2	-16.000	8.000	3.000	-6.000	-16.950	8.000	3.900	-5.050	-16.750	8.000	3.500	-5.250	-17.000	8.000	4.000	-5.000
θ_3	21.250	-10.000	12.500	-1.250	21.250	-10.000	12.500	-1.250	21.250	-10.000	12.500	-1.250	21.250	-10.000	12.500	-1.250
θ_4	-6.950	-4.100	7.000	1.050	-8.000	-2.500	6.500	0.500	-8.125	-2.500	6.150	0.625	-8.125	-2.500	6.150	0.625
θ_5	-24.000	-1.000	6.000	-5.000	-23.750	-1.500	6.000	-4.750	-23.750	-1.500	6.000	-4.750	-23.750	-1.500	6.000	-4.750
θ_6	28.125	-11.500	-5.250	13.375	28.200	-11.500	-4.900	13.300	28.200	-11.500	-4.900	13.300	28.200	-11.500	-4.900	13.300
θ_7	-11.400	13.700	5.900	-4.300	-11.850	13.400	5.900	-4.750	-12.225	13.000	5.750	-4.775	-12.200	13.000	5.800	-4.800
	B5				B6				B7				B8			
	a_i	b_i	c_i	d_i	a_i	b_i	c_i	d_i	a_i	b_i	c_i	d_i	a_i	b_i	c_i	d_i
θ_1	0.425	4.800	0.950	-0.025	0.800	5.000	1.500	-0.200	0.925	5.000	1.750	-0.325	0.225	4.450	1.000	-0.275
θ_2	-17.000	8.000	4.000	-5.000	-17.000	8.000	4.000	-5.000	-17.050	8.000	4.000	-4.950	-16.775	8.000	3.450	-5.225
θ_3	21.300	-10.000	12.400	-1.300	21.250	-10.000	12.500	-1.250	21.250	-10.000	12.500	-1.250	21.250	-10.000	12.500	-1.250
θ_4	-8.250	-2.450	6.350	0.700	-8.100	-2.500	6.100	0.600	-8.125	-2.500	6.350	0.625	-7.400	-3.500	6.700	0.900
θ_5	-23.950	-1.100	6.000	-4.950	-23.750	-1.500	6.000	-4.750	-23.750	-1.500	6.000	-4.750	-23.750	-1.500	6.000	-4.750
θ_6	28.325	-11.750	-4.900	13.425	28.200	-11.500	-4.900	13.300	28.300	-11.500	-4.900	13.200	28.225	-11.500	-4.950	13.275
θ_7	-12.000	14.300	5.700	-4.200	-12.225	12.900	5.850	-4.875	-12.275	12.750	5.700	-4.975	-11.775	14.100	5.550	-4.125
	B9				B10											
	a_i	b_i	c_i	d_i	a_i	b_i	c_i	d_i								
θ_1	0.400	4.850	1.150	-0.050	0.150	4.100	2.100	-0.250								
θ_2	-17.000	8.000	4.000	-5.000	-21.125	10.000	7.750	-3.875								
θ_3	21.250	-10.000	12.500	-1.250	20.500	-6.000	15.000	-4.500								
θ_4	-8.250	-2.500	6.000	0.750	-8.550	2.500	0.600	-3.950								
θ_5	-23.800	-1.500	5.900	-4.700	-26.400	0.000	2.200	-3.600								
θ_6	28.850	-11.500	-3.800	12.650	31.325	-12.350	0.300	11.025								
θ_7	-13.575	12.500	2.550	-3.925	-15.150	11.250	-1.050	-3.600								

Table C-3: Maximum ~ Minimum of coefficients (Model B2 , K_p=0.033 N/deg)

Model B2 , K_p=0.033 N/deg												
Maximum ~ Minimum of coefficients												
	a_i			b_i			c_i			d_i		
	Max	~	Min	Max	~	Min	Max	~	Min	Max	~	Min
θ_1	0.500	~	-0.600	4.900	~	2.750	2.600	~	0.600	0.400	~	-1.150
θ_2	-16.000	~	-21.000	10.000	~	8.000	8.000	~	3.000	-4.000	~	-6.000
θ_3	21.250	~	20.775	-6.500	~	-10.000	14.950	~	12.500	-1.250	~	-4.275
θ_4	-7.000	~	-8.250	0.500	~	-4.050	6.950	~	0.200	1.050	~	-2.550
θ_5	-23.750	~	-26.350	-0.100	~	-1.500	6.000	~	2.200	-3.550	~	-5.000
θ_6	31.400	~	28.125	-11.500	~	-12.500	0.300	~	-5.250	13.375	~	11.100
θ_7	-11.375	~	-14.575	14.100	~	11.900	6.000	~	-1.250	-3.325	~	-4.375

Table C-3 and Table C-4 showed scope of coefficients that was obtained from experiments. Scope of coefficients that was shown in Table A-5 can be understandable easier. Values from this table can help to define variable narrowly and can apply to be the scope of variable definition for optimization in future.

Table C-4: Maximum ~ Minimum of coefficients (Model B2 , K_p=0.034 N/deg)

Model B2 , K_p=0.037 N/deg												
Maximum ~ Minimum of coefficients												
	a_i			b_i			c_i			d_i		
	Max	~	Min	Max	~	Min	Max	~	Min	Max	~	Min
θ_1	3.250	~	0.150	5.100	~	4.100	6.050	~	0.950	0.225	~	-2.700
θ_2	-16.000	~	-21.125	10.000	~	8.000	7.750	~	3.000	-3.875	~	-6.000
θ_3	21.300	~	20.500	-6.000	~	-10.000	15.000	~	12.400	-1.250	~	-4.500
θ_4	-6.950	~	-8.550	2.500	~	-4.100	7.000	~	0.600	1.050	~	-3.950
θ_5	-23.750	~	-26.400	0.000	~	-1.500	6.000	~	2.200	-3.600	~	-5.000
θ_6	31.325	~	28.125	-11.500	~	-12.350	0.300	~	-5.250	13.425	~	11.025
θ_7	-11.400	~	-14.575	14.100	~	11.900	6.000	~	-1.250	-3.325	~	-4.975

Table C-5: Maximum ~ Minimum of coefficients (Compose between K_p= 0.033 and K_p= 0.037 N/deg)

Model B2 , Compose between K_p= 0.033 and K_p= 0.037 N/deg												
Maximum ~ Minimum of coefficients												
	a_i			b_i			c_i			d_i		
	Max	~	Min	Max	~	Min	Max	~	Min	Max	~	Min
θ_1	3.250	~	-0.600	5.100	~	2.750	6.050	~	0.600	0.400	~	-2.700
θ_2	-16.000	~	-21.125	10.000	~	8.000	8.000	~	3.000	-3.875	~	-6.000
θ_3	21.300	~	20.500	-6.000	~	-10.000	15.000	~	12.400	-1.250	~	-4.500
θ_4	-6.950	~	-8.550	2.500	~	-4.100	7.000	~	0.200	1.050	~	-3.950
θ_5	-23.750	~	-26.400	0.000	~	-1.500	6.000	~	2.200	-3.550	~	-5.000
θ_6	31.400	~	28.125	-11.500	~	-12.500	0.300	~	-5.250	13.425	~	11.025
θ_7	-11.375	~	-15.150	14.300	~	11.250	6.000	~	-1.250	-3.325	~	-4.975

Moreover, this table indicated the relation between angles values and coefficients values from gait function equation that included sine and cosine function. This relation showed that low value coefficients of the equation could obtain low angles values too such as θ_1 (θ_1 at hip roll control side to side position). In a similar way, there were higher coefficients values for θ_3 and θ_5 at knee positions than other positions. Angles values were also high along coefficients values.